FINAL REPORT

Investigating Efficient Tar Management from Biomass and Waste to Energy Gasification Processes

SERDP Project WP-2236

APRIL 2015

Patrick Scott
Michael Kiczek
Rick Gower
Kim Magrini
Alliant Techsystems Operations LLC

SERDP
DOD ▪ EPA ▪ DOE

Report Documentation Page

Form Approved
OMB No. 0704-0188

1. REPORT DATE	2. REPORT TYPE	3. DATES COVERED
APR 2015	**N/A**	**-**

4. TITLE AND SUBTITLE	5a. CONTRACT NUMBER
Investigating Efficient Tar Management from Biomass and Waste to Energy Gasification Processes	5b. GRANT NUMBER
	5c. PROGRAM ELEMENT NUMBER
6. AUTHOR(S)	5d. PROJECT NUMBER
	5e. TASK NUMBER
	5f. WORK UNIT NUMBER
7. PERFORMING ORGANIZATION NAME(S) AND ADDRESS(ES) **Alliant Techsystems Operations LLC**	8. PERFORMING ORGANIZATION REPORT NUMBER
9. SPONSORING/MONITORING AGENCY NAME(S) AND ADDRESS(ES)	10. SPONSOR/MONITOR'S ACRONYM(S)
	11. SPONSOR/MONITOR'S REPORT NUMBER(S)

12. DISTRIBUTION/AVAILABILITY STATEMENT
Approved for public release, distribution unlimited

13. SUPPLEMENTARY NOTES
The original document contains color images.

14. ABSTRACT

This effort evaluates enhancements to future development of deployable waste-to-energy (WTE) systems that meet Department of Defense (DoD) needs for efficiency, footprint and reliability. Waste materials and biomass are an energy resource which can be gasified and combusted in electricity generation. Coproduced gasification tars and gas cleanup complicate utilization and reduce conversion efficiency while posing environmental risk. The classical approach breaks tars down completely to carbon monoxide and hydrogen and then combusts these molecules or uses them in liquid fuel production. Literature shows, however, that many of these tars are flammable liquids that would burn in internal combustion engines (via the liquid fuel injection system) with better thermodynamic yield than burning the reformation product of the liquids.

15. SUBJECT TERMS

16. SECURITY CLASSIFICATION OF:			17. LIMITATION OF ABSTRACT	18. NUMBER OF PAGES	19a. NAME OF RESPONSIBLE PERSON
a. REPORT	b. ABSTRACT	c. THIS PAGE			
unclassified	**unclassified**	**unclassified**	**SAR**	**76**	

Table of Contents

Abstract 1
Background 1
Objectives 3
Technical Approach 4
Technical Approach Items 1 & 2: Gasification Method, Feeding and Gas Flow 4
Technical Approach – Items 3 & 4 Gas Delivery and Experiments 7
Technical Approach – Item 4 Plasma & Catalyst Experiments 11
Catalyst Experiment 12
Technical Approach Item 5: System Control. 14
Technical Approach Item 6: Gas Sampling 15
Technical Approach Item 7: Gas and Liquid Characterization. 21
Technical Approach Item 8: Process Gas Temperature and Flow Measurement 27
Integration and Operation Issues Lessons Learned 29
Feeder and Gasifier Issues 30
Heat Trace Lessons Learned 31
Leak Lessons Learned 33
Plasma Lessons Learned 35
Plasma Related Temperature Measurement Lessons Learned 37
Orifice Plate Flow Measurement Lessons Learned 38
Input Air Measurement Lessons Learned 39
Sampling Lessons Learned 40
Results 40
Chemical Mass Balances 41
Syngas Results 43
Discussion 57
8-14-14 Run Gas and Liquid Analysis Results Discussion 58
12-3-14 Run Gas and Liquid Analysis Results Discussion 59
Energy Content Analysis & Discussion 60
Lessons Learned, Conclusions and Implications for Future Research/Implementation 61
Summary 62
Conclusion 63
Recommendation for Future Work 65

Appendices 67
Literature Cited 68

List of Tables

Table 1. Headspace Method for Gas Chromatography Thermal Conductivity Detection 22
Table 2: Liquid Method for Gas Chromatography, Flame Ionization Detection 23
Table 3: Liquid Method for Gas Chromatography, Mass Spectroscopy 24
Table 4. High Temperature Gasket Material Test Results 34
Table 5. Analysis of Feed Stock (70% Wood, 10% Plastic, 10% Paper, 10% Dog Food) 42
Table 6. Headspace Gas Analysis 8-14-14 Run 43
Table 7. Headspace Gas Analysis 12-3-14 Run 45
Table 8: Blank Corrected* Liquid Sample Analysis (GCFID) 8-14-14 Run 46
Table 9. Blank Corrected* Liquid Sample Analysis (GCFID) 12-3-14 Run 47
Table 10. Gravimetric Tar & Water Concentration in Gas 50
Table 11. Table of Alkanes 52
Table 12 Target Tar Concentration and Energy Analysis 61

List of Figures

Figure 1. Pilot Plant Process Flow Diagram with Energy Balance and Sampling Port Indicators 4
Figure 2. Test Waste Stream: 70% Wood, 10% Paper, 10% Plastic, 10% Dog Food. 5
Figure 3. Gasification System and Feeder System in Diagrammatic Cross Section 6
Figure 4. As Built Updraft-Downflow Gasifier and Feed System Prepped for Initial Test 7
Figure 5. Piping Layout and Key System Elements for Gasification, Cracking and Sampling Experiments 8
Figure 6. Gas Flow Diagram for Air, Propane, N2, H2, He 9
Figure 7. Stainless and Incoloy 800H Piping Installed with Plasma and Catalyst Bed, Orifice Plates and Sample Ports. 10
Figure 8. Orifice Plate Flow Meter (Under Insulation) with Nitrogen Purge and Solenoids to Shut off N2 Flow During Flow Measurement. 10
Figure 9. GEK “Ejector Venturi” Drive, GEK Swirl Burner and Fire Eye ™ Flame Monitoring an Active Flare Burning off Syngas 11
Figure 10. Non-Thermal “Gliding Arc” Plasma Shown with Pre-plasma and Post Plasma Sampling Ports. 12
Figure 11. Catalyst Bed Cross Section at ~20^{o} Angle 13
Figure 12. Catalyst Bed as Built with Insulation Applied to withstand 900 ^{o} C. 14
Figure 13. Control Panel 15
Figure 14. Gas Chromatography and Gravimetric Process Gas Sample Ports 16
Figure 15. Gas Chromatography Suction Sampling Tool with Room Temp and Foam Insulated Ice Block Temperature Control 17
Figure 16. Path of Sample Gas through Vials Following European Tar Protocol 17
Figure 17. Gas Chromatography Tool Actively Sampling Tar Laden Syngas from a Process Pipe 18
Figure 18. Gas Chromatography Tubes Visually Indicating Levels of Captured Tars in Solution. 18
Figure 19. Heated Gravimetric Tar Sampling Probe. 19

Figure 20. Heated Gravimetric Sampling Probe and Flanged Airlock 20
Figure 21. Vacuum Flow and Measurement System for Gas Chromatography and Gravimetric Tar Sampling.....20
Figure 22. Heated Probe and Sampling Line for Drawing Tar Laden Syngas from Downstream of the Catalyst Bed. (Valve Heater for ¼ NPT Valve not Shown.).....21
Figure 23. Shimadzu Gas Chromatography Apparatus with PLOT and Siloxane Columns in Chamber Capable of Mass Spectroscopy (MS), Thermal Conductivity Detection (TCD) and Flame Ionization Detection (FID).....22
Figure 24. Calibration Curve Results 26
Figure 25. Cole-Parmer Rotary Vacuum Evaporator.....27
Figure 26. All Power Lab Process Control Unit Arduino Board. 27
Figure 27 Trending Temperature Readings as Measured by the Arduino Board and Recorded by the SmartTerm™ and Excel™ Interface 28
Figure 28. Real Time Temperature and Pressure Data as Presented in Excel™ Spreadsheet on Data Logger PC.....29
Figure 29. Gasifier and Feeder Showing Addition of Poker/Grate Shaker and N2 Blanketed Pneumatic Cylinder. ..30
Figure 30. Gasifier Feed Entry and Down Flow Pipe after Normal Run and after Overfill Condition 31
Figure 31. Condensed Tar that Ran Out of Sampling Port Upon Disassembly. 32
Figure 32. Tar Dripping and Hardening at the Flare.....33
Figure 33. Test Fixture for Verifying Gasket Performance at High Temperatures 34
Figure 34. Plasma - Melted Ceramic Insulator and Powered Electrode with Burn Mark Indicating Arc Location. Electrode Actually Enters Insulator from Side Opposite.....36
Figure 35. Plasma Flow Ports Allowing Insufficient Flow 37
Figure 36. Hole Drilled in Center of Plasmatron in Attempt to Improve Flow of Tar Laden Syngas through the System 37
Figure 37. Ferrite Cores Installed on all Thermal Couple Lines to Reduce Electromagnetic Interference from the Plasma. 38
Figure 38. Rotameter Calibration Data. 40
Figure 39. Real Time Gasifier Temperature Data (500 Data points) during ~9hr Run. 41
Figure 40. Summary of GCTCD Results at Various Sample Ports 8-14-2014 Run 44
Figure 41. Summary of GCTCD Results at Various Sample Ports 46
Figure 42 Percentages of Target Tars Found in the Sampling Fluid from Various Points in the Process 49
Figure 43. GCMS of Liquid from Exit Port of Gasifier from Vials in Sampler Path 50
Figure 44. FTIR Transmission of Tar at Exit of System Near Flare.....51
Figure 45. FTIR Transmission of Brown Condensed & Hardened Tar at Exit of System Near Flare.....52
Figure 46. Differential Scanning Calorimeter Analysis of Brown Waxy Exudate From the Flare. Run 1 Melt Temperature Approximately 77^{o}C.....54
Figure 47. Differential Scanning Calorimeter Analysis of Brown Waxy Exudate From the Flare. Run 1, Sample 2 Melt Temperature Approximately 76^{o}C 54
Figure 48. Differential Scanning Calorimeter Analysis of Brown Waxy Exudate From the Flare. Run 2, Sample 2 Possible Combustion at 330^{o}C.....55
Figure 49. Differential Scanning Calorimeter Analysis of Brown Waxy Exudate from the Flare. Run 2, Sample 2 Area around Melt of Figure 47 Expanded. 56
Figure 50. Differential Scanning Calorimeter Analysis of Brown Waxy Exudate from the Flare. Run 1, Sample 3..56
Figure 51. Brown Waxy Exudate (Stalagmite) Dissolving into R8 Fuel.....57
Figure 52.Filtration Result of Brown Waxy Exudate, Indicating that 64% of the Material is Soluble in Diesel Fuel.57
Figure 53. Pilot Plant Diagram with Test Ports Labelled. 58
Figure 54. Optimized Waste to Energy System for Maximized Conversion of Waste Energy into Electricity 64
Figure 55. Existing Lockheed Capital Scrubber Ready for Integration to a Gasification Unit.....66

List of Appendices

Appendix A: Exceptions to the European Tar Protocol.....67

List of Acronyms

BTX	Benzene, Toluene, Xylene
CFM	Cubic Feet per Minute
CO	Carbon Monoxide
CO2	Carbon Dioxide
CONUS	Continental US
DoD	Department of Defense
DSC	Differential Scanning Calorimeter
ETP	European Tar Protocol (CEN-143)
EPO	Emergency Power Off
FID	Flame Ionization Detection
FOB	Forward Operating Base
FTIR	Fourier Transform Infrared (Spectroscopy)
GC	Gas Chromatography
GCFID	Gas Chromatography Flame Ionization Detection
GCMS	Gas Chromatography Mass Spectroscopy
GCTCD	Gas Chromatography Thermal Conductivity Detection
GEK	Downdraft gasifier & equipment from All Power Labs, Inc.
GVn	Gate Valve Number (n = 1-7)
H2	Hydrogen
HDPE	High Density Polyethylene
IPA	Isopropyl Alcohol
ICE	Internal Combustion Engine
JP-8	Mil Spec Diesel & Aviation Fuel
LM	Lockheed Martin
MS	Mass Spectroscopy
NREL	National Renewable Energy Laboratory
N2	Nitrogen
NTP	Non-Thermal Plasma
PLC	Programmable Logic Controller
PLOT	Porous Layer Open Tubular gas chromatography column.
RTV	Room Temperature Vulcanizing Rubber (Silicone)

R-8	Renewable JP-8 by Dynamic Fuels
SERDP	Strategic Environmental Research and Development Program
TQG	Tactical Quiet Generator
TCD	Thermal Conductivity Detection
VOC	Volatile Organic Compounds
WTE	Waste to Energy

Keywords

Waste to Energy, Syngas, Reformation, Plasma, Catalyst, Diesel Fuel Based Scrubber, Tar Sampling, Gas Chromatography Mass Spectroscopy

Acknowledgements

Much thanks to the SERDP team for funding this effort!

Abstract

This effort evaluates enhancements to future development of deployable waste-to-energy (WTE) systems that meet Department of Defense (DoD) needs for efficiency, footprint and reliability. Waste materials and biomass are an energy resource which can be gasified and combusted in electricity generation. Co-produced gasification tars and gas cleanup complicate utilization and reduce conversion efficiency while posing environmental risk. The classical approach breaks tars down completely to carbon monoxide and hydrogen and then combusts these molecules or uses them in liquid fuel production. Literature shows, however, that many of these tars are flammable liquids that would burn in internal combustion engines (via the liquid fuel injection system) with better thermodynamic yield than burning the reformation product of the liquids. This study uses an updraft gasifier to generate a tar rich gas stream then evaluates minimized plasma and catalytic tar reformation of the gas stream to make more of this tar gas stream usable in the engine. Gas sampling at the process steps allows analytical (GCMS/TCD/FID) and gravimetric analysis of the gas and tar stream. The sampling techniques simulate a scrubber using methyl chloroform (for gas chromatography), and isopropyl alcohol or renewable JP-8 (R-8) engine fuel as the working fluid for the gravimetric sampling. The simulated scrubber aspect of this work is focused on capturing tars in R8 fuel that could later be burned in existing diesel generator sets to enable maximum conversion of waste to electricity. The gasification system, tar cracking experiments, and analytical techniques were put in place and shown to perform as expected to some degree. Hydrogen was produced by the gasifier at 16% maximum concentration (10% average); carbon monoxide was produced at 6% maximum and 4% average. Tar was generated from the gasifier at a minimum concentration of 150g/m^3. It is estimated that the usable portion of this tar is over 100g/m^3. The tar was decreased by the catalyst experiment but was not used to generate statistically significant data due to technical startup problems that consumed time and funding availability. The plasma system had flow and arc instability problems coupled with a hard failure (melted insulator) but did show a decrease in H_2, CO and CH_4 concentration in the limited data obtained. The plasma system has been repaired and is functional, but meaningful data has not yet been generated. Scrubbing with R8 removed all aromatic and heavy tar from the syngas. An amber ~30 carbon long straight alkane material was found running out from the flare that is mostly soluble in R8 implying the soluble portion would be an acceptable engine fuel additive and significant energy source depending on the amount of plastic in the waste stream.

Background

Base waste disposal (CONUS and FOB) is the fundamental issue that drove this research. Waste generation estimates are 4-8 lb/person/day at FOBs[i]. Current base disposal methods include landfill and incineration. Both have limited long term sustainability because of limited landfill space (particularly at FOBs) and the increasingly documented unhealthy effects of open burn pits[ii]. The US Department of Veterans Affairs' position is that current research does not prove long term health problems associated with burn pits, yet it has a registry to document health effects and provide opportunity to file compensation claims[iii]. Converting waste to energy cleanly and efficiently through gasification has long been desired to address waste disposal incineration limitations and exposures while providing an energy source.

Tars are one of the more technically challenging obstacles to the use of gasification as a waste-to-energy approach. Co-produced tars have complicated gasification and limited its

implementation because incomplete conversion to gas represents lost energy potential. The effort expended in cracking the tars results in plant complexity and cost, as does the gas cleanup required. Gas cleanup typically results in water treatment requirements and can lead to potential environmental releases of contaminated water. Milne[iv] summarizes gasification history and development in this landmark study. Tars are classified as primary, secondary and tertiary based on chemistry resulting from the chosen gasification method, the time at higher temperature, and oxygen exposure. Milne follows with a compilation of tar reference studies, including methods used and tar levels obtained. More recently Basu[v] has written extensively on Gasification, Pyrolysis, Torrefaction and design of these systems. He further explains the effects of time and temperature on tars and with Milne provides the basis for the conception of this research: ***It is found in this data that more 70% of the tars from gasification should easily be combustible in an engine, particularly if they are dissolved in a standard fuel at an acceptable percentage.*** For an updraft gasifier these tars are mostly simple aromatic hydrocarbons like benzene, toluene, xylene, with smaller amounts of methanol and ethanol, which are all flammable liquids. A current manual for a COTS diesel genset allows 35% aromatic fuel in the mix. As a result, the goal should be to replace more than 1/3 of the liquid fuel going into stationary diesel gensets with scrubber-captured low molecular weight tars while separating out then cracking or combusting the high molecular weight polyaromatic compounds as the heat source for gasification.

Most gasification work in the 20th century focused on downdraft gasification as a method of providing a low tar syngas when the burning char at the exit of the gasifier creates a zone where tar cracking can naturally occur in a simple format. The Department of Energy published a handbook on downdraft gasification which documents these systems in wide use during World War II.[vi] The current manifestation of these systems are highly advanced, computer controlled versions which have been tried in the field with limited success on pre-sorted waste streams[vii]. Other types of gasification include updraft, fluidized bed (circulating and bubbling types) and cross draft, with many variations on the themes of injecting controlled amounts of air at various points in the gasification process to optimize temperatures and syngas characteristics.

Methods of tar cracking involve electrical discharges including high temperature plasma torches[viii], microwave[ix], corona[x] and as related to this study, gliding arc nonthermal plasma[xi] and catalysts[xii]. Non-thermal plasma systems, including low-pressure glow, radio frequency and corona discharges, offer high chemical selectivity and relatively energy efficient plasma enhanced chemical reactions. Recent advances in gliding arc non-thermal plasma achieve excellent mixing of gas and plasma, which results in very highly active, non-equilibrium reactions. The gliding arc plasma technology was demonstrated effective at reforming JP-8 to hydrogen-rich fuel at about 1-3% energy input of the fuel stream. Again, the goal of the work referenced is to break down the tars to carbon monoxide and hydrogen which may be burned in an engine, or sent to Fischer Tropsch type processes for the production of synthetic fuels.

Lastly, gas scrubbing/cleanup has typically been accomplished with water, but focus on scrubbing with oily materials shows promise for the future and is a partial focus of this effort[xiii]. See Borrigter[xiv] and Scott[xv] for potential applications of scrubbing with fuels, or even better, renewable fuels such as biodiesel, as a path to enhanced energy recovery and minimization of waste water cleanup concerns. In general if the tar is diluted in a bulk fuel the water should separate and tend to lose organic material to the organic phase.

Objectives

The primary objective of this work is to develop fundamental methods to maximize delivery of *usable* waste chemical energy to the combustion chamber of an internal combustion engine (ICE[1]) in the simplest and most robust method possible. The work is novel in that it evaluated potential delivery of the chemical energy to the engine via the liquid fuel injection system as captured tars in addition to the traditional gas phase as syngas. The delivered chemical energy must: be combustible in the engine, not foul air and gas intakes, and not corrode or foul fuel injection systems. This work looks at pilot scale production of tars and evaluates plasma and catalytic cracking the tars to the minimal extent possible (to benzene, toluene, and xylene as opposed to H_2 & CO) to allow ICE utilization.

The objectives may be summarized graphically in Figure 1, where the waste is shown entering the gasifier and approximately10% of the chemical energy is consumed in the process of gasifying the solid material to a tar- syngas mix. The potential usable combustion energy at any point in the process is the syngas combustion potential plus the combustion potential of the usable tars. The usable tars are captured tars which, for this evaluation, distill off in a rotary vacuum evaporator at 65^{o}C or may pass through a filter as organic materials soluble in R8. The red arrows indicate where sampling (GC and gravimetric) ports were provided. On the gasifier, for example, samples can be taken at the top and bottom of the updraft down-flow gasifier. The objective was to understand the usable energy at each of the sampling points and apply that information towards the overall biomass gasification and tar recovery system design. Sampling is based on the "European Tar Protocol"[xvi] (ETP) which bubbles the syngas through impinger tubes in a sequence of warm and cold tubes to optimize condensation of the liquid tars in the fluid. The classical ETP uses isopropyl alcohol to determine gravimetric amounts of tar coupled with Gas Chromatography (GC) to analyze the fluids. In this study samples are taken directly using the GC vials filled with methyl chloroform to allow rapid acquisition and analysis via an auto handler on the gas chromatography machine. An additional test involves filling the classical ETP impingers with a renewable JP-8 diesel fuel (R-8) to simulate scrubbing with a fuel as method of capturing tars for use in the engine while evaluating the gas cleanup potential of the R-8 fuel.

[1] In this work internal combustion engine (ICE) can mean spark ignition or diesel (compression ignition). It is likely that the light tars could be made to burn in either style engine at significant (30%) concentration.

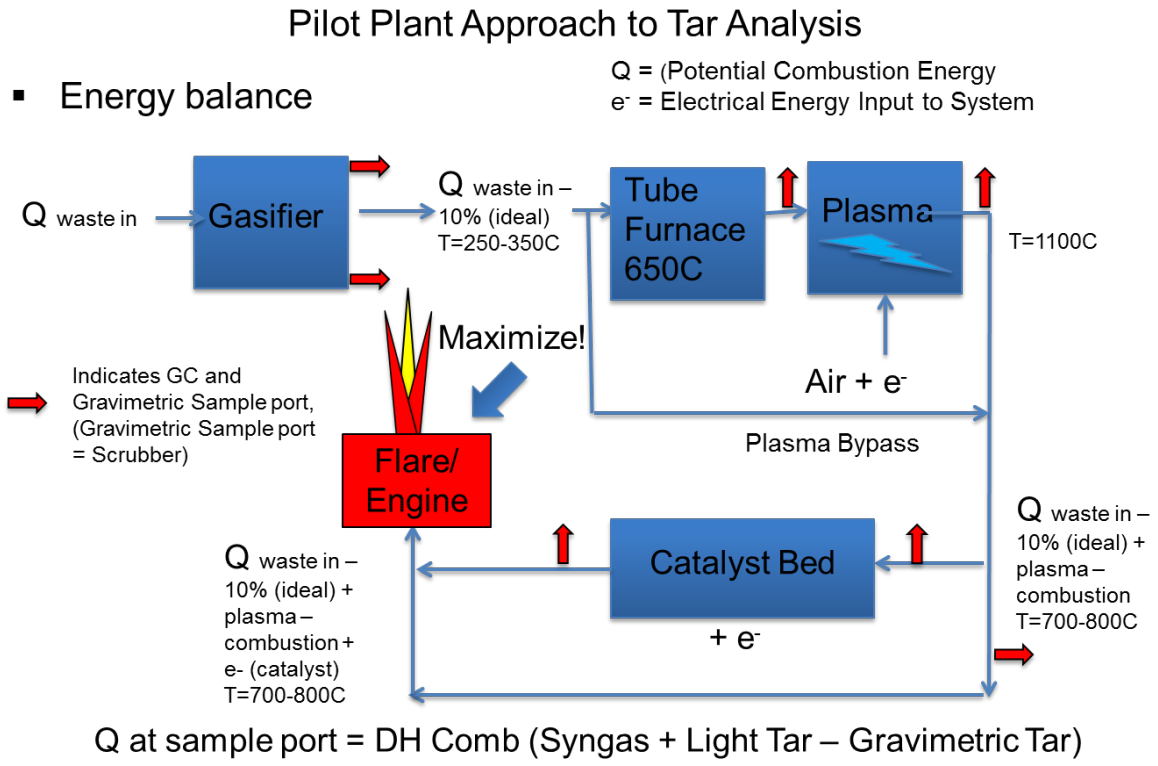

Figure 1. Pilot Plant Process Flow Diagram with Energy Balance and Sampling Port Indicators

Technical Approach

To accomplish the objectives the following Technical Approach Items be in place: 1) the waste must be fed to a gasifier with minimal entrained air; 2) the waste must be gasified in a repeatable manner; 3) the produced gas must be fed at a non-condensing temperature to the two tar cracking experiments (the plasma and the catalytic system); 4.) the two tar cracking experiments must operate and not produce confusing results (accumulation of tar or soot that confounds true tar elimination results); 5.) the experiments, heaters and safety monitoring system must be developed and verified; 6.) the resulting gas stream must be captured in a repeatable manner at key points in the gas stream before and after each experimental section; 7.) the gas and captured liquid tars must be characterized and quantified in a repeatable manner; 8.) the temperature and flow rates must be measured and recorded to allow understanding of energy and mass balances.

Technical Approach Items 1 & 2: Gasification Method, Feeding and Gas Flow

Lockheed Martin's approach is to first develop a gasification system that converts the maximum amount of waste material into a gas phase in the simplest and most reliable method possible. Updraft gasification was chosen because it uses air, provides maximum thermal efficiency in the simplest geometry possible, and generates a tar rich stream consisting of mostly chemicals that should be combustible directly in the engine[xvii]. Further, SERI[xviii] states that updraft gasification allows up to 90% of a dry biomass stream to be gasified to a tar rich stream which is about 20% better than the most advanced downdraft gasifiers.

This study uses a feedstock that is a mixture (by weight) of 70% wood chips, 10% paper & cardboard, 10% plastic, and 10% dry dog food to simulate waste and provide a repeatable (non-decaying and non-odor generating) energy source, Figure 2.

Figure 2. Test Waste Stream: 70% Wood, 10% Paper, 10% Plastic, 10% Dog Food.

The waste is fed to the gasifier via a PLC controlled double dump valve and pneumatic ram. The feed system may be triggered manually or via nitrogen-inerted level sensors that detect low level feed in the gasifier and overfill conditions that may result from bridged feed conditions. The system, as designed, lets the level sensors modulate ram travel until the end of ram stroke. At the end of the stroke, the ram returns, the double dump valve cycles (a nitrogen purge reduces oxygen in the feed) and the ram proceeds forward till the level sensors trigger. Gas flow through the system is driven by a GEK Gasifier[xix] "Ejector Venturi" that draws gas through the entire system including the experimental sections. The venturi blows the product gas into a GEK swirl burner to prevent buildup of syngas. Propane is added to the gas stream immediately before the venturi to provide a stable flame in the swirl burner. Nitrogen is provided for Emergency Power Off (EPO) conditions at various locations to shut the combustion process down. On an EPO, the drive venturi solenoid shuts, the propane is shut off and the nitrogen is turned on to prevent flame and an air fuel mix from combusting in the process lines or equipment. Figure 3 shows the gasification system in cross section. For simplicity, the drive venturi is shown on the gasifier. In practice, the drive venturi, swirl burner, propane connection and nitrogen EPO blanket are located outside of the building. The air intakes at the bottom of the gasifier have a flow meter to verify and measure flow. The system may also be air blown to assist in gas flow through the plasma and catalyst.

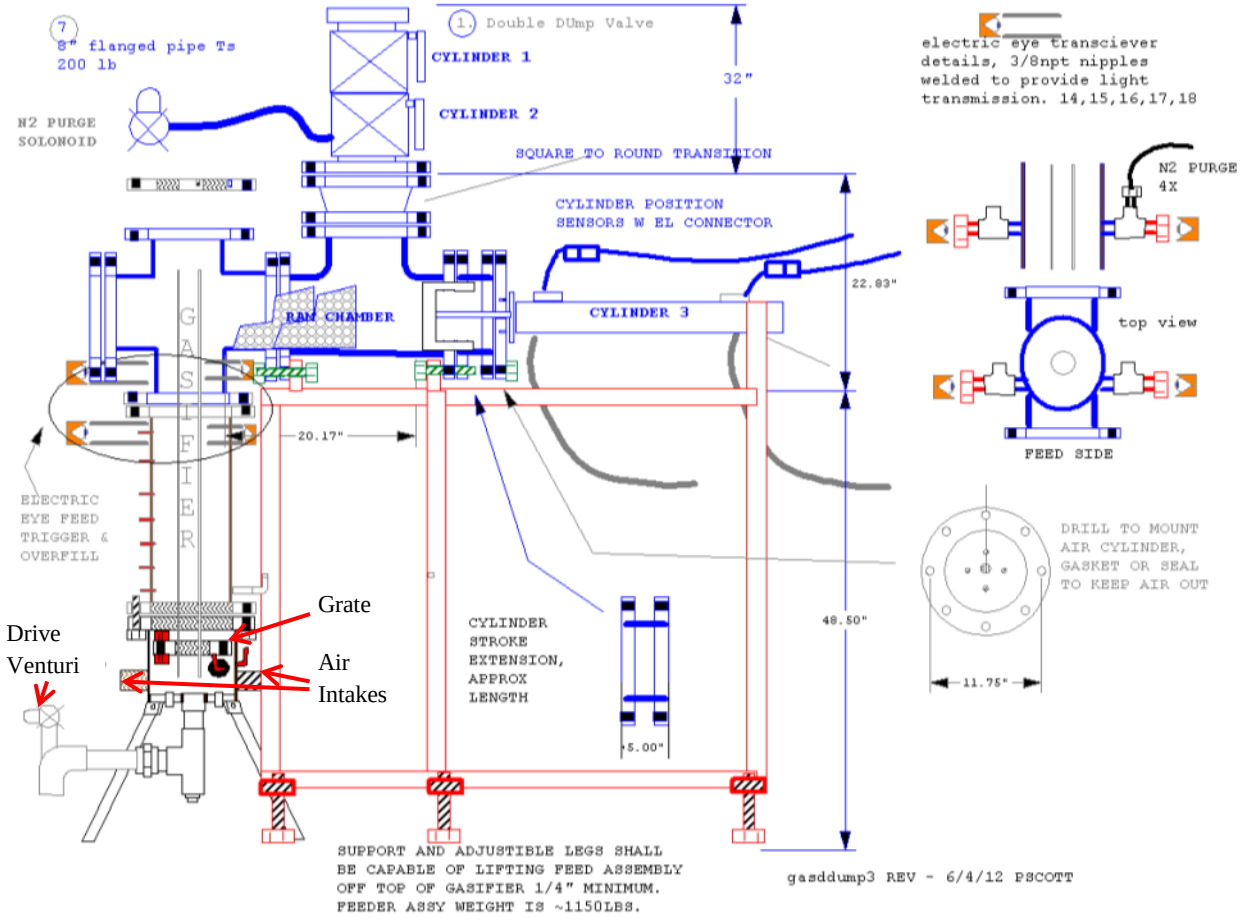

Figure 3. Gasification System and Feeder System in Diagrammatic Cross Section

One of the benefits of the gasifier used in this work is that it is reconfigurable. In Figure 3, a central pipe runs up the center of the gasifier and draws gas from the top back through the combustion zone to heat the produced tar-laden gas and prevent/reduce condensation. If this pipe is removed, the gasifier becomes a downdraft gasifier, and, if gas is sampled near the top of this down-flow pipe, the gasifier is effectively a straight updraft gasifier. Sample ports allow gas evaluation at each of these points.

Figure 4 shows the gasifier and feeder as-built with thermocouples installed and hooked up directly to the gas outflow pipe and venturi for initial burn tests.

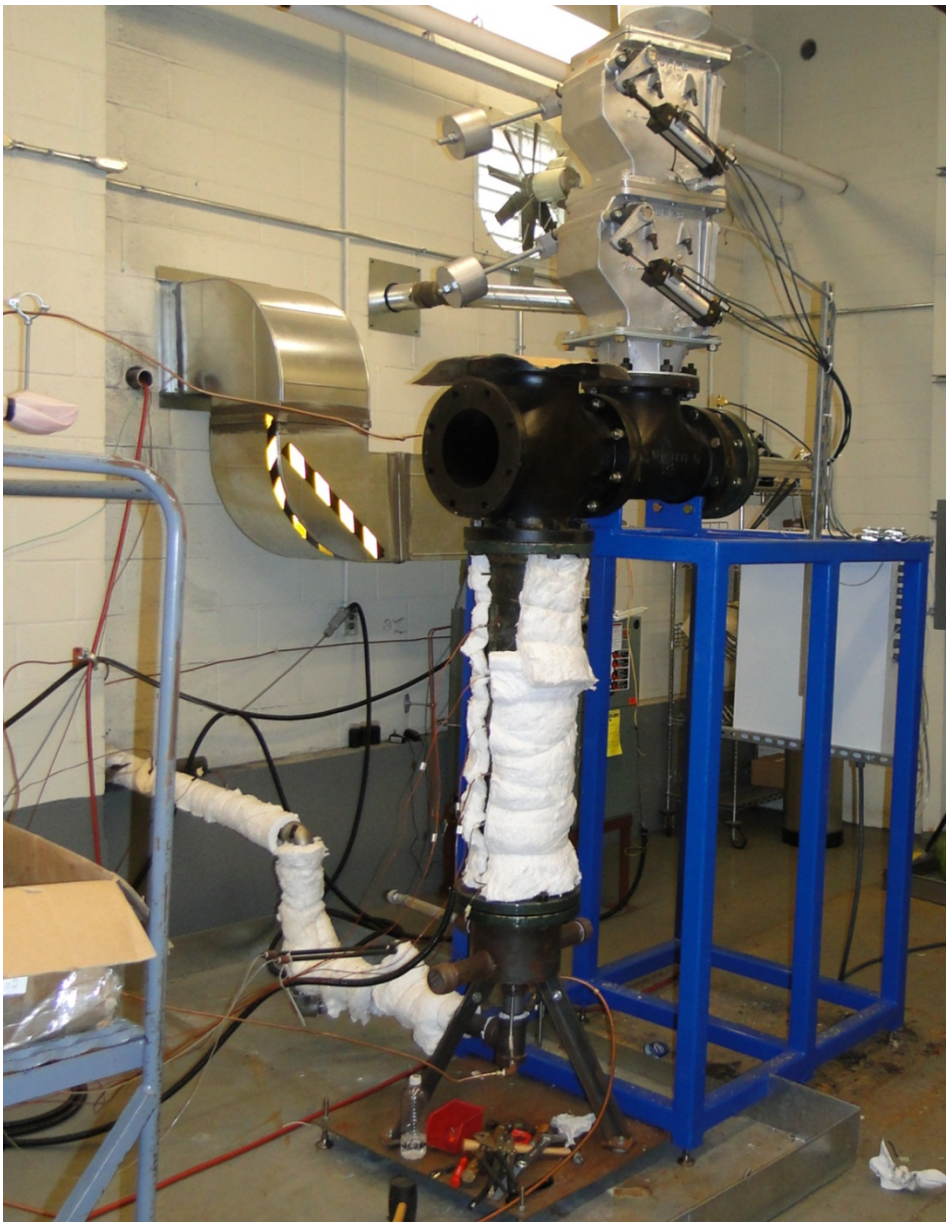

Figure 4. As Built Updraft-Downflow Gasifier and Feed System Prepped for Initial Test

Technical Approach – Items 3 & 4 Gas Delivery and Experiments

As stated above, the process gas is drawn through the gasifier by a venturi drive system located at the end of the process pipe. The gas is flared off along with propane to ensure a stable combustion of syngas. Gas delivery to the experimental sections occurs through 316 stainless steel or Incoloy 800H pipes in the very high temperature sections (after plasma preheat, the catalyst bed and catalyst exit sections). All pipes leading to these sections are heat traced with 40 Watt/foot single circuit Chromalox mineral-insulated heater capable of 480^{o}C operation and 1000^{o}C non-operational temperatures. The PLC controls temperature to set points subject to maximum individual pipe location limits. (i.e. the non-used bypass may cool while the very high temperature plasma exit gas flows from the system). This limitation was imposed by the heater

design and amperage parameters. Figure 5 shows the piping layout and indicates the locations of the key system elements.

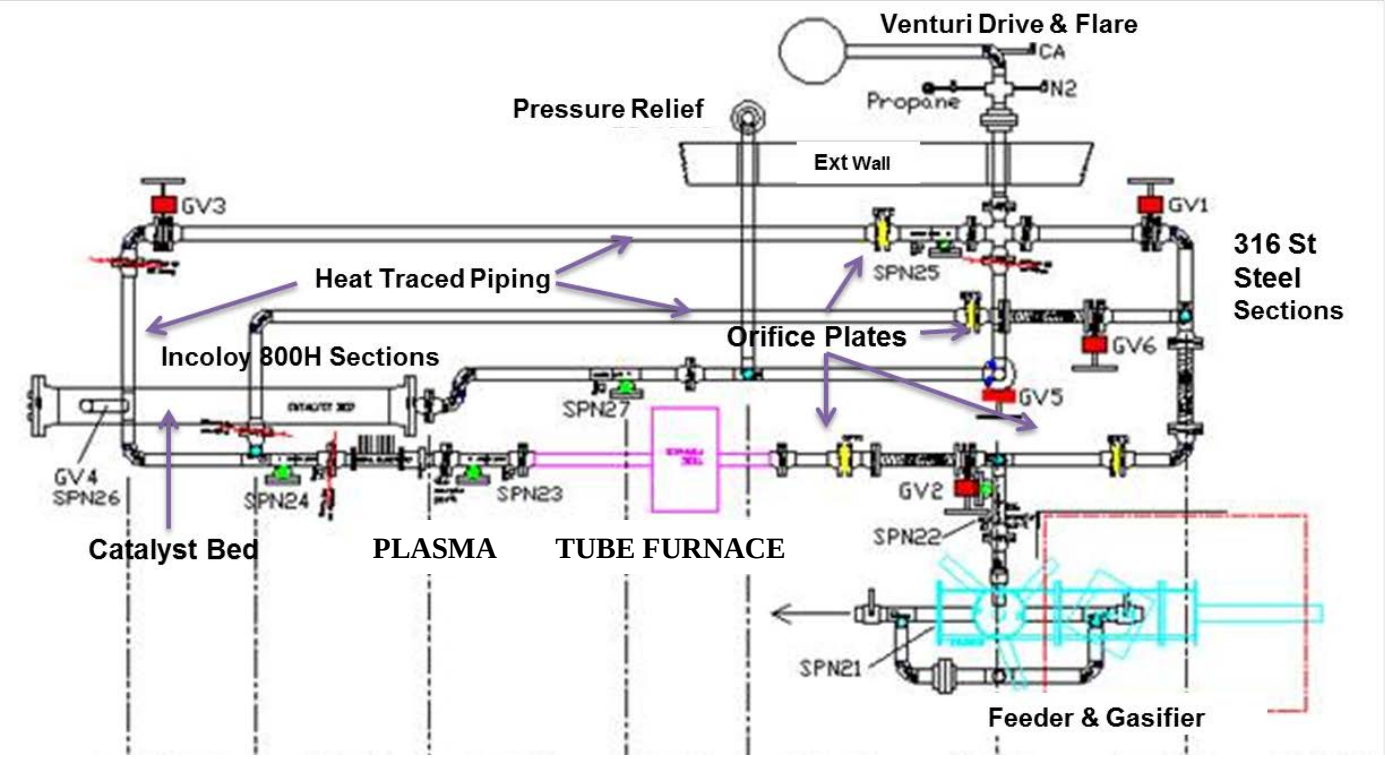

Figure 5. Piping Layout and Key System Elements for Gasification, Cracking and Sampling Experiments

For lighting and burn stabilization, gate valve 1 (GV1) is opened and all experiments are bypassed. To run the plasma, GV2 and GV3 are opened and GV1 is shut. To blend bulk flow with plasma GV6 is opened. To engage the catalyst bed GV4 and GV5 are opened, GV3 is shut.

Orifice plates are used to monitor flow through the various sections of piping. They are nitrogen inerted on the pressure sensor lines to prevent tar buildup in the orifice plate pressure sensor ports. The nitrogen lines have independent solenoids and flow controllers in order to maintain a nitrogen bleed that may be turned off when flow measurement is desired.

Figure 6 shows the overall utility gas flow diagram (for all the gases other than syngas). Nitrogen is provided to the feeder electric eyes, orifice plates, poker and pneumatic cylinder interface to keep tar from plugging and interfering with operation. The sampling ports have nitrogen valves to flood the GCMS entry ports so that air doesn't enter the port during sampling, which may affect the catalyst bed. Lastly, nitrogen is provided to the EPO system to quench the gasifier and the flare in the event of an emergency shutdown. The flare quench is designed to open and reduce air intrusion into the system in the event that the flare and venturi are lost. If the venturi were lost air can draw back into the process pipe creating an air fuel mixture that may ignite.

Hydrogen is used to activate the catalyst bed and Helium may be used as a tracer gas to get flow measurements and to determine dilution related changes after reformation.

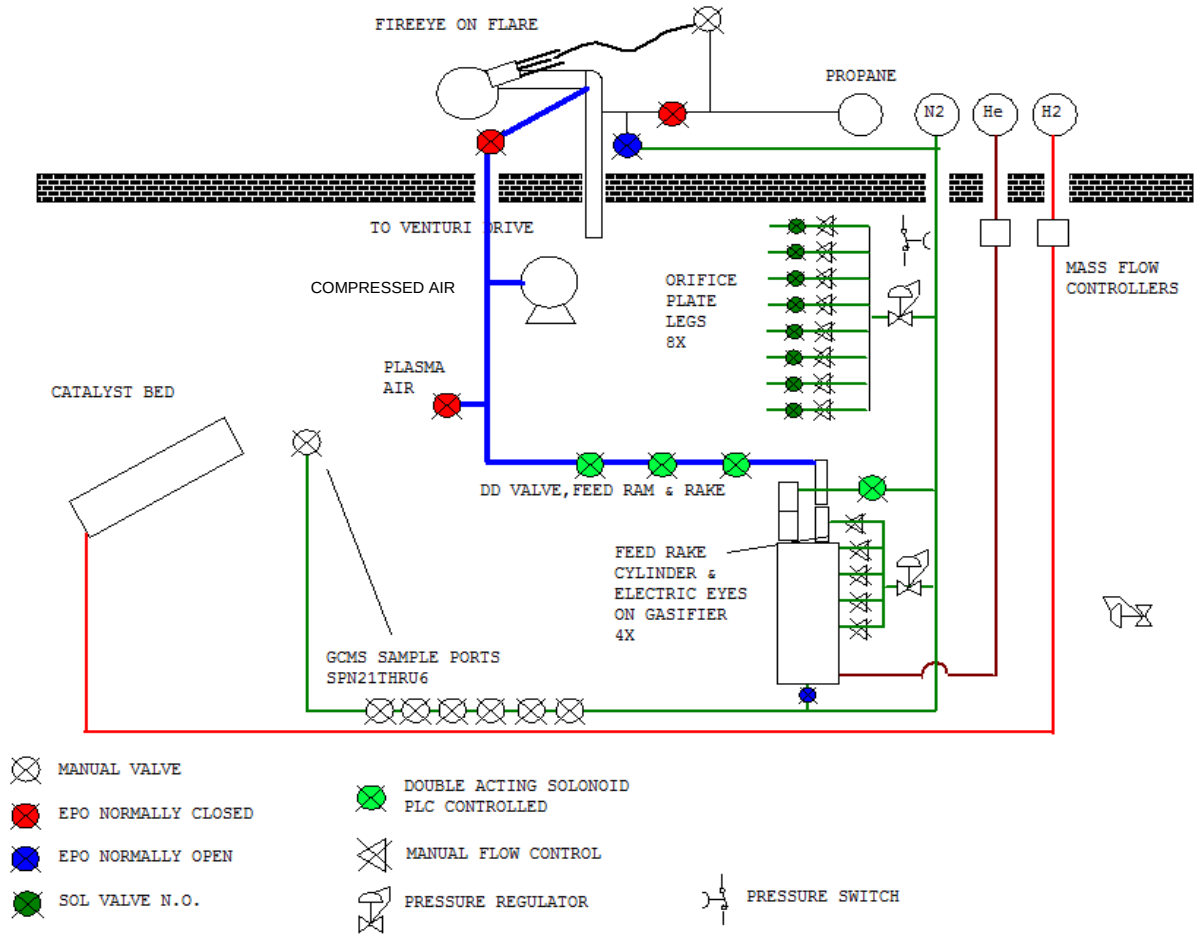

Figure 6. Gas Flow Diagram for Air, Propane, N2, H2, He

The nitrogen supply is a 40 gallon liquid reservoir with a 50 psi set point for the EPO system. Normal nitrogen use rate is minimal for the purge of the electric eyes and orifice plates.

Figure 7 shows the as built configuration prior to application of pipe heat tracing, orifice plate nitrogen purge, orifice plate pressure sensor lines and pipe insulation.

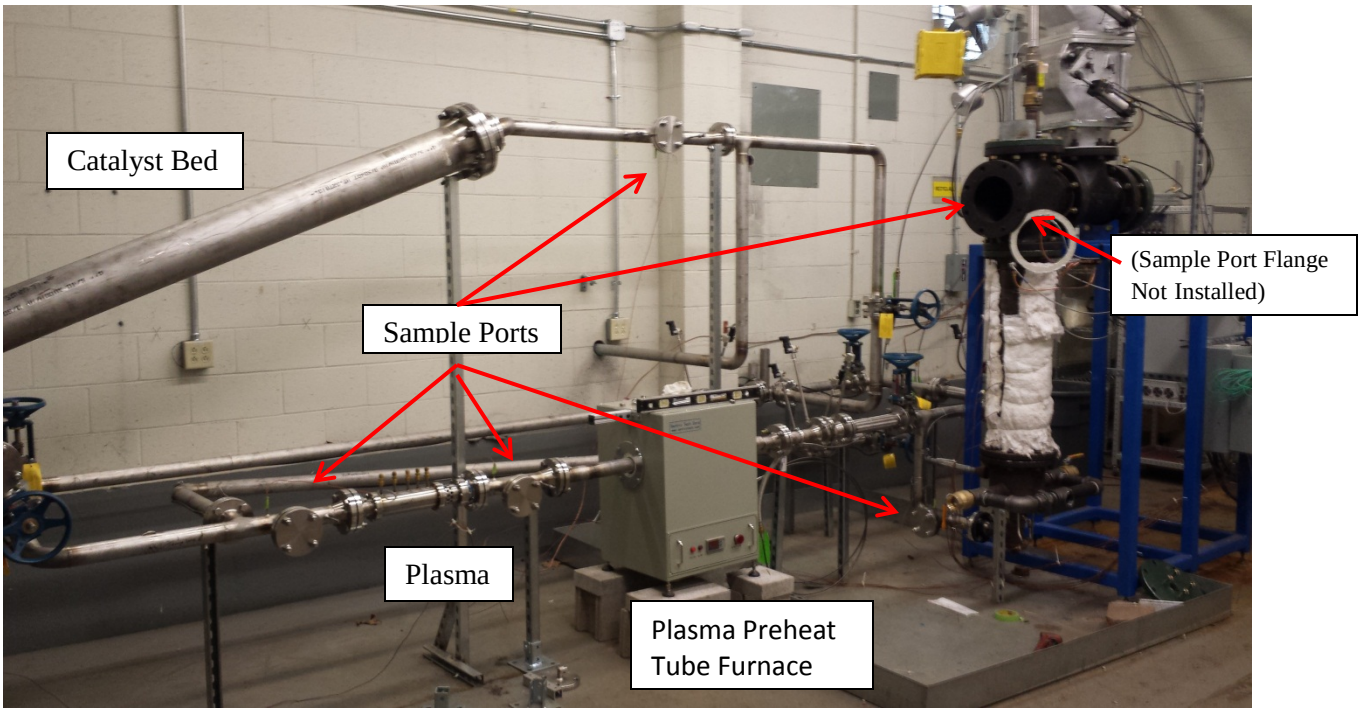

Figure 7. Stainless and Incoloy 800H Piping Installed with Plasma and Catalyst Bed, Orifice Plates and Sample Ports.

Figure 8 shows the orifice plate configuration. Solenoids control flow of nitrogen from flow controllers to keep the lines free of tar.

Figure 8. Orifice Plate Flow Meter (Under Insulation) with Nitrogen Purge and Solenoids to Shut off N2 Flow During Flow Measurement.

Figure 9 shows the GEK “Ejector Venturi” and swirl burner flare. A Fire Eye ™ igniter and flame monitor verifies the flare combustion process and is tied to the EPO system to prevent buildup of carbon monoxide and hydrogen should the flare go out. The Fire Eye utilizes plasma ion (fire) conductivity to verify ground and attempts re-ignition with a high voltage arc before initiating a shutdown process.

Figure 9. GEK “Ejector Venturi” Drive, GEK Swirl Burner and Fire Eye ™ Flame Monitoring an Active Flare Burning off Syngas

Technical Approach – Item 4 Plasma & Catalyst Experiments

The Non-Thermal “Gliding Arc” plasma system used is from Advanced Plasma Solutions. This system is shown in Figure 10 in cross section and as installed in the piping system with pre-plasma and post-plasma sampling ports that allow GC samples to be drawn through ¼ OD tubes and gravimetric tar samples through flanged connections.

This experiment uses the non-thermal gliding arc technology for tar reformation and to heat the syngas by using controlled combustion air. The plasma effluent is then blended with the bulk process gas flow to tailor the temperature for the catalyst bed where it is hoped that reformation can occur at lower overall temperatures.

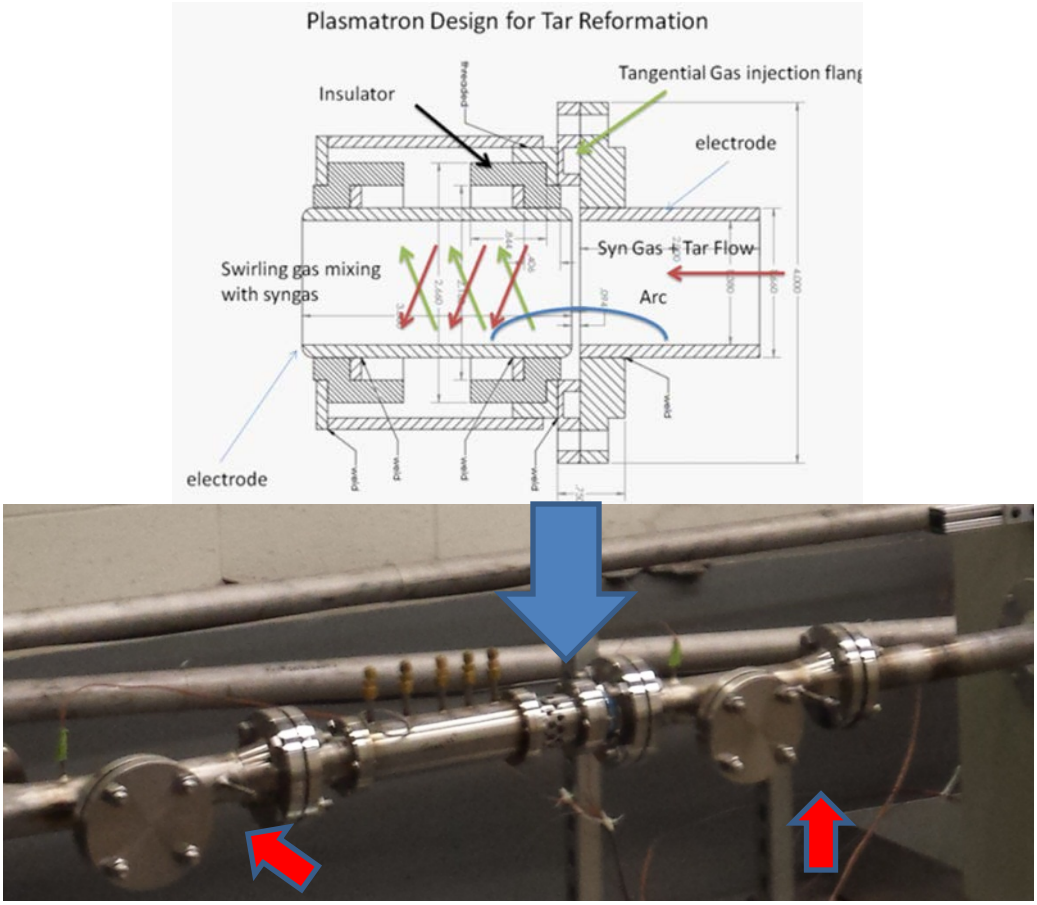

Figure 10. Non-Thermal "Gliding Arc" Plasma Shown with Pre-plasma and Post Plasma Sampling Ports.

During the design phase, the plasma manufacturer recommended that the gas feeding the plasma be preheated to 1000°C to minimize plugging and to facilitate reformation. This heating will have a negative effect on the energy balance. If the gas has to be at or near reformation temperatures as a result of electrical heating there may not be much to gain from an energy standpoint. For a future plant or overall system a gasifier redesign may allow direct chemical energy to provide this heat, which may be a net benefit, but for the purposes of this experiment the net energy balance effect would have to be negative.

Because of the 1000°C requirement, a Sentrotech tube furnace was procured and added to the system to maintain the gas feed to the plasma at the required temperature. The initial design had an alumina tube with a 3/8 OD tube planned to run through it. It was believed (and later verified) that the pressure drop would be too large for proper flow through this system. As a result an Incoloy 800H pipe was installed with flanges permanently welded into place directly upstream of the plasma. This can be seen as implemented in Figures 5 and 7.

Catalyst Experiment

The catalyst bed is shown in Figure 11. It consists of a 6' long 6" diameter Incoloy 800H pipe with three heating elements, each of which has 3 zones of independent temperature control for a

total of 8900W of total input power. A three point thermocouple runs through the center of the bed to monitor the temperature of the 3 zones. The first 4' of bed is filled with untreated ¼" alumina spheres. The last 2' has the nickel oxide coated spheres that can be activated by exposure to hydrogen at 850°C.

This work was done with non-activated (non-reduced) catalyst because NREL data suggests the catalyst is effective at reformation to benzene, toluene and xylene in a very poison tolerant manner. Follow-on work should be with hydrogen activation of the catalyst to produce higher CO and H_2%.

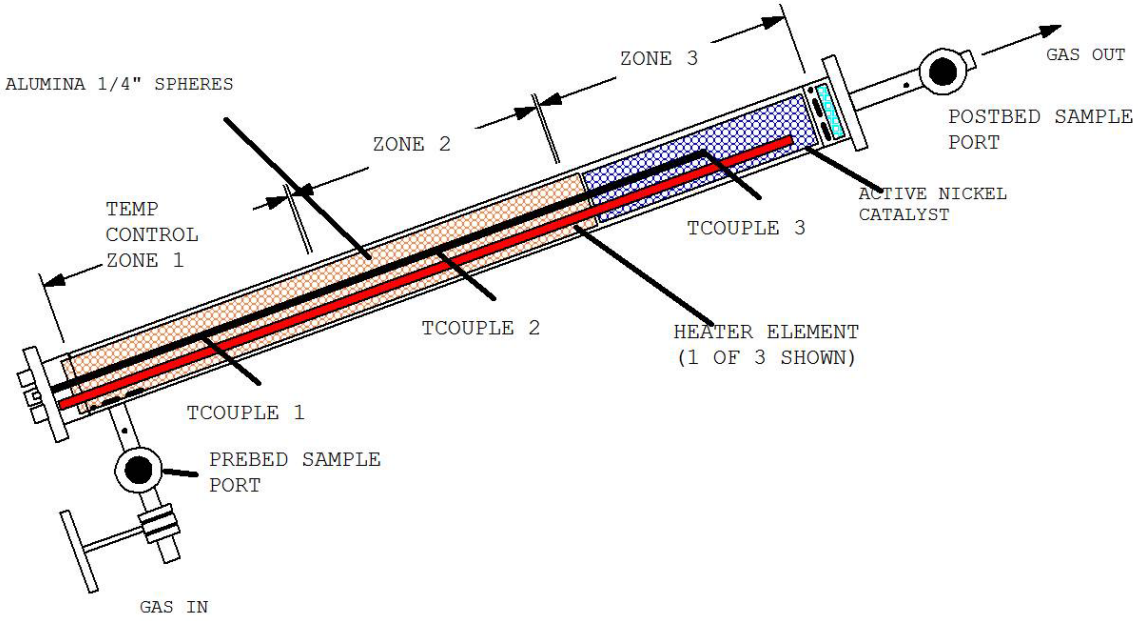

Figure 11. Catalyst Bed Cross Section at ~20° Angle

Figure 12 shows the as built system including the catalyst with all the insulation in place.

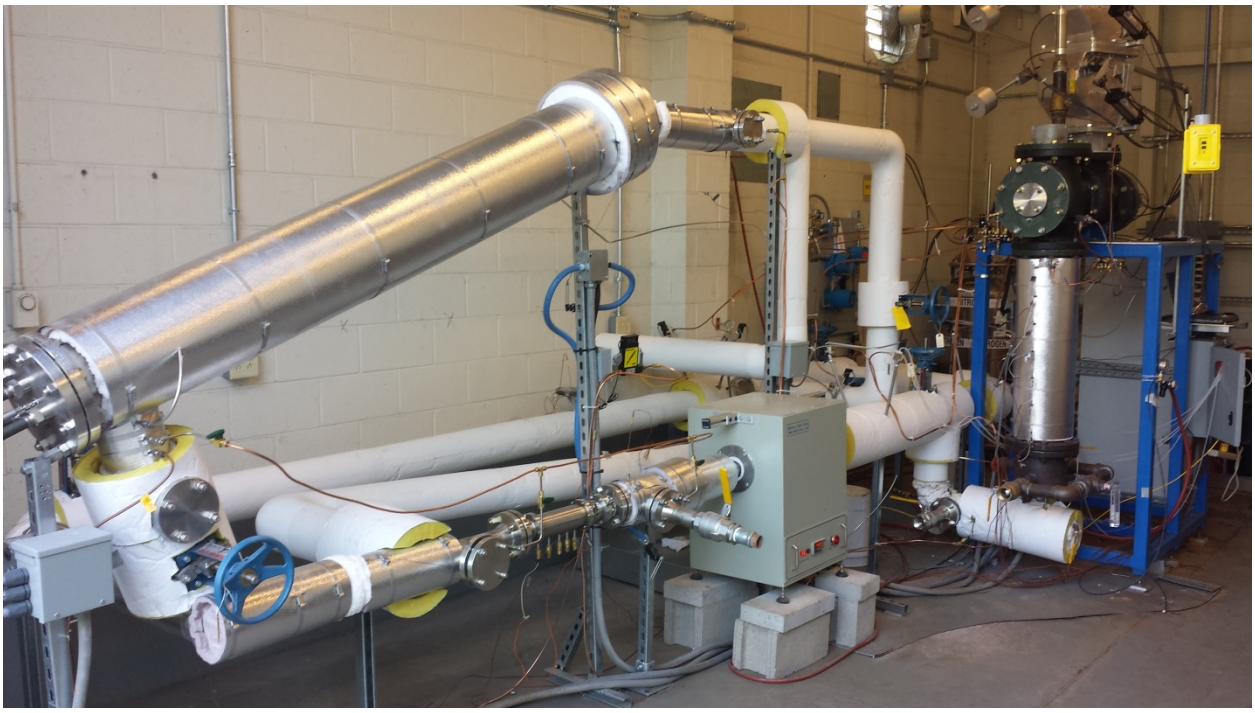

Figure 12. Catalyst Bed as Built with Insulation Applied to withstand 900 ^{o} C.

Technical Approach Item 5: System Control.

The pipe heat trace temperature control, catalyst bed heating, feeder control and EPO safety controls are all operated on an Allen Bradly 1763 Micrologix 1100 Series B Programmable Logic Controller (PLC) coupled with a 1762 -IQ16 expansion module for digital input and 1762-OB16 for digital output. A 1762-IT4 provides for 8 temperature inputs. The PLC drives the feeder using a Festo valve manifold using 3 independent air cylinders with 6 cylinder position sensors with a "pinch off" solenoid that allows incremental feeding as driven by the electric eye. The EPO is an independent circuit which monitors safety data, including: that the overhead door is open, the exhaust fan is on, the flare fire is burning, the exit from the high temperature zones (post plasma and post catalyst bed) is not over 900^{o}C (due to unplanned combustion of process gas), and that the nitrogen pressure is adequate for EPO conditions. If these conditions are not met, PLC executes a safe shutdown, including: the drive venturi air is shut off, the heating elements are all shut down and nitrogen purge of the gasifier takes place. The controller and software were partially developed under LM capital and SERDP funding. Figure 13 shows the completed system control panel.

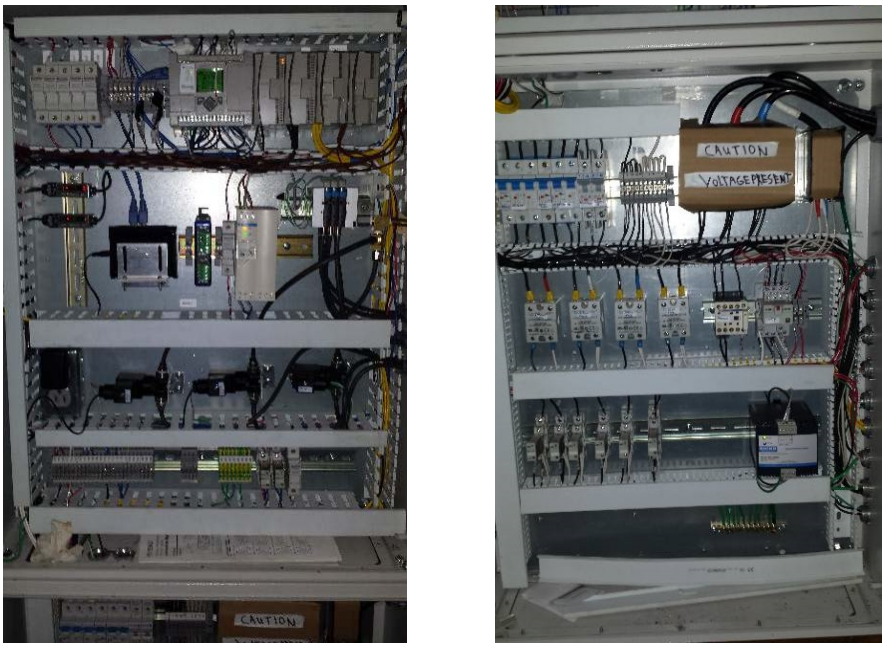

Figure 13. Control Panel

Technical Approach Item 6: Gas Sampling

The product gas sampling approach involves bubbling the process gas through a series of impinger tubes where glass beads perturb the flow and increase surface area for contact of gas and liquid. There are 2 types of product gas sampling based on the types of analysis to be performed. The first involves sampling for gas chromatography (GC) analysis. In order to streamline this work, the gas and tars are caught directly in the sample tubes that are usable by the auto handler of the GC. This method allows analysis of the gas and liquid phases from the same sample. The second involves use of larger impingers designed for longer sample times and accumulation of significant quantities of tars in the liquid phase (no gas analysis is involved). The goal of this work is to provide gravimetric (weight based) analysis of the tars to determine how much of the nonvolatile tars (nonvolatile at ~80°C) are in the gas phase at the particular point in the process.

Figure 14 is the standard sample port that allows both types of samples to be taken. It consists of a ¼” tube welded into the 2” process pipe for the GC work and a 2”open pipe flange to be used for the gravimetric analysis.

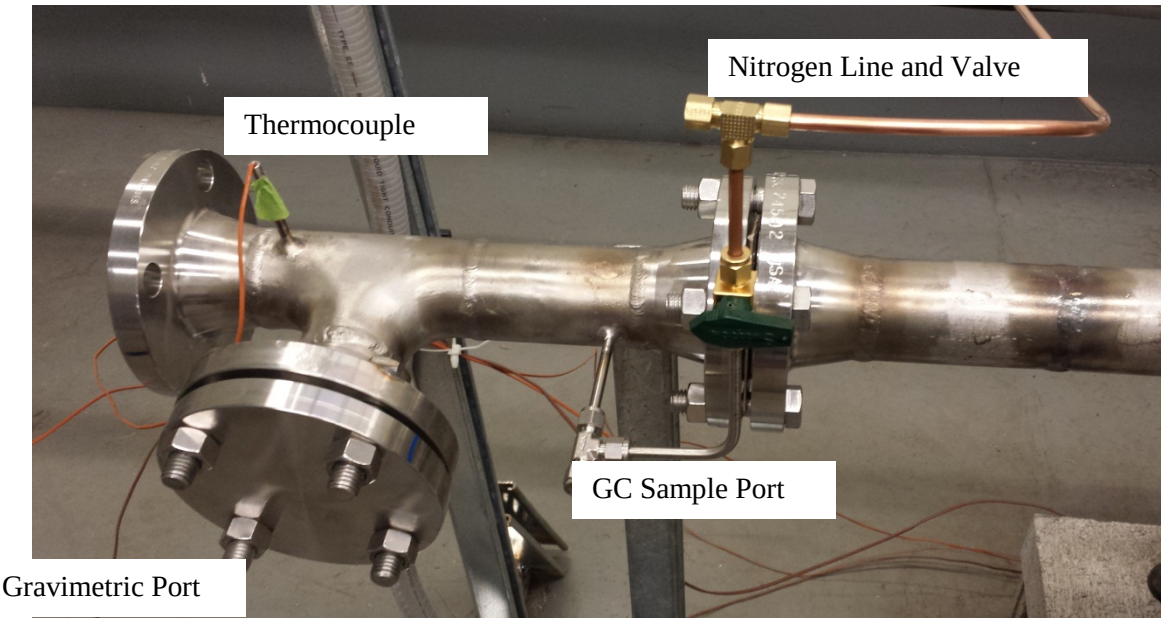

Figure 14. Gas Chromatography and Gravimetric Process Gas Sample Ports

The GC sample port has provisions to flood the port with nitrogen during removal of the compression tube fitting to prevent or reduce air intrusion during insertion of the sampling probe. This is critical during sampling upstream of a catalyst bed where air intrusion would deactivate the catalyst. The insertion process is to momentarily stop process gas flow, turn on the nitrogen flow, remove the compression tube cap, quickly insert the sampling tube until the sealing bead of high temperature putty seals against the compression tube fitting, and then to resume process gas flow.

Figure 15 shows the GC sampling apparatus. The six 20 ml tubes are filled with 8 ml of 0.023 – 0.033" glass beads and 10ml methyl chloroform to capture gas and liquid samples simultaneously. The first 3 tubes are room temperature; the last three are pre frozen in blocks of ice. The gas flows through the tubes as follows:

> Room Temp→Room Temp→Cold→Room Temp→Cold→Cold→Vacuum. This is in accordance with the principles of the European Tar Protocol. The warm tubes create vapor that condenses on the tar aerosol particles, increasing their diameter. These larger aerosols are then caught in the colder tubes more effectively.

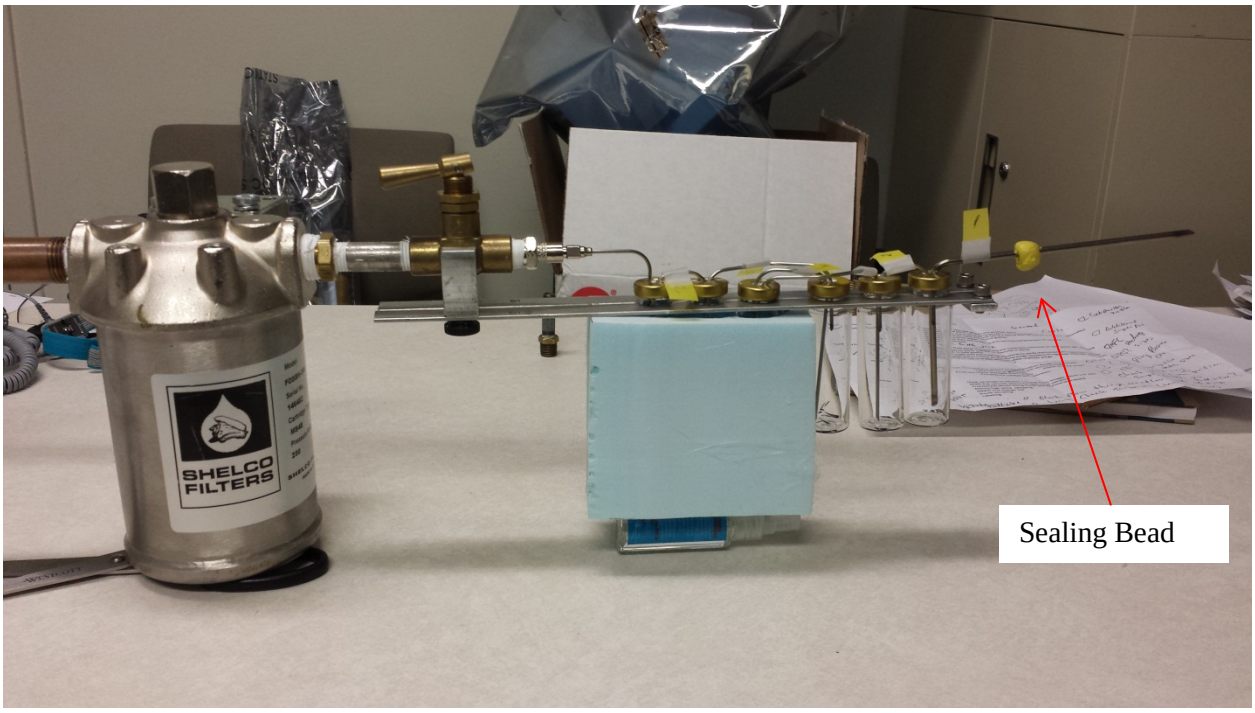

Figure 15. Gas Chromatography Suction Sampling Tool with Room Temp and Foam Insulated Ice Block Temperature Control

Figure 16 shows the path the gas takes through the room temperature then cold vials in the sampling apparatus in partial accordance with the European Tar Protocol.

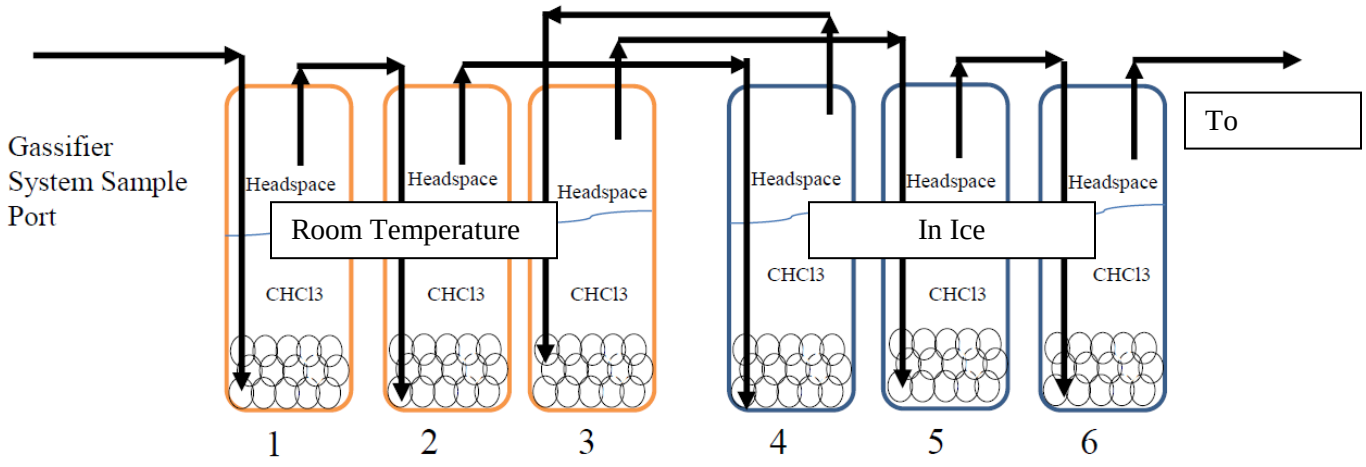

Figure 16. Path of Sample Gas through Vials Following European Tar Protocol

Figure 17 shows the GC capture system in operation with the vigorous bubbling action taking place during sampling.

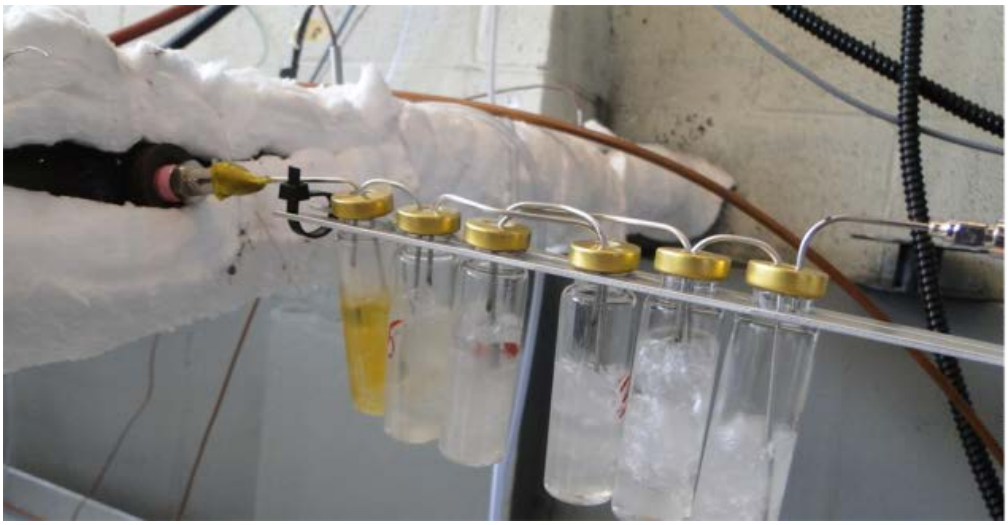

Figure 17. Gas Chromatography Tool Actively Sampling Tar Laden Syngas from a Process Pipe

Figure 18 Shows the resulting tar laden liquid samples that result from the sampling operation.

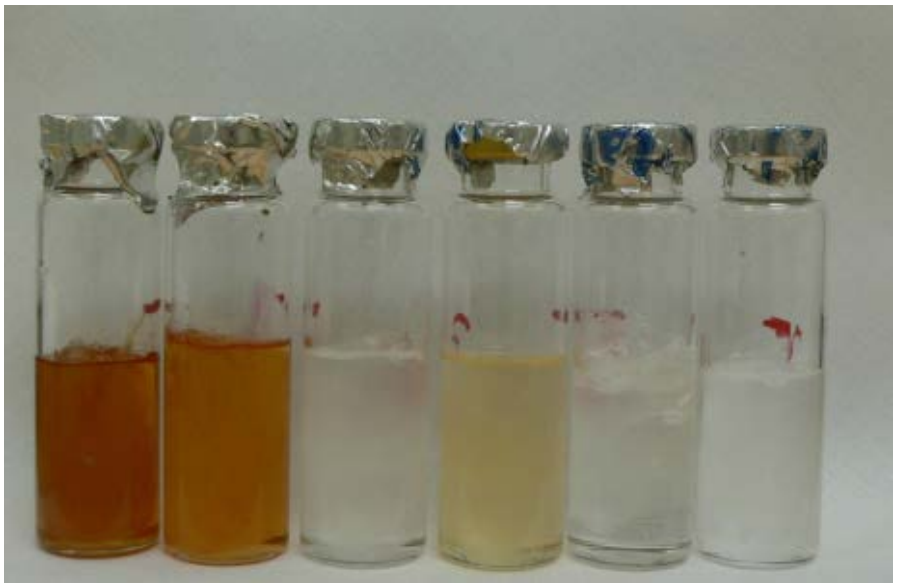

Figure 18. Gas Chromatography Tubes Visually Indicating Levels of Captured Tars in Solution.

Figure 19 shows the gravimetric sampling port in cross section. The as built system used a flanged fitting to allow transfer of a single sample port to multiple locations. The sampling is done through heated elements operating at about 125°C, per the European Tar Protocol, for pyrolysis or updraft gasification. This temperature is intended to prevent or minimize condensation while not being so hot as to thermally decompose the tars or allow them to react excessively. A collet creates a minimal air leak path while the ball valve is opened and the probe is slid into position. Once in position, the collet is tightened to prevent further air intrusion. The initial design had a heated particle filter that was to be washed out of captured particulates with the element pre-weighed and post weighed after washing. The filter canister delivered wasn't designed for a thimble type filter as necessary to perform this washing and it was agreed that the

labor hours necessary to perform this reflux washing didn't justify this type of measurement, particularly for updraft gasification where the there is little ash particulate in the output stream.

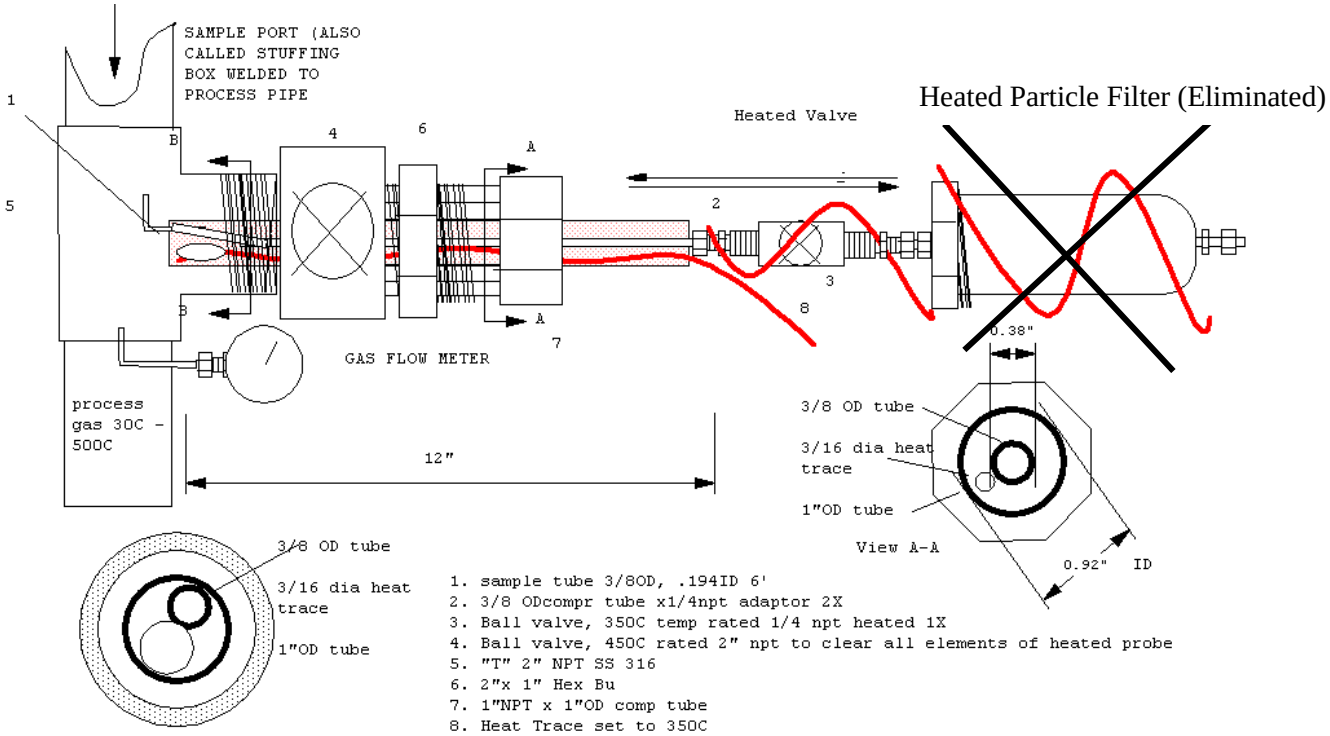

Figure 19. Heated Gravimetric Tar Sampling Probe.

Figure 20 shows the actual heated probe along with the airlock system of the 2" ball valve and collet that allows the probe to slide into the process stream with minimal air intrusion.

Figure 20. Heated Gravimetric Sampling Probe and Flanged Airlock

Gas flow for gas chromatography and gravimetric tar sampling is controlled and measured by the same precision flow bench shown in Figure 21.

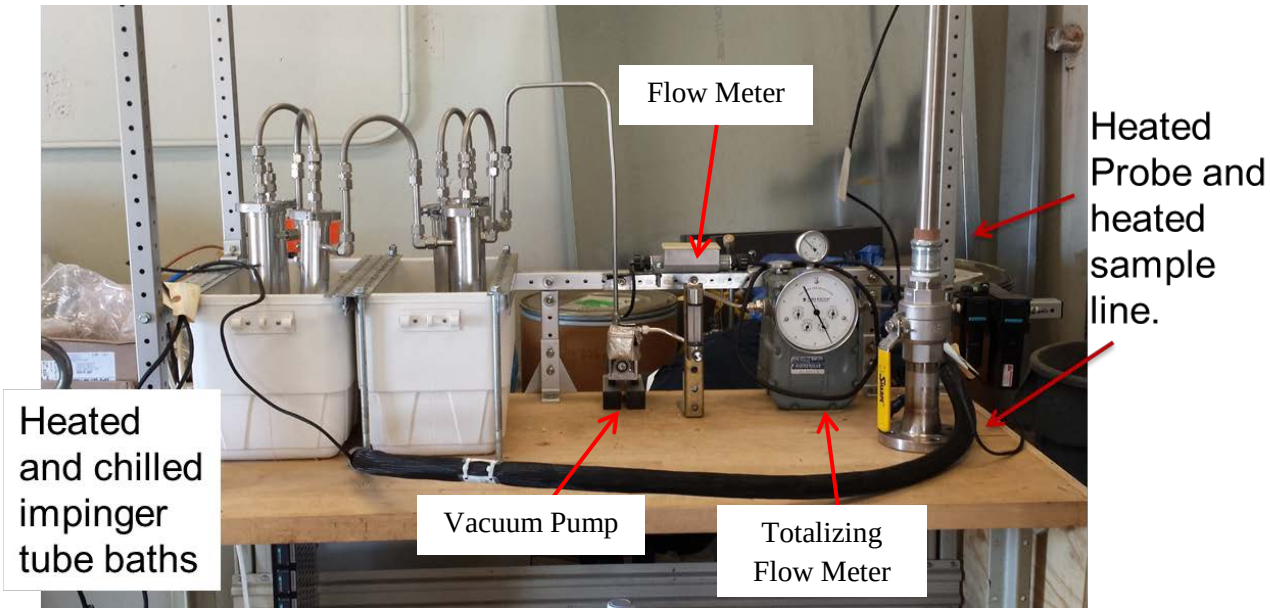

Figure 21. Vacuum Flow and Measurement System for Gas Chromatography and Gravimetric Tar Sampling

The impinger tubes for gravimetric sampling are 15.5”L X 2-7/8”ID stainless steel filled with 100 ml of isopropyl alcohol and 100 ml of glass beads. The totalizing flow meter is an American Meter DTM 115-3. The start and stop of each run is recorded.

Figure 22 shows use of the probe being inserted for sampling downstream of the catalyst bed.

Figure 22. Heated Probe and Sampling Line for Drawing Tar Laden Syngas from Downstream of the Catalyst Bed. (Valve Heater for ¼ NPT Valve not Shown.)

When switching from gravimetric to GC sampling, the compression tube connection to the vacuum pump is removed and a flexible stainless line is connected to the vacuum pump. The other end of the line contains a Luer Lock ™ or equivalent 0.051" needle that punctures the septa on the last vial of Figure 17 to draw gas and tar through all 6 sample vials. GC sampling is done at1/10th liter per minute, while gravimetric tar sampling is done at 3 liters per minute.

Technical Approach Item 7: Gas and Liquid Characterization.

Once samples are taken they are processed according to type.

For gas chromatography, needles are pulled from the sample vials and vials are capped with aluminum foil tape to reduce loss of hydrogen. There is a technical concern that since the gasification system runs at vacuum and the samples are drawn by means of a higher vacuum, the sample tubes have an inherent residual vacuum that may draw air in over time and/or create a vacuum in the GC sampling needle after extraction from the vial. In either case, the result will be air intrusion into the vacuum samples.

Samples are loaded into an auto handler on the Shimadzu QP 2100 Gas Chromatography (GC) system that allows unattended operation of the system (some runs take 20 minutes or more for the larger molecules to travel through the 30 meter long column). The system is first used to analyze the headspace of the vials to characterize and quantify the gas with Thermal Conductivity Detection (TCD) and a Porous-Layer Open-Tubular (PLOT) column that separates gases effectively using argon as the carrier gas. After the gas phase samples are processed, the column is changed out in the injection port and the liquid samples are taken from the same vials (again, the runs are 20 minutes or more for each sample). This time, the samples go to a Flame Ionization Detector (FID) to determine chemical composition. The system is also capable of

Mass Spectroscopy (MS) where the molecules are ionized and then accelerated by magnetic fields and smashed into a detector. The location of impact (or impacts of fragments) is related to mass of the molecule (or fragments).

Figure 23 is the Shimadzu QP 2100 GCMS, GCTCD, GCFID with the auto handler system capable of running 32 samples at a time.

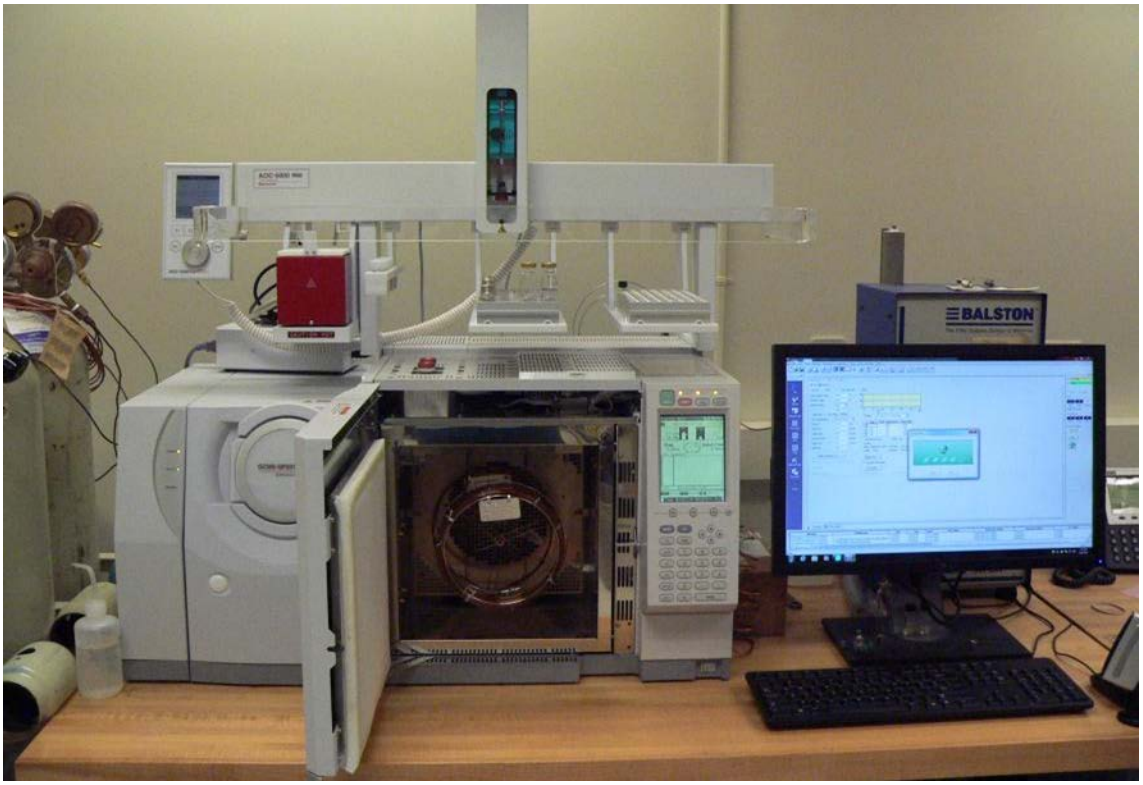

Figure 23. Shimadzu Gas Chromatography Apparatus with PLOT and Siloxane Columns in Chamber Capable of Mass Spectroscopy (MS), Thermal Conductivity Detection (TCD) and Flame Ionization Detection (FID).

Before gas chromatography results could be obtained a great deal of background work had to be done to establish methods for MS, FID, and TCD (for the permanent gases) and calibration curves for several of the target tar molecules including methanol, ethanol, isopropyl alcohol, benzene, toluene, xylene & phenol. Table 1 summarizes the method used for the generation of the gas phase sample data.

Table 1. Headspace Method for Gas Chromatography Thermal Conductivity Detection

- System Configuration
  - Shimadzu GC-2010
    - Injection Port: 200°C
    - Carrier Gas: Argon (Ar) Primary Pressure 500-900kPa
    - Flow Control
    - Automated Flow Controller (AFC-2010)
    - Mode: Velocity

- Pressure: 43.9 kPa
- Total Flow: 14.6 mL/minute
- Column Flow: 1.14 mL/minute
- Linear Velocity: 20 cm/second
- Purge Flow: 2.0 mL/minute
- Split Ratio: 10.0

- Detector
  - Thermal Conductivity Detector (TCD)
  - Temp: 230°C
  - Sample Rate: 40msec
  - Current: 25mA
  - Makeup Gas: Ar
  - Makeup Flow: 3.0mL/minute
- Auto Sampler
  - AOC 5000
  - 2.5mL Heated Injection Needle
  - Sampler Method: 50C needle temperature
    10minute 50C incubation bath prior to injection
- Column
  - Type: Carboxen 1010 PLOT
  - SN: 49437-01A
  - Length: 30.0m
  - ID: 0.32mm
  - Max Temp: 250C
- Method Profile
  - Initial Column Temp: 35C
  - Injection Volume: 1500uL
  - Injection directly from incubation bath
  - Hold 35C for 7.5minutes
  - Ramp to 230C at 24C/min
  - Hold at 230C for 9.38min
  - Total Program time = 25minutes
  - 10minute 50C incubation bath prior to injection

Table 2 summarizes the methods used for analyzing the liquid tar samples GC/FID.

Table 2: Liquid Method for Gas Chromatography, Flame Ionization Detection

- System Configuration
  - Shimadzu GC-2010
    - Injection Port: 200C
    - Carrier Gas: Argon (Ar) Primary Pressure 500-900kPa
    - Flow Control: Automated Flow Controller (AFC-2010)
    - Mode: Velocity
    - Pressure: 112.9 kPa
    - Total Flow: 87.1 mL/minute
    - Column Flow: 4.00 mL/minute
    - Linear Velocity: 33.1 cm/second
    - Purge Flow: 3.0 mL/minute

        - Split Ratio: 20.0
    - Detector
        - Flame Ionization Detector (FID)
        - Temp: 250C
        - Sample Rate: 40msec
        - Current: 25mA
        - Makeup Gas: Ar
        - Makeup Flow: 8.0mL/minute
        - H2 Flow: 50.0mL/minute
        - Air Flow: 500.0mL/minute
    - Auto Sampler
        - AOC 5000
        - 2.5mL Heated Injection Needle
        - Sampler Method:
        - 50C needle temperature
    - Column
        - Type: RTX-502.2
        - SN: 446197
        - Length: 75.0m
        - ID: 0.45mm
        - Max Temp: 300C
    - Method Profile
        - Initial Column Temp: 100C
        - Injection Volume: 2uL
        - Injection directly from incubation bath
        - Hold 100C for 24minutes
        - Ramp to 150C at 50C/min
        - Hold at 150C for 5min
        - Total Program time = 30minutes

Table 3 documents the GCMS method for the liquid tars from the samples captured in the liquid phase of the vials.

Table 3: Liquid Method for Gas Chromatography, Mass Spectroscopy

- System Configuration
    - Shimadzu GC-2010
        - Injection Port: 200C
        - Carrier Gas: Helium (He) Primary Pressure 500-900kPa
        - Flow Control: Automated Flow Controller (AFC-2010)
        - Mode: Velocity
        - Pressure: 73.0 kPa
        - Total Flow: 22.0 mL/minute
        - Column Flow: 1.00 mL/minute
        - Linear Velocity: 37.2 cm/second
        - Purge Flow: 1.0 mL/minute
        - Split Ratio: 20.0
    - Detector

  - Mass Spectroscopy (MS)
  - Ion Source Temp:300C
  - Interface temp = 285C
  - Solvent cut Time: 2.5min
  - Start Time: 2.5min
  - End time 35 min
  - Scan speed: 666
  - Event Time: 0.50
  - Start m/z: 40.0
  - End m/z: 350.0
- Auto Sampler
  - AOC 5000
  - 10uL Injection Needle
  - Sampler Method:
  - 2.0uL injection
- Column
  - Type: SHRXI-5MS
  - SN: 1059287
  - Length: 30.0m
  - ID: 0.25mm
  - Max Temp: 330C
- Method Profile
  - Initial Column Temp: 100C
  - Injection Volume: 2uL
  - Hold 100C for 5minutes
  - Ramp to 300C at 20C/min
  - Hold 17.5 min
  - Total Program time = 35minutes

Lastly, GCFID calibration curves had to be developed for several of the target tar molecules including methanol, ethanol, benzene, toluene, xylene, naphthalene & phenol. Figure 24 shows the calibration curve results where samples at 2500, 5000 and 10000 ppm were used to calibrate the systems sensitivity levels. A “check standard” with all of the materials at 7500 ppm was injected and as can be seen the results correlated very well with each of the standard chemicals coming out in the 7500ppm range.

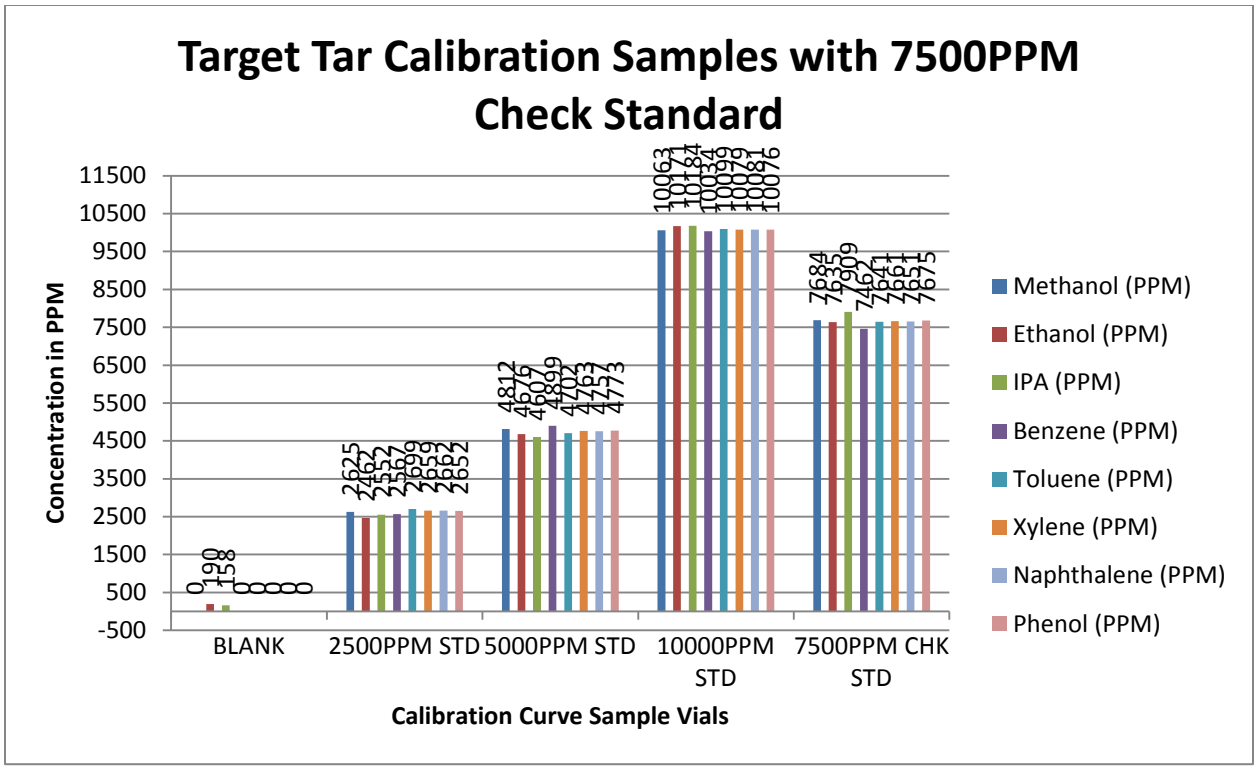

Figure 24. Calibration Curve Results

Gravimetric Tar Samples were handled as follows: The six impingers were opened, drained and rinsed into a brown glass bottle through a funnel to separate out the glass beads. The heated sample line and probe were rinsed into the same brown bottle until the liquid ran free of amber color. The sample was then placed in a rotary vacuum evaporator to determine solids content in accordance with the European Tar Protocol. Figure 25 shows the rotary evaporator in cross section and in physical embodiment.

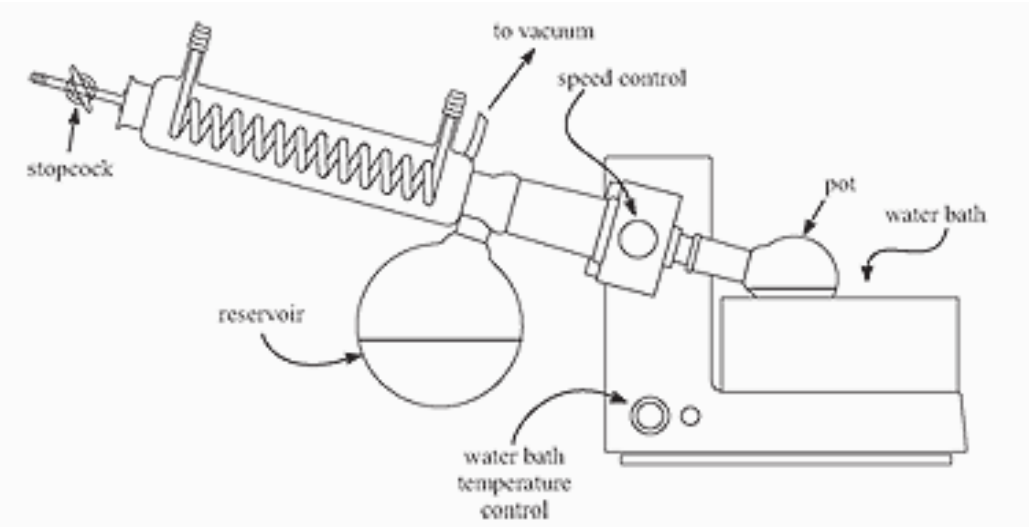

Figure 25. Cole-Parmer Rotary Vacuum Evaporator

Technical Approach Item 8: Process Gas Temperature and Flow Measurement

The temperature and flow measurements were taken with an All Power Labs Process Control Unit (PCU) as shown in Figure 26. This is an Atmel AVR processor with Arduino software and firmware operating on it. The board has 16 thermocouple inputs and 5 pressure sensors for the orifice plates.

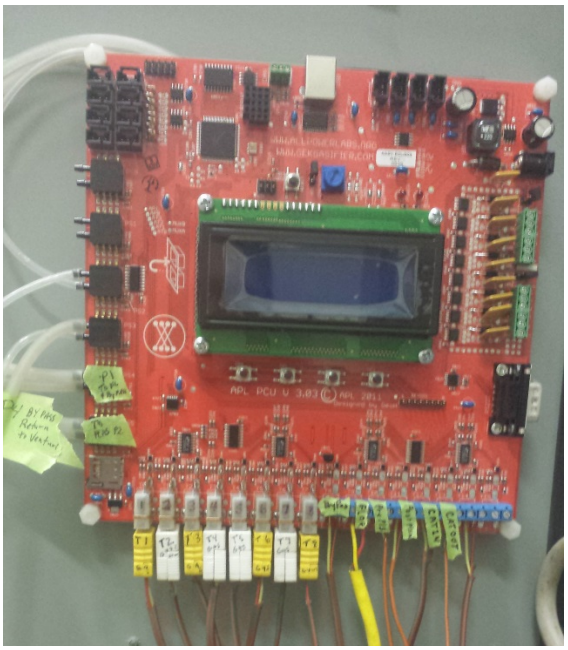

Figure 26. All Power Lab Process Control Unit Arduino Board.

The PCU device communicated to a laptop computer via USB output. A Smarterm™ terminal emulation program allowed the device to communicate to an Excel program to allow run and data accumulation real time. Figure 27 contains the graphical user interface showing the trending temperature data along with the real time data shown on a top and side view graphical representation of the system, Figure 28.

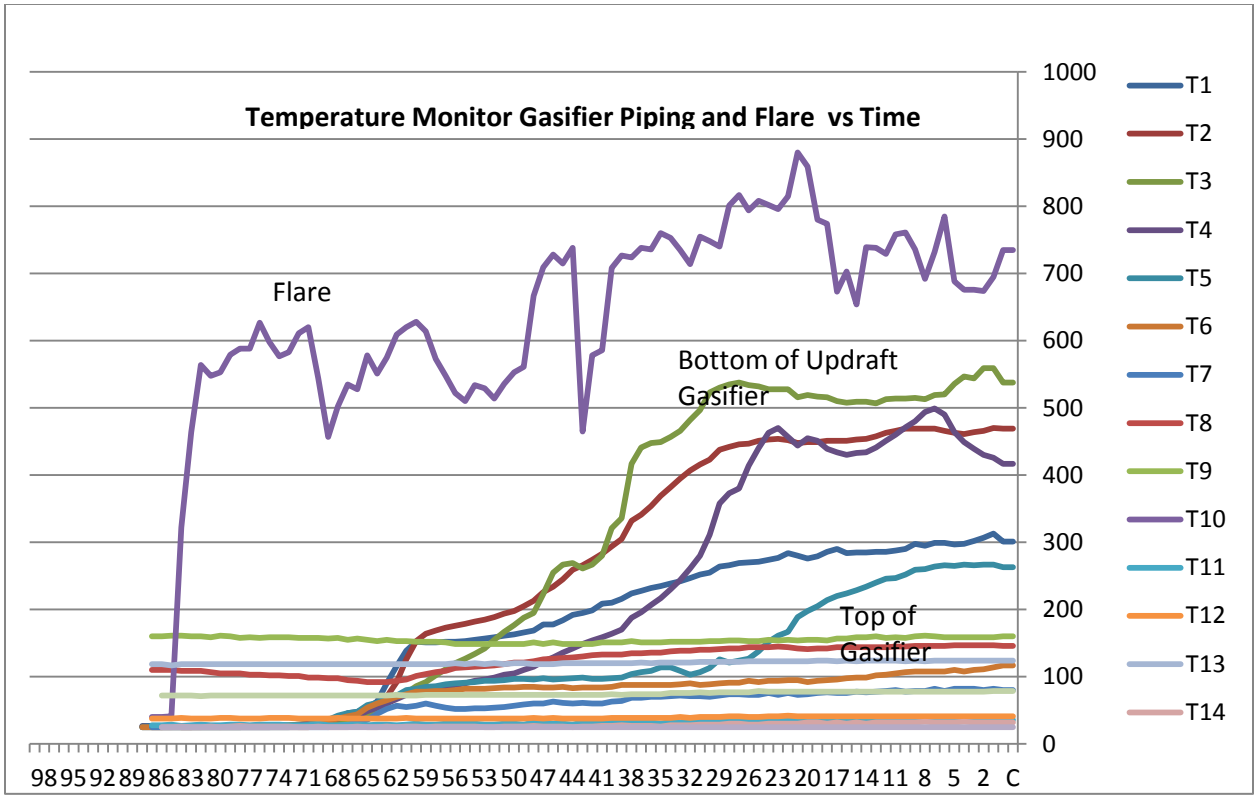

Figure 27 Trending Temperature Readings as Measured by the Arduino Board and Recorded by the SmartTerm™ and Excel™ Interface

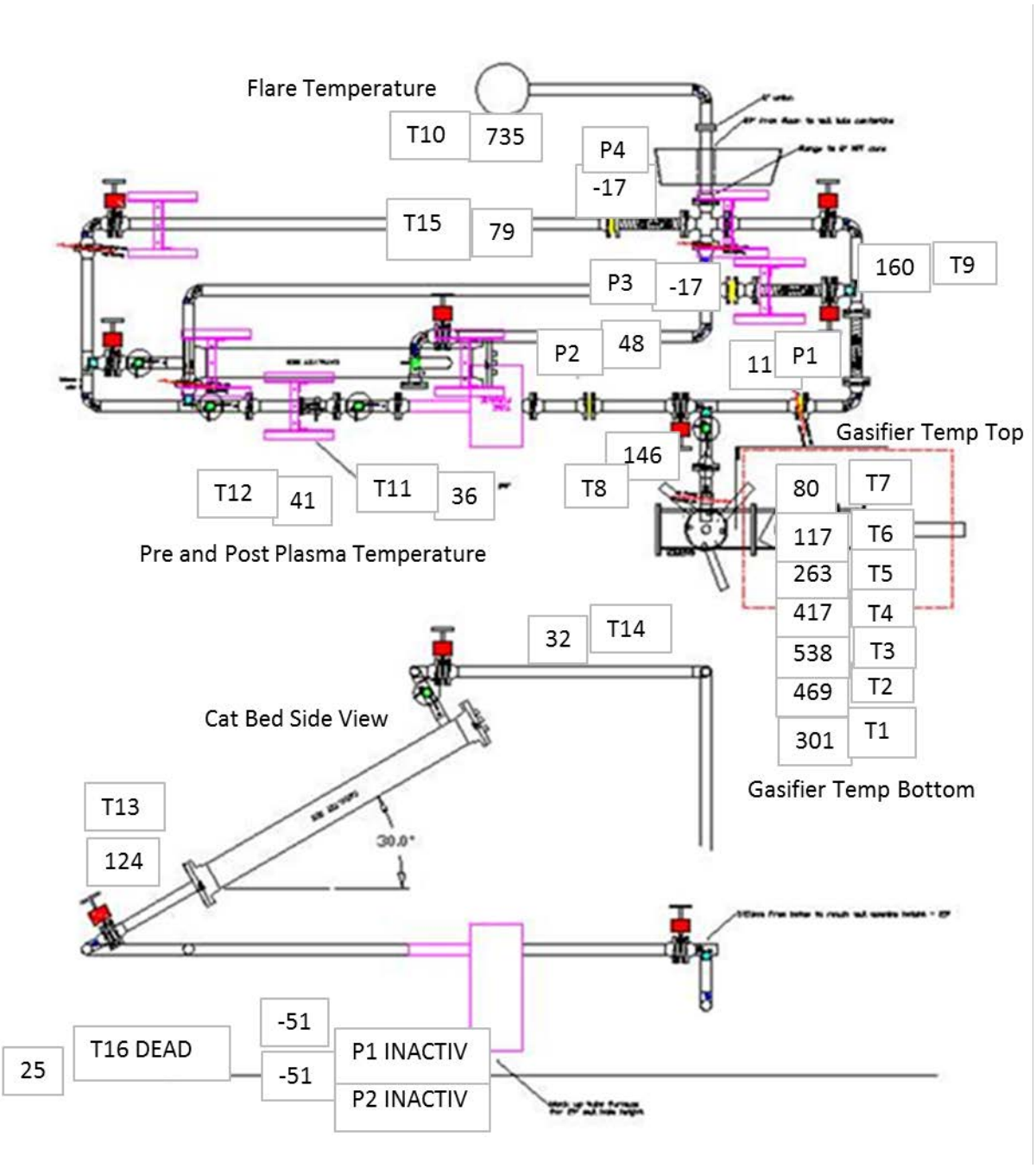

Figure 28. Real Time Temperature and Pressure Data as Presented in Excel™ Spreadsheet on Data Logger PC.

Integration and Operation Issues Lessons Learned

This project involved integration of many technologies and provided engineering challenges from the beginning. In the order of Technical Approach Items listed above the lessons learned and problem solutions were as follows:

Feeder and Gasifier Issues Lessons Learned

The feeder worked flawlessly on woodchips, however when the mix of shredded paper, plastic and dog food was added, it became evident that the shredded material had a different angle of repose and would not drop freely into the gasification chamber, binding up against the down flow pipe. A multi-forked poker was added with a drive cylinder to force the material down the infeed side of the pipe while pushing some to the opposite side of the gasifier. Figure 29 shows the feeder and gasfier with the pneumatic poker added.

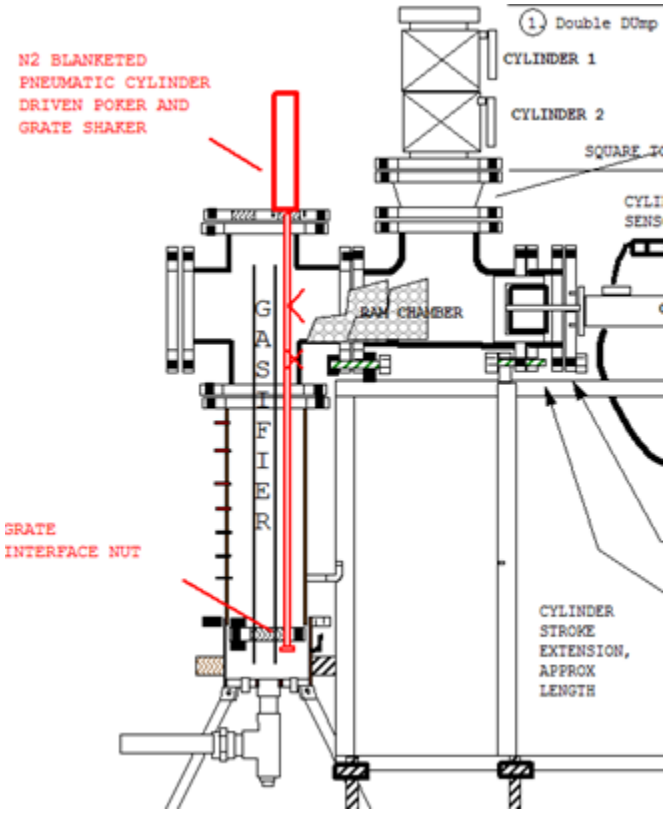

Figure 29. Gasifier and Feeder Showing Addition of Poker/Grate Shaker and N2 Blanketed Pneumatic Cylinder.

To automate grate shaking and ash flow, the design was modified so that the poker rod penetrated the burning pile and interfaced with the grate. A nut was placed on the end of the rod and when fully retracted would “bump up” the grate to knock ash to the bottom of the gasifier. The PLC was reprogrammed to operate this poker at varying stroke frequencies with movement speed controlled by cylinder speed controls. The head of the cylinder was sealed to the top gasifier flange and packed with glass fiber and then nitrogen blanketed to keep tar out of the cylinder.

The nitrogen blanketed electric eyes worked on wood chips, seeing through the smoke with gain adjustments. However, when operated on paper, shreds of tar-coated paper eventually blocked the holes and rendered them nonfunctional. This led to feeding with the poker operating continuously, at 1 stroke every 10 seconds. The ram would be cycled about every 2 minutes and fresh feed would be added when the ram was able to complete a forward stroke.

This worked well during a run that was intended to include the plasma and catalyst, but then the temperature began to drop in the combustion area, implying instabilities in the burn. It was discovered that a bridge had occurred and the upper portion of the gasifier had completely plugged with feed. Figure 30 shows inside the top of the gasifier after a normal run and after the overfill condition.

Figure 30. Gasifier Feed Entry and Down Flow Pipe after Normal Run and after Overfill Condition

During a normal run, the feed at the entry forms a plug that prevents tar from entering the feed ram and double dump valve mechanism. The slight amber colored feed can be seen in the left view of Figure 30. It also should be noted that jacking bolts were used to tip the entire gasifier and feeder assembly forward, as it was found that condensed tar was pooling under the feed and running back towards the feed ram.

The bridge and plug problems may have been able to be solved with a second automated poker/bridge breaker, but schedule and funds mandated that this would remain a manual operation. At 15 minute intervals a plug was pulled from the top gasifier flange and a 3/8" x 4' rod was rammed down the hole to stir the feed, break bridges and force feed into the combustion zone on the side opposite the poker. This cannot be done during active sampling or during runs involving the catalyst bed because this adds oxygen to the syngas flow leaving the top of the gasifier.

Heat Trace Lessons Learned

The mineral insulated heaters were rated to 480^{o}C operational temperature. They were clamped to the pipe with stainless steel worm gear hose clamps at regular intervals and fastened to valves and flanges as effectively as possible while maintaining a 3" minimum bend radius. Thermocouples were fastened to the elements at 2 locations to provide element failure protection at set points of 400^{o}C. With these set points, the controller registered near continuous duty cycle

and maintained a pipe temperature of 180^{o}C. With this temperature, per literature, it was expected that most of the tars would remain in gas phase and transfer through the pipe while not reacting too quickly. Figures 31 and 32 somewhat confirm the tars are indeed transferring, but certainly imply tar loss or condensation could be occurring along the experimental apparatus. Figure 28 shows the liquid that had condensed near the updraft-down flow gravimetric tar sampling flange and poured out upon disassembly.

Figure 31. Condensed Tar that Ran Out of Sampling Port Upon Disassembly.

Although it is good that the tar was getting to the sampling point, because it was condensing on the flange, all of the available tar was not making it into the sampling port which detracted from data accuracy.

Figure 32 shows a “stalagmite” of tar that collected from a leak near the flare directly downstream of the venturi drive system.

Figure 32. Tar Dripping and Hardening at the Flare

Although it is obvious that the tar is transferring to end of the process flow, it is not known whether it is transferring in the gas or liquid phase (or both). The tar-laden gas may be cooling and condensing tar upon contact with the expansion cooled venturi air. Later in the results section, this material's chemical analysis, solubility in renewable JP-8 and utilization potential is discussed.

Leak Lessons Learned

Significant leaks were addressed in the system, requiring some pipe welds to be reworked, the top flange system to be tightened, the double dump flapper valve rod packing glands to be tightened, RTV and a Teflon release liner to be added to the dump valve surfaces, large weights to be added to increase the closing force, and the ram cylinder to be sealed to the feeder flange with RTV. Even with these in place, when the air pressure is turned on with all valves shut, it was still difficult to get even a few psi pressure rise at flow rates approaching normal operating conditions. The safety blow offs may leak and contribute to the problem, but leak locations could not be identified with ultrasonic leak detectors or pressurized smoke bomb experiments (some were identified with smoke tests and fixed). Most sampling runs show O2 gas in effluent from the gasifier. As discussed in results section this may be due to vacuum extraction of samples from a process running at a vacuum.

A number of leak experiments were run using a flanged test jig shown in Figure 33 and a heat treat oven to expose the gasket to the temperatures involved in conditions matching the process temperatures.

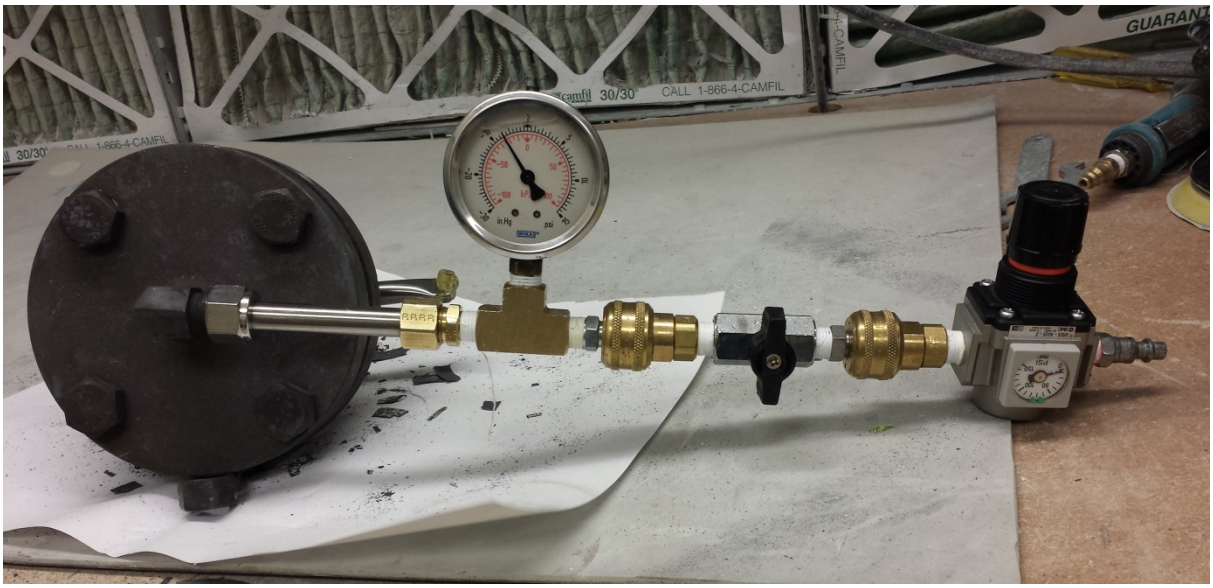

Figure 33. Test Fixture for Verifying Gasket Performance at High Temperatures

Table 4 shows the test matrix and results of testing.

Table 4. High Temperature Gasket Material Test Results

Gaskett Type	Sealant	Result	Post Heat Treat 1200F	Comment
Metal Faced	None	Leak		Head Gasket Material
Metal Faced	Hi Temp RTV	Pass	Leak	RTV Burns out with time
Metal Faced	Copaltite	Pass	Leak Minimal	Burns out som material left
Ceramic	None	Leak		Fibrous material
Ceramic	Firebrick Mortar	Pass	Leak - Minimal	Mortar is brittle
Ceramic	Pyroputty ™	Pass	Leak	Organic Burns out
Ceramic	Deacon 8875™	Pass	Leak	Organic Burns out
Ceramic	Copaltite	Pass	Leak Minimal	Organic Burns out
Spirowound Graphite	None	Pass	Leak	Graphite Burns out
Spirowound Cogebi	None	Pass	Leak Minimal	Fastener Stretching at Temp

After much work with proprietary high temperature sealants which weren't effective, it was determined that Spiro wound Monel and Cogebi gaskets would be used. Even these were not perfect after high temperature exposure. Stainless steel bolts were used throughout the system and in the test fixture. High strength steel bolts may have provided more high temperature creep resistance. In the interest of moving forward gaskets were installed and the system was insulated. High temperature RTV and the metal faced gaskets were used in many of the lower temperature locations and on the sample port flanges which were not insulated or exposed for a very long time. The process valves used were gate valves with compressed glass packing. During the seal testing, it was observed that compressed fibrous materials did not form a tight seal.

Plasma Lessons Learned

The plasma as described above was originally intended to take 200-400°C gas from the gasifier, add swirl gas air and reform the syngas stream while combusting some of the stream to heat the bulk process flow. The goal was for blending to occur immediately after the plasma, resulting in 750^{o}C gas for optimal catalyst bed activity. It was noted that flow through the plasma was greatly diminished when everything was up to temperature. The reason for this was unclear. It could be volume heating plus reformation in the 1000^{o}C tube furnace or it could be combustion taking place in the tube furnace when coupled with stray oxygen also leading to an increase in the number of gas molecules. The system was run with flow through the plasma for approximately 2 hours while gas and tar samples were taken upstream of the plasma on 8-14-14. Downstream samples were also being taken, but there were changes in the electrical performance. When the plasma is operating it is desirable to have an input power control reading of 1kV and about 0.6 amps. After ~2 hours of operation the voltage began to drop and the amperage spiked upward. The system was shut off and restarted several times but the readings remained off specification. The system was cooled and disassembled. Figure 34 shows the damaged ceramic insulator and the pockmark where the arc blew through the insulator and apparently caused the amperage spike. There is also evidence that the ceramic melted and began to flow.

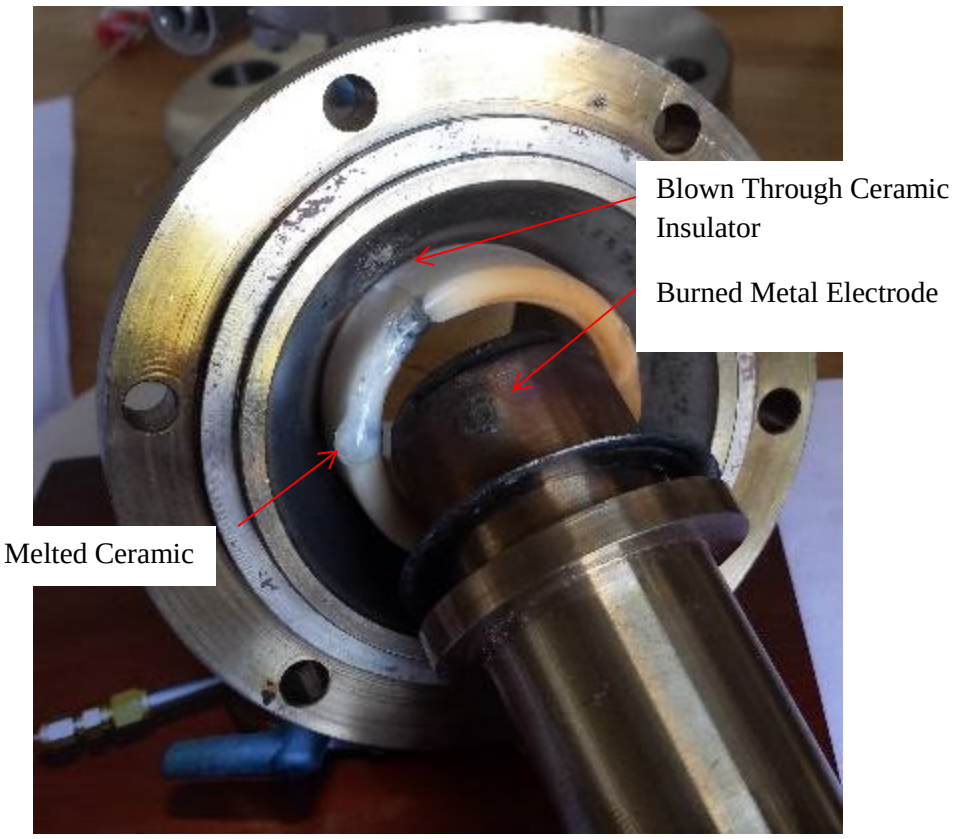

Figure 34. Plasma - Melted Ceramic Insulator and Powered Electrode with Burn Mark Indicating Arc Location. Electrode Actually Enters Insulator from Side Opposite

The flow rate drop due to temperature increase may have resulted in excess localized heating. As stated in the technical section, the manufacturer of the plasma advised preheating the gas to 1000^{o}C to facilitate reformation. It is likely that the 1000^{o}C starting point coupled with air (leading to combustion) and the electrical heating resulted in the over-temperature condition for the ceramic insulator. Upon investigation of the plasma system further with the manufacturer, the ceramic used is Macor machinable ceramic, which has a maximum operating temperature of 1000^{o}C! The plasmatron was sent back to the manufacturer for repair and the repaired system was subsequently lost in shipping and had to be remanufactured, resulting in a 3 month delay and significant funding impact. After everything was re-installed, it was determined that follow-on operation would be with only a 650^{o}C set point on the tube furnace.

Figure 35 shows the flow ports as designed in the plasma system. Analysis revealed that these ports do not provide significant enough flow to accomplish the temperature rise desired for the bulk syngas flow heading to the catalyst. Further, when coupled with a tar and particulate-laden syngas, there was almost un-measurable flow through the plasma system unless the flow venturi was turned up to maximum which overloaded the compressor and all flow went through the plasma (no bypass).

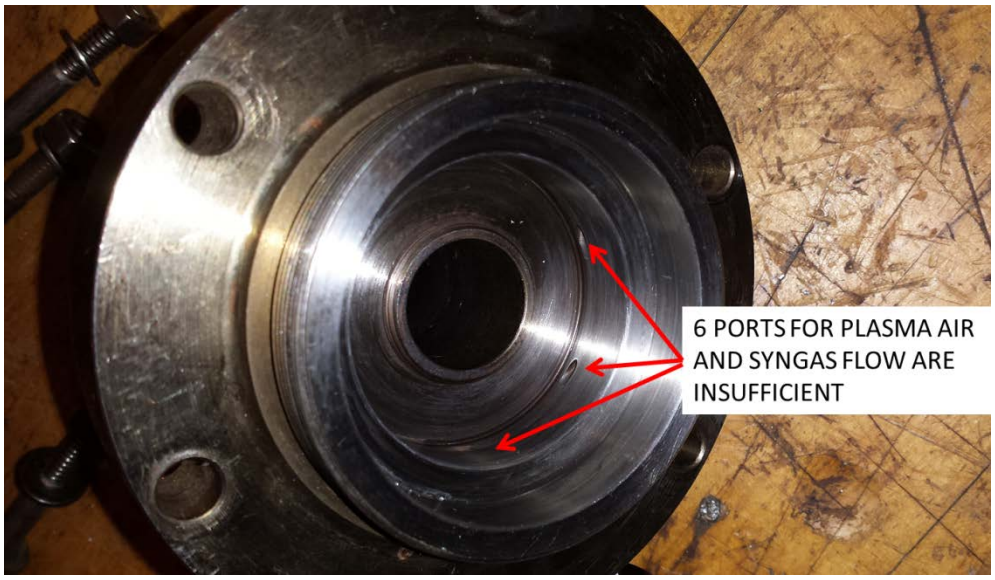

Figure 35. Plasma Flow Ports Allowing Insufficient Flow

In an attempt to get meaningful results (and against the advice of the plasma supplier) the central plug of the plasma reactor was drilled out as shown in Figure 36.

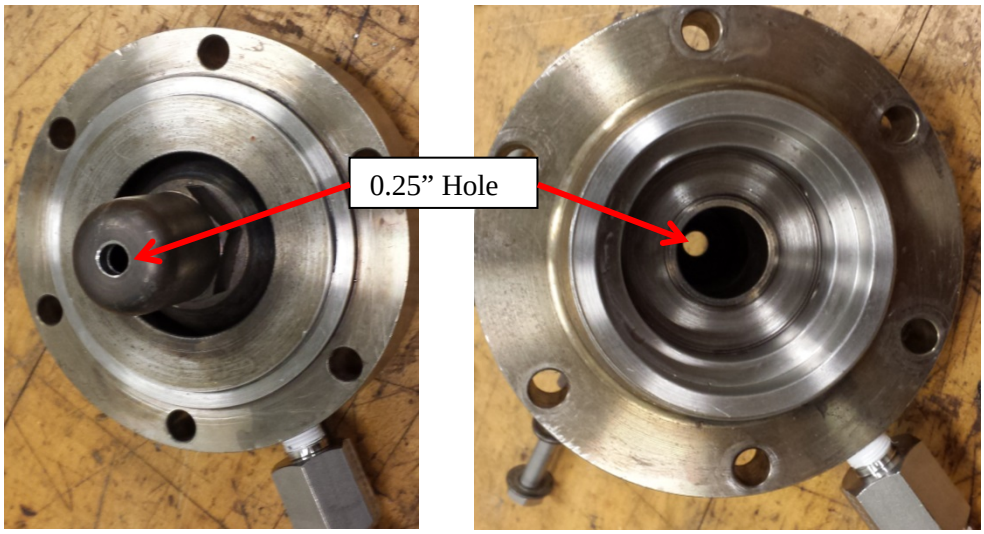

Figure 36. Hole Drilled in Center of Plasmatron in Attempt to Improve Flow of Tar Laden Syngas through the System

This additional flow caused slight changes to the voltage and amperage performance of the system when operated on air (gasifier non-operational).

Plasma Related Temperature Measurement Lessons Learned

In integrating the system, it was noted that some of the temperature channels, including the critical measurement point downstream of the plasma, were not functioning. It was determined

that the plasma current (or generated field) was doing the damage, shutting down communication between the GEK PCU measurement board and the data logger PC. The system was metered for safety reasons on initial startup and no stray voltages were measured on the well-grounded system. However, there apparently are induced fields that follow the thermocouples back to the measurement board and damage channels of thermocouples located within several feet of the plasma. This is of considerable concern as there is no way to determine the effect of the plasma on the bulk heat flow of the process gas entering the catalyst bed. To remedy this, ferrite cores were installed on the thermocouple wires in the vicinity of the plasma with 3 turns of wire going through the core to impede these stray voltage spikes. This stopped permanent damage to the thermocouple channels, but still caused communication to be lost during plasma operation. Ferrite cores were installed on all thermal couple lines leading to the GEK PCU board (as shown in Figure 37), but communication would still be lost. Aluminum shielding tape was installed on the high voltage cables that energize the plasma system. This shield was tied to the pipe near the plasma. Lastly, the power supply to the measurement board and the data logger laptop were plugged into a different panel circuit via an extension cord. Only when all these changes were instituted did reliable operation with the damaged Arduino board result. After operation was verified, a replacement Arduino board was installed and operation was re-verified with the new board.

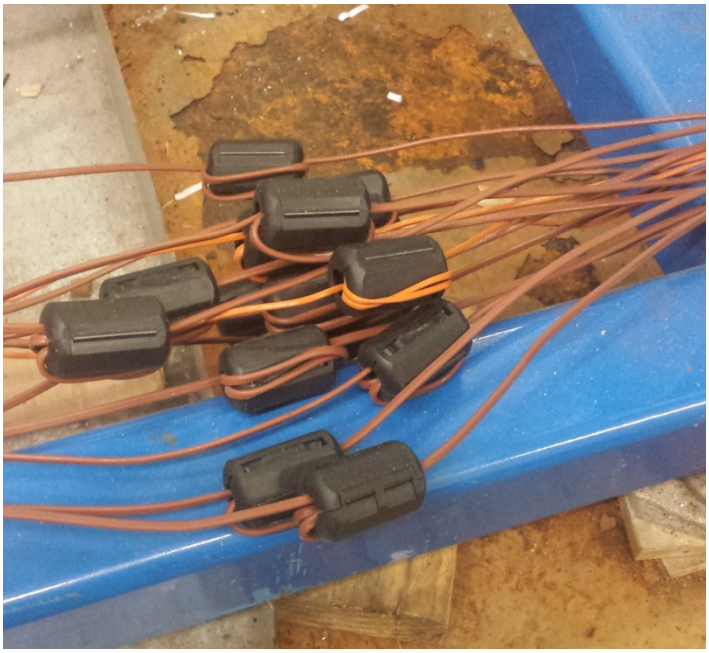

Figure 37. Ferrite Cores Installed on all Thermal Couple Lines to Reduce Electromagnetic Interference from the Plasma.

The plasma operation also affected the hydrogen mass flow controller located 4’ from the plasma. The unit was on but not actively controlling gas flow at the time. The display values oscillated wildly whenever the plasma was operational.

Orifice Plate Flow Measurement Lessons Learned

From the beginning, it was known that it would be difficult to get accurate measurements of the flow rates through the system. The tarry mixture of gas posed obvious concerns. Coriolis systems would likely plug rapidly, so Rosemount orifice plate systems were the most attractive approach for this type of measurement, but the cost was prohibitive. Dwyer F-1 and F-2 flow plates were chosen and interfaced to the make the best solution for the project. They were nitrogen blanketed during non-measurement time periods to keep tar from flowing into the cooler sections in the measurement tubes and plugging them up. The measured pressure differential was very small and the readings were not repeatable, particularly in the plasma area. It was discovered that only 2 of the 6 pressure transducers were of the sensitivity needed to measure the flow rates involved. These were used to calibrate and relate the flow through the orifice plate at room temperature to the input flow rate of air through the rotameter at the entrance to the gasifier.

Input Air Measurement Lessons Learned

The flow rate to the venturi was controlled with a needle valve and this governed airflow through the system all the way back to the input air through the flow meter. A King Instruments rotameter was used to measure flow rate with results reported in CFM. The scale was found to be wholly inaccurate for the situation at hand upon verification with the sample bench totalizing flow meter [2] and simple experimentation. Figure 38 shows the results of the measurement experiments. As can be see the variation between flowing from the rotameter to the totalizing meter (red), and then flowing from the totalizing meter to the rotameter (blue) gave readings off by a factor of 3 even in the center part of the rotameter scale. The red and blue lines begin to deviate from each other as a result of pressure differences when flowing from one meter to the next through tubing. In both cases, however they are far off from the instrument scale. The accepted calibration method was to use thin, plastic garbage bags of published and verified volume and to measure the time it takes to evacuate them using the venturi drive pulling the air through the piping and the gasifier filled with feed as is the case during an actual run.

[2] The totalizing flow meter gave excellent correlation to a precision air flow meter that was integral to the sample bench.

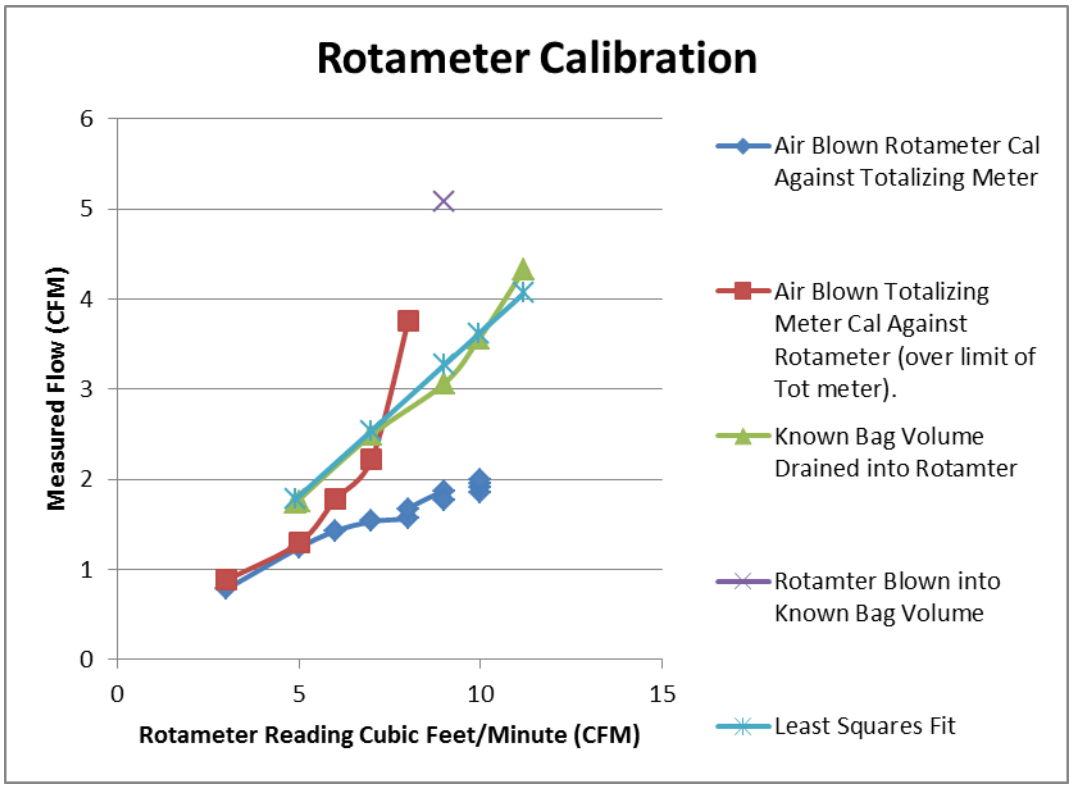

Figure 38. Rotameter Calibration Data.

The gasifier was typically run with the needle valve for the venturi set to pull through the rotameter with a reading of 10. Per Figure 38 and the least squares fit of the bag draining flow experiments this equates to a flow rate of 3.6 CFM.

Sampling Lessons Learned

In one attempt the GC vials were lost: The vials were turned upside down to reduce hydrogen loss through the punctured septa by keeping the gas phase trapped above the liquid. The methyl chloroform swelled the punctured septa and all liquids and gas leaked out (it was previously verified the methyl chloroform would not swell un-punctured septa).

Results

A typical gasifier temperature profile is shown in Figure 39 during a 9 hour run. The fluctuations on this run were related to a run capacitor slowly burning out on the compressor motor. The electrical panel circuit breaker tripped out twice during the run. It was originally attributed to additional non-related work consuming electrical load in the building, but after the other work was halted, the problem still existed. The repair was made to the compressor, the run and sampling continued.

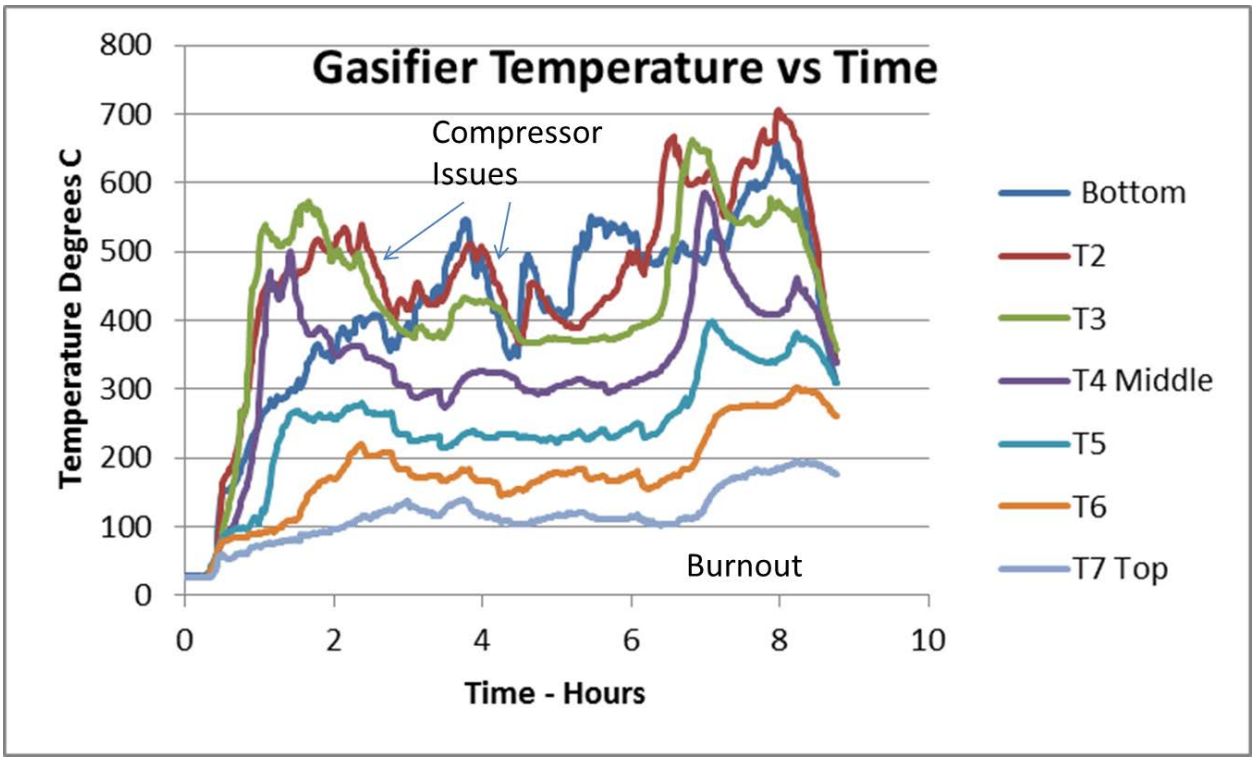

Figure 39. Real Time Gasifier Temperature Data (500 Data points) during ~9hr Run.

The feeding stopped and burnout started at 6.5hours which caused the temperature rise. The flare temperature typically runs about ~700^{o}C but fluctuated wildly with wind gusts and is therefore not shown.

Chemical Mass Balances

A sample of the feed was sent to KMT Labs in Newtown, Iowa for Proximate and Ultimate Analysis. Table 2 shows the results for this relatively dry feed.

Table 5. Analysis of Feed Stock (70% Wood, 10% Plastic, 10% Paper, 10% Dog Food)

Results as Received			
Moisture	6.87	wt %	ASTM E1755
Ash	3.13	wt %	ASTM E1755
Volatile Matter	80.46	wt %	ASTM E1755
Fixed Carbon	9.54	wt %	ASTME1755
Carbon	42.65	wt %	ASTM D5291
Sulfur	0.07	wt %	ASTM E3177
Hydrogen	6.54	wt %	ASTM D5291
Nitrogen	<0.10	wt %	ASTM D5291
Oxygen by Difference	47.81	wt %	ASTM D5291
Low Heat Value	5933	BTU/lb	ASTM E711
High Heat Value	6539	BTU/lb	ASTM E711
Results Dry Weight Corrected			
Ash	3.12	wt %	ASTM E1755
Volatile Matter	86.40	wt %	ASTM E1755
Fixed Carbon	10.24	wt %	ASTM E1755
Carbon	45.83	wt %	ASTM D5291
Sulfur	0.07	wt %	ASTM E3177
Hydrogen	6.20	wt %	ASTM D5291
Nitrogen	<0.10	wt %	ASTM D5291
Oxygen by Difference	44.76	wt %	ASTM D5291
Low Heat Value	6374	BTU/lb	ASTM E711
High Heat Value	7025	BTU/lb	ASTM E711

The carbon, hydrogen and oxygen ratios of the corrected dry weights have a reasonable correlation to wood:

Ash	Carbon	Sulfur	Hydrogen	Nitrogen	Oxygen Difference	Sum
3.12	45.83	0.07	6.2	0.09	44.76	100.07
Divide by Atomic masses of CHO						
	3.815669		6.150793651		2.7975	
Multiply by 2	7.6		12.3		5.6	
	Chemical Formula: C7.6H12.3O5.6					

Wood is generally of the formula $C_6H_{10}O_5$, so the added polyethylene from the plastic (very long straight chain $(–CH_2-)n$, where n=up to several hundred or even thousands depending on type of polyethylene) resulted in a slightly higher ratio of carbon and hydrogen to oxygen as expected. The gasifier can consume about 500 lbs/day of this material. If we assume it has a “molecular

weight"[3] of 194.34lbs/lb. mole the gasifier is consuming 0.001787 lb moles of this material per minute. For complete combustion of this material to CO2 and H2O the stoichiometry is:

$$C7.6H12.3O5.6 + 10.98\ O2 \rightarrow 7.6\ CO2 + 12.3\ H2O$$

The oxygen flow for complete combustion is therefore 0.019626 lb. moles O2/minute which with nitrogen added equates to 0.0935 lb. moles air/minute

From the ideal gas law PV=nRT or V=nRT/P.

From Himmelblau[xx] $R=10.73(psia)(ft^3)/(lbmole)(^oR)$

$V= [(0.0935\ lbmoles\ Air/minute)*(10.73(psia)(ft^3)/(lbmole)(^oR)*(562\ ^oR)]/(14.7psia)$

Volumetric Flow Rate for Complete Combustion = 38.4 ft^3/min

So for complete combustion the air flow would be 38.4 CFM. The measured flow is 3.6 CFM as estimated from Figure 35 or about 9.4% of that for complete combustion. This measured flow rate relate correlates well to the data provided by SERI[v] in the Gasifier Handbook where it states that an updraft gasifier will combust only about 10% of the chemical energy of the biomass (or waste) in the production of a tar laden syngas mixture. This system appears to be running leaner than the data would suggest based on carbon and hydrogen input from the Proximate and Ultimate analysis. Perhaps the pyrolyzed plastic exiting as a waxy material (Figure 29) skews the results by taking significant portions of the combustible material (reported in Table 5) in a very energy rich polymer molecular fragment.

Syngas Results

With the gasification system, feeder, piping, experiments and sampling system in place, several daylong burns took place where some of the samples were successfully acquired. Analytical data from the runs comes in two types: the headspace (gas) analysis from the vials as shown in Figure 14 and the liquid (tar) analysis as shown in Figure 14. Typically, only the first 3 vials in the flow path are analyzed and reported. The results of 2 data runs for gas phase are shown in Table 6 and 7.

Table 6. Headspace Gas Analysis 8-14-14 Run

[3] This is not truly a molecule with this formula, but it does serve to provide ratios of elements in the feed mixture based on chemical analysis and can be used for calculation of air flow rates O:C ratios, etc.

SAMPLE	Volume (L)	He%	H2 %	O2%	N2%	CO%	CH4%	CO2%	Total
Blank		0.0	0.0	24.5	75.5	0.0	0.0	0.0	100.0
TOP Pre-Light	0.5	3.5	0.0	22.2	74.3	0.0	0.0	0.0	100.0
TOP Post-Light	0.5	2.2	3.1	11.6	72.5	1.6	0.0	9.0	100.0
TOP-PS-1	0.5	0.0	1.4	15.1	69.6	0.0	0.0	13.9	100.0
TOP-PS-2	0.5	0.0	3.9	12.2	65.0	2.2	1.9	14.8	100.0
TOP-PS-4	0.5	0.0	6.2	9.8	66.5	2.5	2.4	12.6	100.0
TOP - 1	1.0	0.0	0.0	18.8	78.5	0.0	0.0	2.7	100.0
TOP - 2	1.0	0.0	0.0	20.7	77.4	0.0	0.0	1.9	100.0
TOP - 4	1.0	0.0	1.5	14.5	68.5	0.0	0.0	15.5	100.0
BOTTOM - 1	1.0	1.7	5.3	3.7	66.9	2.8	1.8	17.8	100.0
BOTTOM - 2	1.0	1.9	5.2	4.3	68.7	3.3	1.8	14.8	100.0
BOTTOM - 4	1.0	0.0	0.0	19.0	67.7	0.0	0.0	13.3	100.0
Post Plasma-2-1	2.0	1.3	3.8	9.7	71.1	1.6	1.1	11.4	100.0
Post Plasma-2-2	2.0	1.2	2.9	10.9	73.5	1.6	0.0	9.9	100.0
Post Plasma-2-4	2.0	0.0	1.9	12.9	74.1	0.0	0.0	11.1	100.0
Post Catalyst-1	2.0	1.5	0.0	6.2	75.2	0.0	0.0	17.1	100.0
Post Catalyst-2	2.0	0.0	0.0	14.3	65.7	0.0	0.0	20.0	100.0
Post Catalyst-4	2.0	1.2	0.0	6.5	71.5	0.0	0.0	20.8	100.0
Averages		**0.8**	**2.0**	**13.2**	**71.2**	**0.9**	**0.5**	**11.5**	**100.0**

TOP-PS means premature stop of gasifier due to feed jam.

These results are summarized graphically in Figure 40

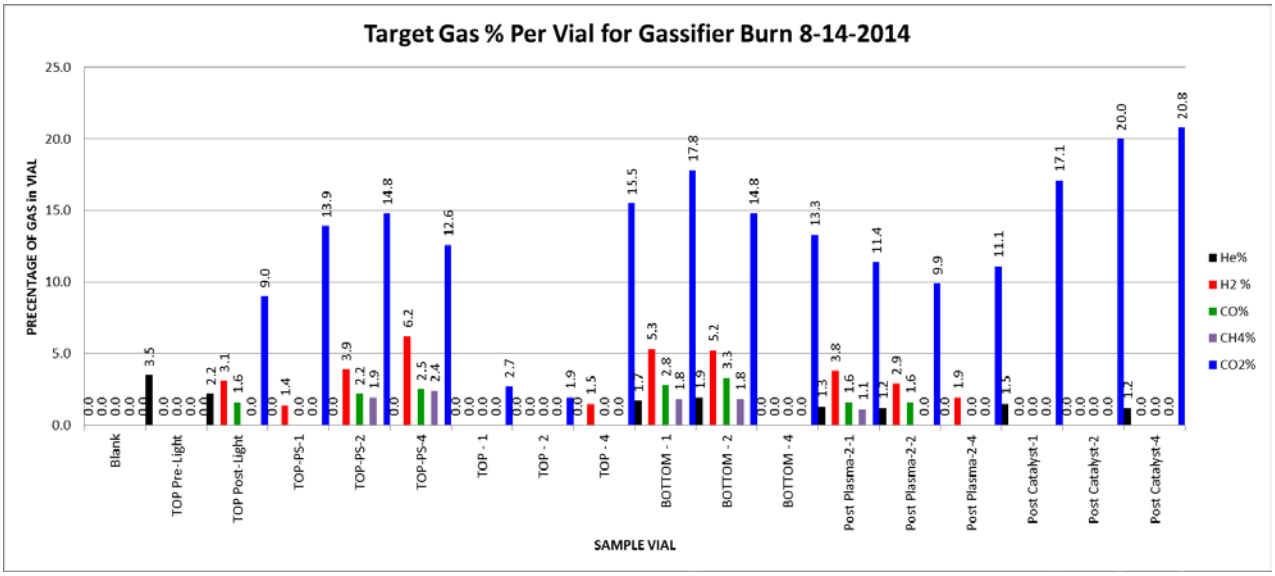

Figure 40. Summary of GCTCD Results at Various Sample Ports 8-14-2014 Run

Table 7. Headspace Gas Analysis 12-3-14 Run

SAMPLE	Volume (L)	H2 %	O2%	N2%	CO%	CH4%	CO2%	Total
Blank		0.0	24.5	75.5	0.0	0.0	0.0	100.0
Top Vial 1	3.0	1.4	0.0	6.6	0.4	5.8	21.4	35.6
Top Vial 2	3.0	13.1	3.1	61.5	4.2	0.0	18.1	100.0
Top Vial 3	3.0	9.8	4.2	62.2	4.5	0.0	19.2	100.0
Pre-Plasma Vial 1	3.0	0.0	22.5	77.5	0.0	0.0	0.0	100.0
Pre-Plasma Vial 2	3.0	0.0	24.0	76.0	0.0	0.0	0.0	100.0
Pre-Plasma Vial 3	3.0	0.0	23.5	76.5	0.0	0.0	0.0	100.0
Post Plasma Vial 1	3.0	0.0	23.4	76.6	0.0	0.0	0.0	100.0
Post Plasma Vial 2	3.0	0.0	22.4	77.6	0.0	0.0	0.0	100.0
Post Plasma Vial 3	3.0	0.0	23.5	76.5	0.0	0.0	0.0	100.0
Pre-Catalyst-PMS-1	3.0	6.8	14.4	68.8	0.0	0.0	10.1	100.0
Pre-Catalyst-PMS-2	3.0	0.0	23.6	76.4	0.0	0.0	0.0	100.0
Pre-Catalyst-PMS-3	3.0	0.0	22.5	77.5	0.0	0.0	0.0	100.0
Pre-Catalyst-Vial 1	3.0	0.0	19.6	72.7	0.0	0.0	7.7	100.0
Pre-Catalyst-Vial 2	3.0	0.0	23.1	74.8	0.0	0.0	2.2	100.0
Pre-Catalyst-Vial 3	3.0	0.0	22.1	75.4	0.0	0.0	2.6	100.0
Post-Catalyst-Vial 1	3.0	7.6	0.0	64.1	2.2	0.0	26.2	100.0
Post-Catalyst-Vial 2	3.0	6.4	0.0	63.8	1.9	0.0	27.9	100.0
Post-Catalyst-Vial 3	3.0	5.2	2.7	64.4	2.1	0.0	25.7	100.0
Post-ETP-Vial 1	3.0	15.6	9.1	61.2	4.7	2.7	6.8	100.0
Post-ETP-Vial 2	3.0	16.4	4.9	51.6	5.9	4.1	17.1	100.0
Post-ETP-Vial 3	3.0	11.0	7.6	45.8	3.7	4.7	27.2	100.0

The results for the 12-3-14 run are summarized in Figure 41.

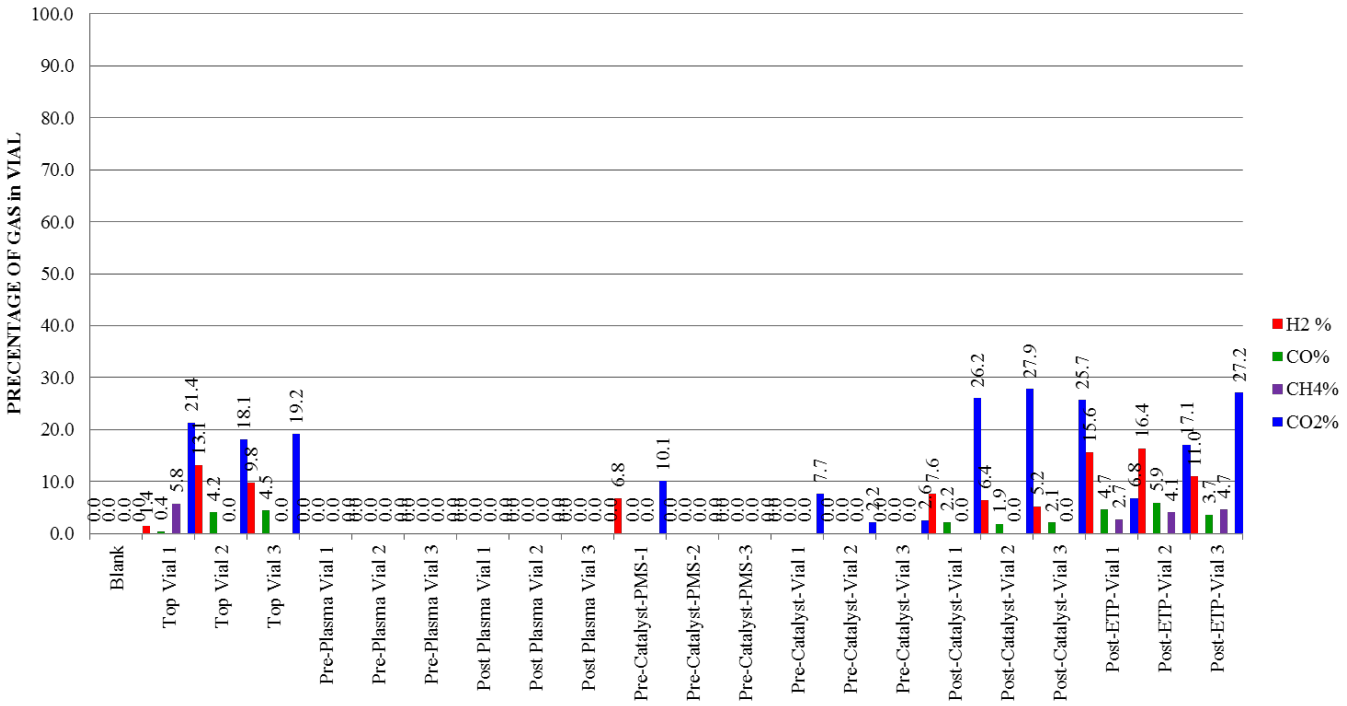

Figure 41. Summary of GCTCD Results at Various Sample Ports

Table 8 shows the liquid tar captured in the GC sampling system at various points in the pilot plant on the 8-14-14 run.

Table 8: Blank Corrected* Liquid Sample Analysis (GCFID) 8-14-14 Run

SAMPLE	Methanol (PPM)	Ethanol (PPM)	Benzene (PPM)	Toluene (PPM)	Xylene (PPM)	Naphthalene (PPM)
BLANK	0	0	0	0	0	0
2500PPM STD	2622	2979	2481	2472	2549	2558
5000PPM STD	4816	5290	5028	5041	4926	4913
10000PPM STD	10061	10127	9990	9986	10028	10029
7500PPM CHK STD	7390	7920	7623	7619	7718	7699
PRE-LIGHT VIAL 1	0	3260	0	(21)	(13)	0
POST-LIGHT VIAL 1	525	203	0	(22)	(11)	0
TOP-PS-VIAL 1	1112	3422	0	(19)	26	0
TOP-PS-VIAL 2	497	3319	0	0	0	0
TOP-PS-VIAL 3	0	1835	0	0	0	0
TOP-PS-VIAL 4	0	473	0	0	(13)	0
TOP-PS-VIAL 5	0	51	0	0	(12)	0
TOP-VIAL 1	601	3537	487	(19)	33	0
TOP-VIAL 2	501	3212	0	0	0	0
TOP-VIAL 3	0	2710	0	0	0	0
TOP-VIAL 4	0	3395	0	0	0	0
TOP-VIAL 5	0	3298	0	0	0	0
BOTTOM-VIAL 1	1080	(381)	496	(15)	64	0
BOTTOM-VIAL 2	495	2088	0	0	0	0
BOTTOM-VIAL 3	0	1410	0	0	0	0
BOTTOM-VIAL 4	0	(2805)	0	0	(13)	0
BOTTOM-VIAL 5	0	(171)	0	0	(12)	(28)
BOTTOM-VIAL 6	0	224	0	0	0	0
POST PLASMA-2 VIAL 1	702	2827	407	(22)	329	0
POST PLASMA-2 VIAL 2	550	3139	0	0	0	0
POST PLASMA-2 VIAL 4	499	883	0	0	(13)	0
POST CATALYST VIAL 1	0	(1428)	0	0	0	0
POST CATALYST VIAL 2	0	(1207)	0	0	0	0
POST CATALYST VIAL 4	0	129	0	0	(13)	0

Table 9 shows the sampling results from the 12-3-14 run.

Table 9. Blank Corrected* Liquid Sample Analysis (GCFID) 12-3-14 Run

SAMPLE	Methanol (PPM)	Ethanol (PPM)	IPA (PPM)	Benzene (PPM)	Toluene (PPM)	Xylene (PPM)	Naphthalene (PPM)	Phenol (PPM)
BLANK	0	0	0	0	0	0	0	0
2500PPM STD	2625	2273	2394	2567	2699	2659	2662	2652
5000PPM STD	4812	4486	4449	4899	4702	4763	4757	4773
10000PPM STD	10063	9981	10026	10034	10099	10079	10081	10076
7500PPM CHK STD	7684	7445	7751	7462	7641	7661	7651	7675
Top Vial 1	2044	(1656)	766	3405	1730	3903	1105	626
Top Vial 2	2011	(450)	72	0	0	0	0	521
Top Vial 3	879	(428)	(35)	0	0	0	0	168
Top Vial 4	795	135	(42)	0	0	0	0	84
Top Vial 5	0	(268)	(42)	0	0	0	0	82
Top Vial 6	0	(236)	(50)	0	0	0	0	0
Pre-Plasma Vial 1	0	(203)	(40)	0	0	0	0	0
Pre-Plasma Vial 2	0	(122)	(41)	0	0	0	0	0
Pre-Plasma Vial 3	0	(416)	(47)	0	0	0	0	0
Post Plasma Vial 1	0	(335)	(42)	0	0	0	0	0
Post Plasma Vial 2	0	(86)	(41)	0	0	0	0	0
Post Plasma Vial 3	0	(423)	(45)	0	0	0	0	0
Pre-Catalyst Vial 1	1443	(740)	237	2499	602	1068	576	424
Pre-Catalyst Vial 2	915	(109)	46	0	0	0	0	209
Pre-Catalyst Vial 3	794	(700)	(48)	0	0	0	0	83
Post Catalyst Vial 1	0	(2383)	(42)	0	0	0	0	0
Post Catalyst Vial 2	0	(394)	(38)	0	0	0	0	0
Post Catalyst Vial 3	0	(439)	(42)	0	0	0	0	0
Post ETP Tubes Vial 1	766	(199)	2821	0	0	0	0	0
Post ETP Tubes Vial 2	1635	(583)	2921	0	0	0	0	0
Post ETP Tubes Vial 3	765	(4236)	49	0	0	0	0	0
Post ETP Tubes Vial 4	0	(657)	(39)	0	0	0	0	0
Post ETP Tubes Vial 5	0	(863)	(38)	0	0	0	0	0
Post ETP Tubes Vial 6	0	(457)	(44)	0	0	0	0	0

*Methanol, Ethanol and IPA showed up in unexpected quantities. A blank sample (not exposed to the tar laden syngas) was run through the system and used to make a correction factor. Ethanol and IPA were driven negative by this correction factor.

Figure 42 graphically summarizes the liquid results of the 12-3-14 sampling.

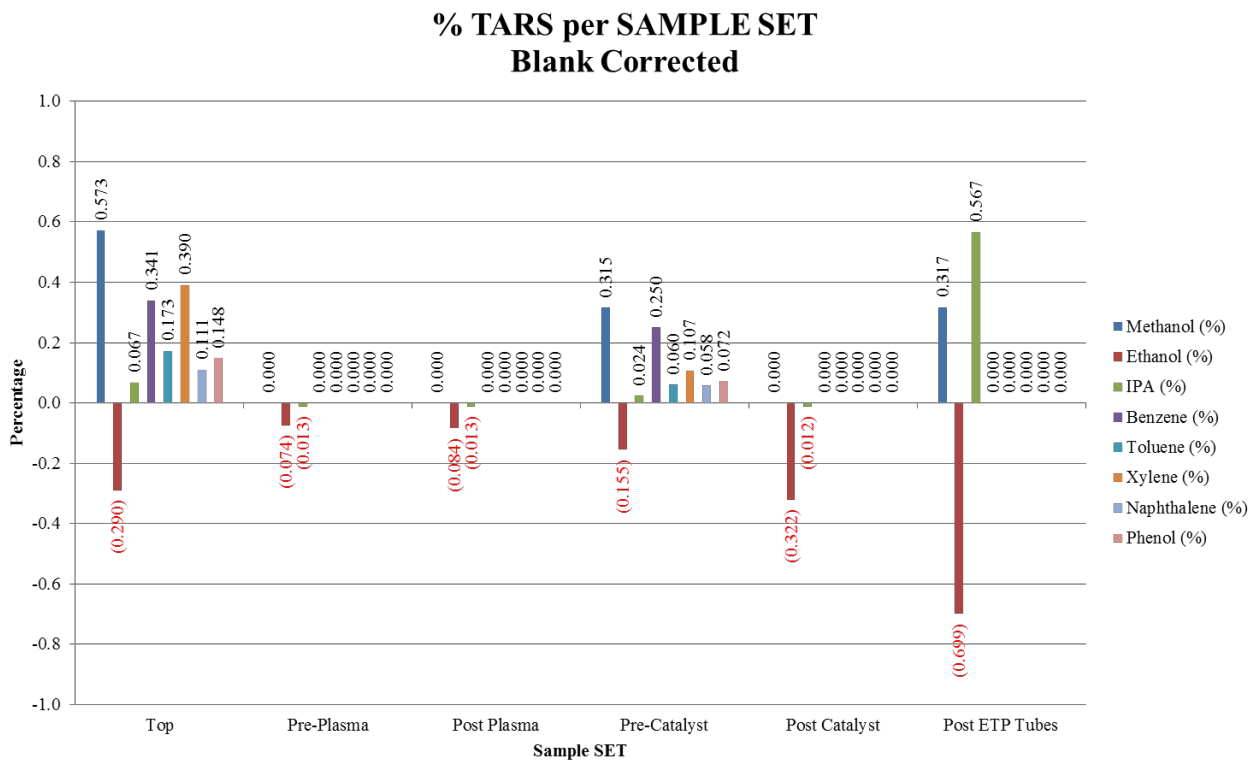

Figure 42 Percentages of Target Tars Found in the Sampling Fluid from Various Points in the Process

The high IPA reading coming out of the Post ETP Tubes results from the pump and totalizing meter having drawn IPA vapor out of the impingers on earlier runs. When the same system was used to draw syngas through renewable JP-8 and force it into the GC sampling tubes, it apparently transferred some of the IPA with it. The methanol throughout the results is difficult to explain other that it is being produced in significant quantity and showing up throughout, or there is a problem with the GC set up. Blank standards seem correct on methanol. It is also not clear why the ethanol readings are negative throughout.

Figure 43 shows a GCMS run on the vials as sampled from the downflow port at exit of gasifier. One can see that the majority of tars were captured in the first 2 or 3 vials corresponding to the change in liquid color in Figure 18.

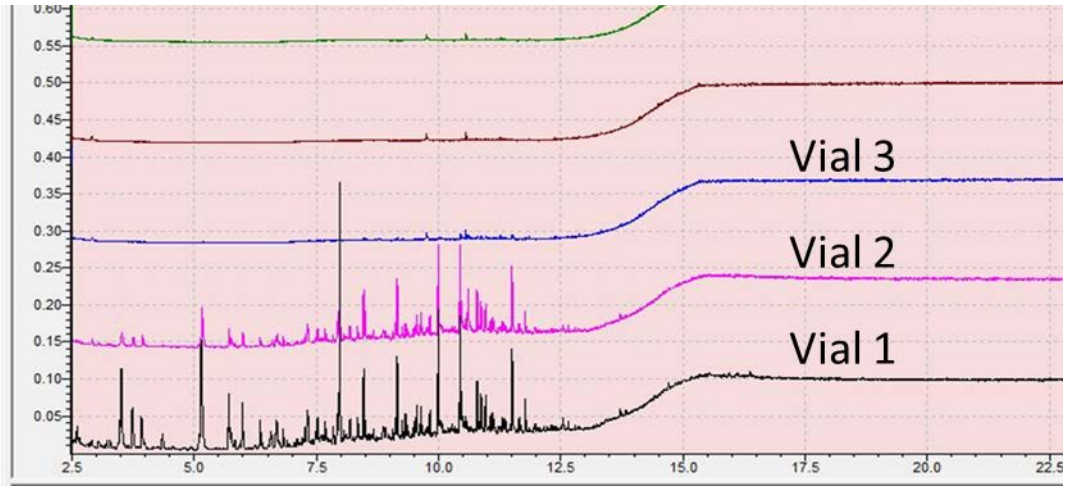

Figure 43. GCMS of Liquid from Exit Port of Gasifier from Vials in Sampler Path

Gravimetric Results are summarized in Table 10. The water % was measured using Karl Fischer Titration.

Table 10. Gravimetric Tar & Water Concentration in Gas

SAMPLE DATE	SAMPLE LOCATION	LITERS OF GAS WITHDRAWN	COLLECTION BOTTLE I.D.	GRAMS TAR PER LITER GAS WITHDRAWN	WATER % IN IPA IN IMPINGERS	WATER % IN IPA IN DISTILLATE
6/26/2014	gasi-top	30	A	0.0114	1.0	1.2
8/6/2014	gasi-bot	50	B & C	0.1134	2.4	1.5
8/6/2014	pre-plasma	50	D	0.0030	1.4	1.1
8/18/2014	post-plasma	50	E	0.0019	0.7	0.5
12/3/2014	gasi-top	30	J*	0.0980	1.7	0.8

*The “gasi-top” evaluation was sampled through renewable JP-8. As such, the material could not be boiled off in a rotary evaporator because the boil point is too high. Instead, it was performed on an aluminum dish on a hot plate, so the results are likely somewhat low.

After operating the gasifier, a light brown waxy substance was found accumulating near the exit flare where the last of any combustible gases and tars are consumed as they exit the last stage of the gasifier system (see Figure 32). It was not part of the original test plan for this project but a Fourier Transform Infrared Spectroscopy (FTIR) analysis of this material best matches a mixture of polyethylene and polypropylene as they appear in references of pyrolyzed samples (see Figures 44 and 45).

It is likely that the small differences between the unknown and reference spectra shown below are due to additional unknown materials originating from the combustion of the mixture of fuels used. The source of plastic was the various food containers from the Lockheed cafeteria which

are Low and High Density Polyethylene (HDPE). The major peaks clearly match the basic ethylene and propylene materials that have been pyrolyzed.

Scans of the unknown sample were made using a Nicolet FTIR in transmission mode. A thin film of the sample was transferred to a sodium chloride salt flat simply by rubbing the sample on one surface (see Figures 44 & 45).

Red: brown residue in question
Violet: reference of a known ethylene-propylene copolymer.

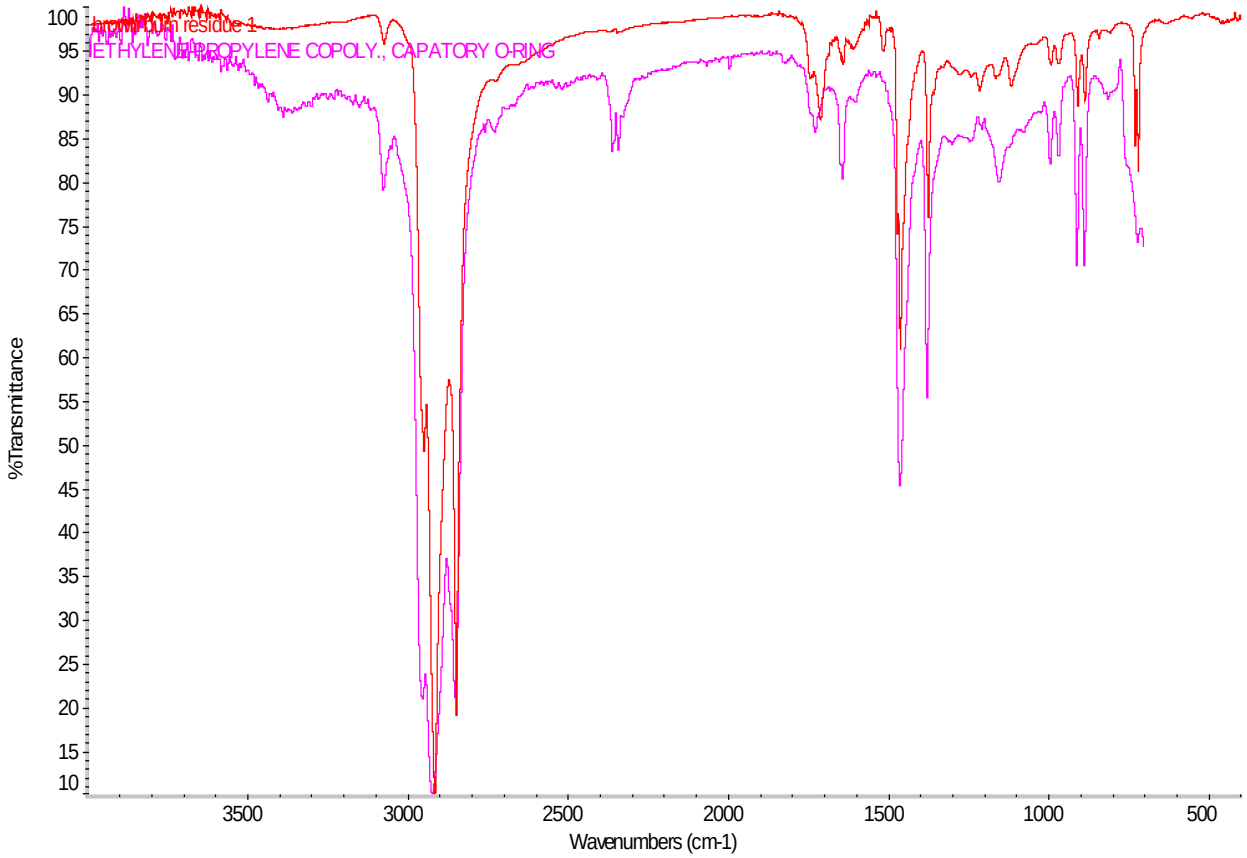

Figure 44. FTIR Transmission of Tar at Exit of System Near Flare

Red: brown residue in question
Green: reference of a pyrolyzed sample of EPTR (ethylene propylene thermoplastic polymer)

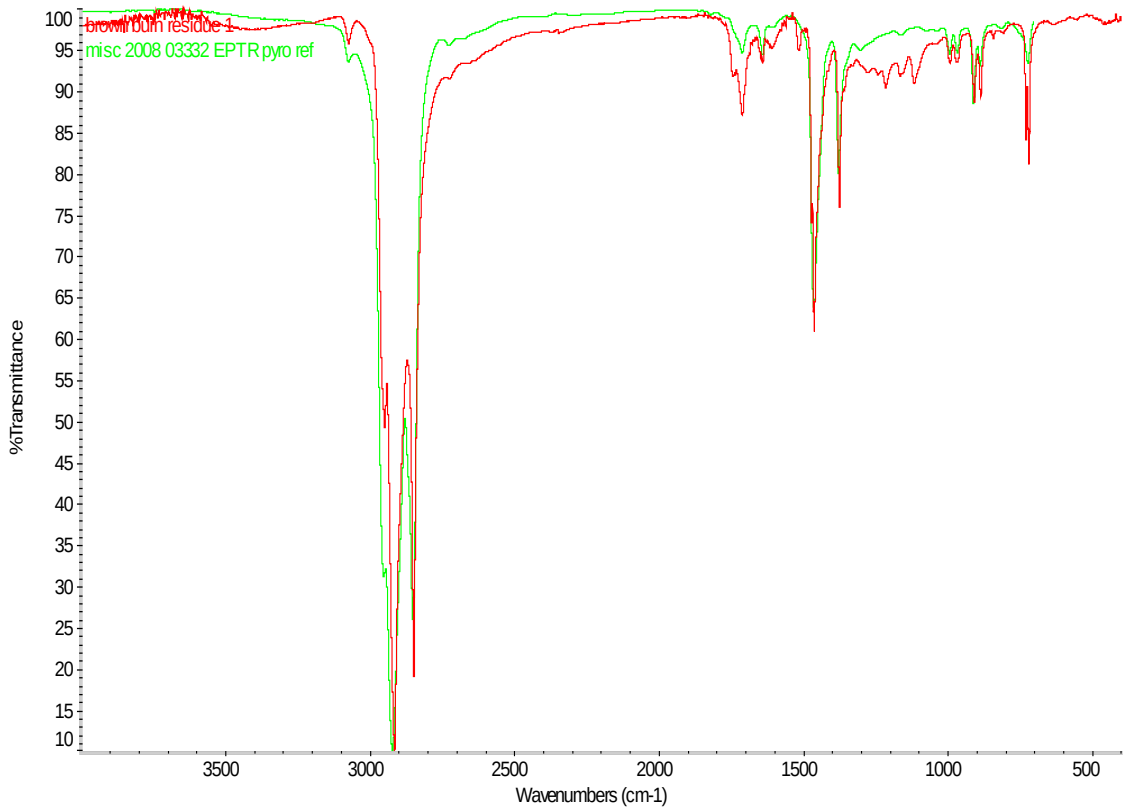

Figure 45. FTIR Transmission of Brown Condensed & Hardened Tar at Exit of System Near Flare

It was also not part of the original test plan, but the brown waxy material found near the exit flare was subject to a Differential Scanning Calorimeter (DSC) to attempt to analyze it further.

The three scans below are DSC runs to identify phase changes in the light brown material which makes up 99% of the stalagmite. It must be noted that the DSC is not normally artificially cooled so the lowest starting temperature is slightly above room temperature.

The scans were done with a goal of determining the melt temperature of the stalagmite material and previous FTIR scans suggest that the material is a waxy alkane. Table 11 implies that the alkane is in the range of 30 to 35 carbons long. Because branching tends to reduce the melt point, if the unknown substance is highly branched, more carbon atoms would be present in the molecule than estimated. The lack of a doublet peak at 1385 wave numbers in Figure 44 and 45 suggests that there is not a lot of branching on these hydrocarbon chains and that they are mostly straight chain hydrocarbons.

Table 11. Table of Alkanes

Alkane	**Formula**	**Boiling point [°C]**	**Melting point [°C]**	**Density [g·cm^{-3}] (at 20 °C)**

Methane	CH_4	−162	−182	Gas
Ethane	C_2H_6	−89	−183	Gas
Propane	C_3H_8	−42	−188	Gas
Butane	C_4H_{10}	0	−138	Gas
Pentane	C_5H_{12}	36	−130	0.626 (liquid)
Hexane	C_6H_{14}	69	−95	0.659 (liquid)
Heptane	C_7H_{16}	98	−91	0.684 (liquid)
Octane	C_8H_{18}	126	−57	0.703 (liquid)
Nonane	C_9H_{20}	151	−54	0.718 (liquid)
Decane	$C_{10}H_{22}$	174	−30	0.730 (liquid)
Undecane	$C_{11}H_{24}$	196	−26	0.740 (liquid)
Dodecane	$C_{12}H_{26}$	216	−10	0.749 (liquid)
Hexadecane	$C_{16}H_{34}$	287	18	0.773 (liquid)
Icosane	$C_{20}H_{42}$	343	37	Solid
Triacontane	$C_{30}H_{62}$	450	66	Solid
Tetracontane	$C_{40}H_{82}$	525	82	Solid
Pentacontane	$C_{50}H_{102}$	575	91	Solid
Hexacontane	$C_{60}H_{122}$	625	100	Solid

1st run, 1st brown sample. Approximate melt temperature is 77°C. This sample was rather large (not weighed) and once melted, filled the cup. For this reason it was terminated well below any potential boiling point to prevent contamination of the DSC furnace from possible violent overflow if allowed to boil.

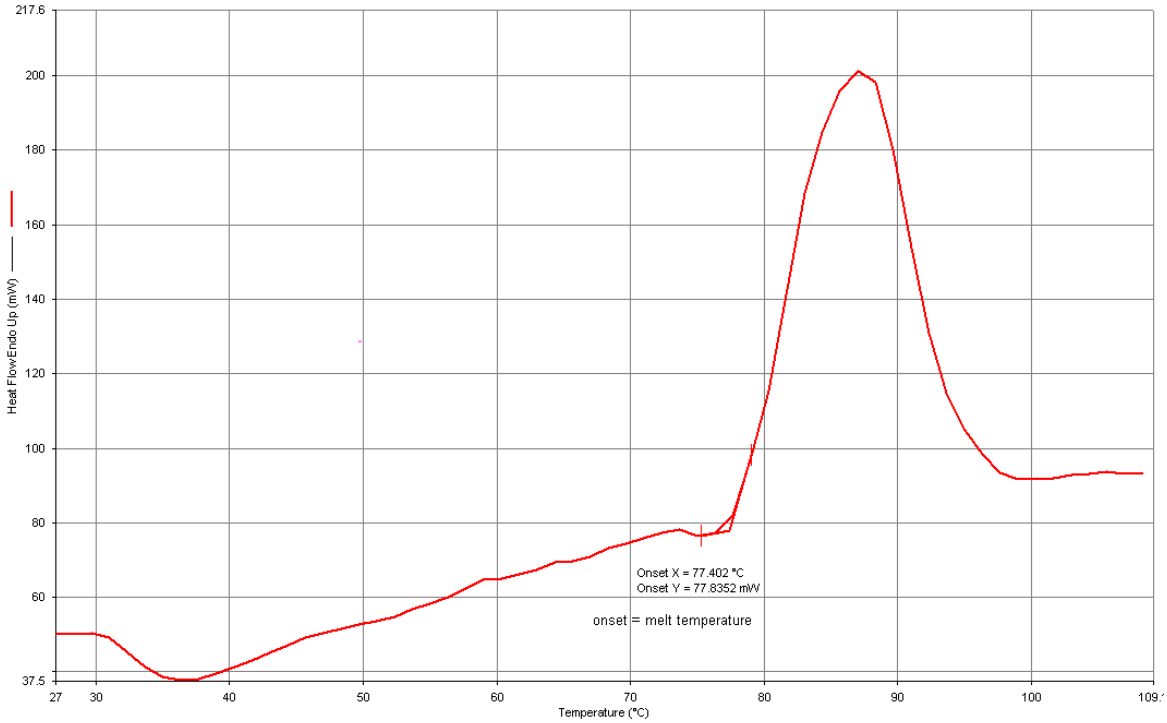

Figure 46. Differential Scanning Calorimeter Analysis of Brown Waxy Exudate From the Flare. Run 1 Melt Temperature Approximately 77°C.

1st run, 2nd sample, 7.69mg in weight.

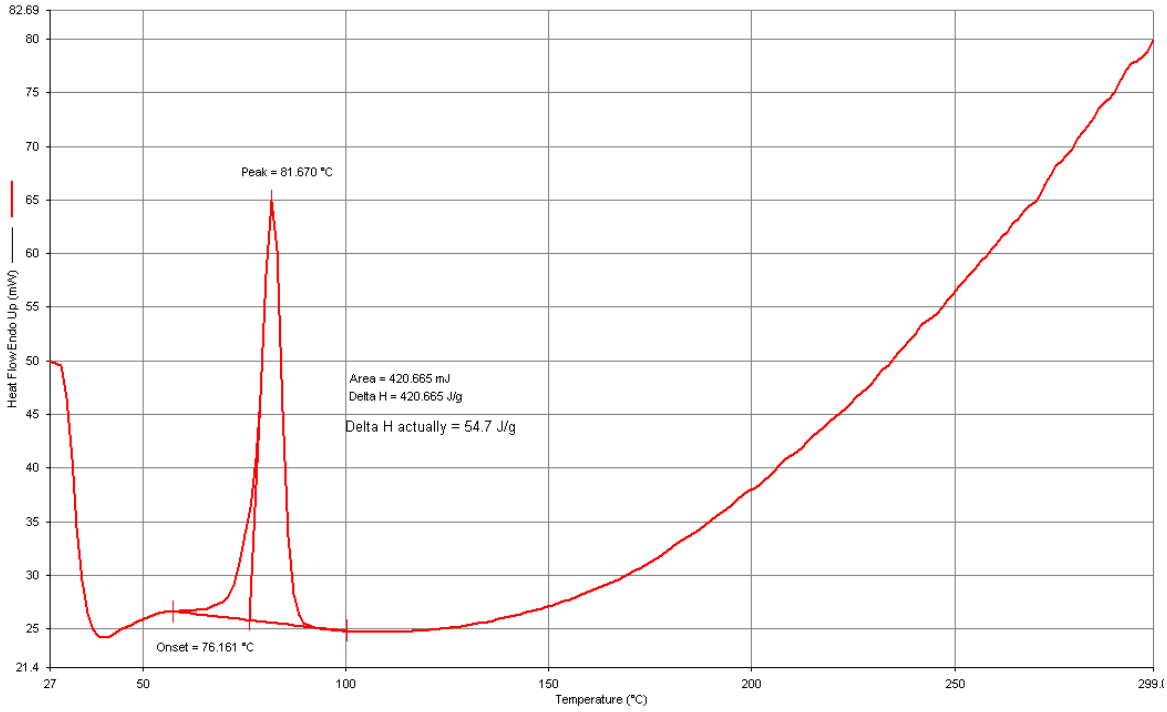

Figure 47. Differential Scanning Calorimeter Analysis of Brown Waxy Exudate From the Flare. Run 1, Sample 2 Melt Temperature Approximately 76°C

2nd run, 2nd sample, weight dropped to 5.28mg. Max temp was 390°C. Exothermic event may have been combustion since this was done in normal atmosphere with an open cup to prevent gumming up the DSC furnace. Boiling was not observed, but the autoignition temperature of alkanes are typically in the low 200°C range, so as the vapor pressure rises these materials should spontaneously ignite.

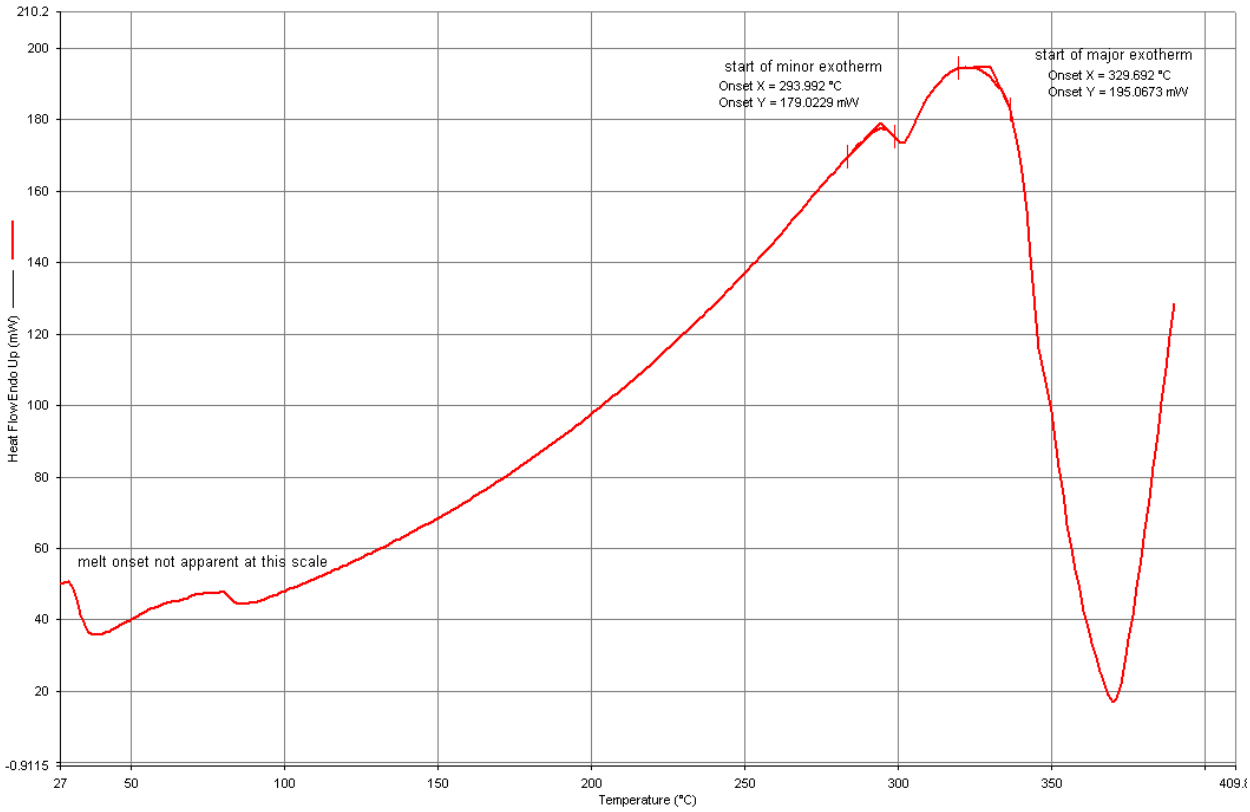

Figure 48. Differential Scanning Calorimeter Analysis of Brown Waxy Exudate From the Flare. Run 2, Sample 2 Possible Combustion at 330°C

If the area around the melt temperature (75°C) of Figure 48 is expanded a melt event did occur.

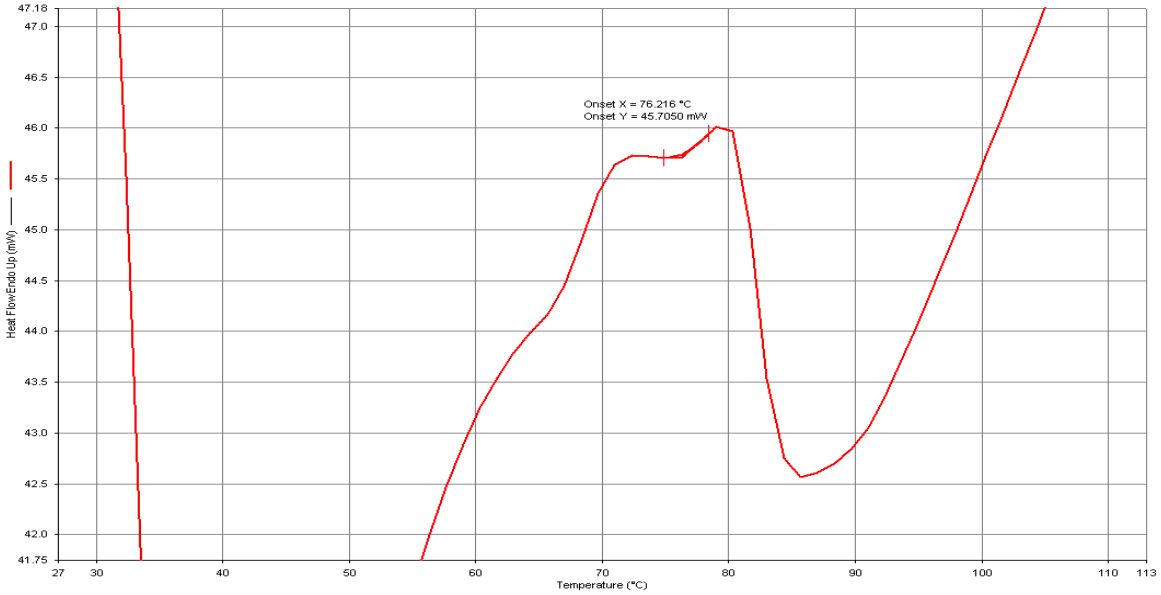

Figure 49. Differential Scanning Calorimeter Analysis of Brown Waxy Exudate from the Flare. Run 2, Sample 2 Area around Melt of Figure 47 Expanded.

1st run, 3rd sample, 4.39mg weight. Shows clear melt as first run of previous sample did (although about 10°C lower than previous sample) and also small and large exotherms as the second run of the previous sample did.

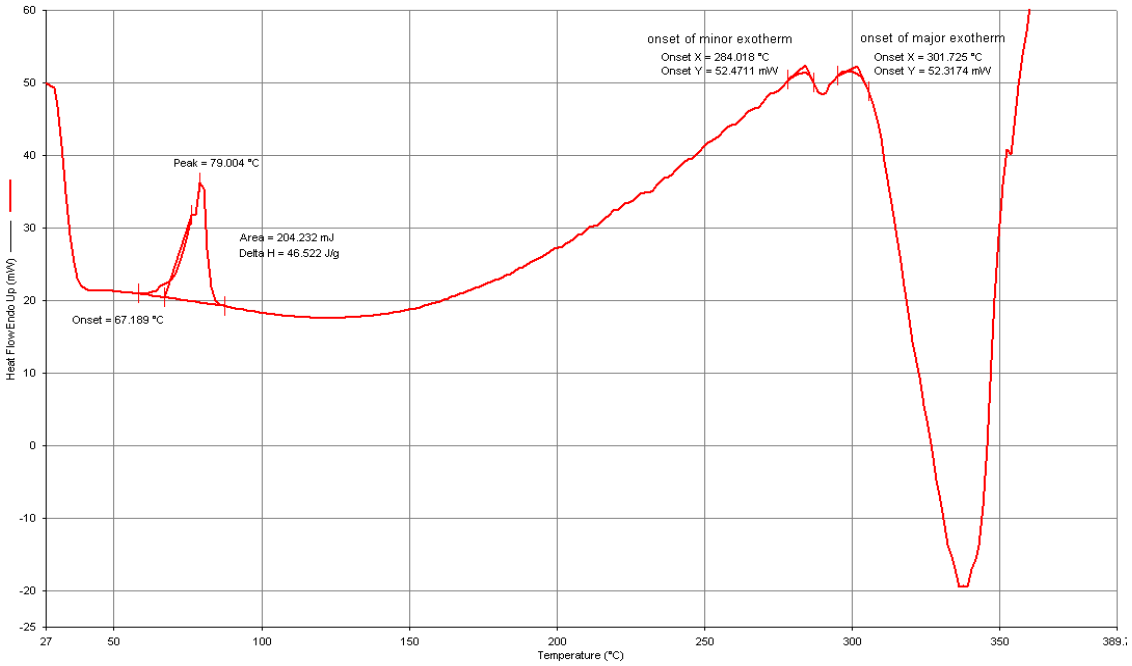

Figure 50. Differential Scanning Calorimeter Analysis of Brown Waxy Exudate from the Flare. Run 1, Sample 3.

The material of the stalagmite was further analyzed for solubility in R-8. Figure 51 shows the material as originally placed in the R-8, after 60 minutes at 60°C and the filtration results.

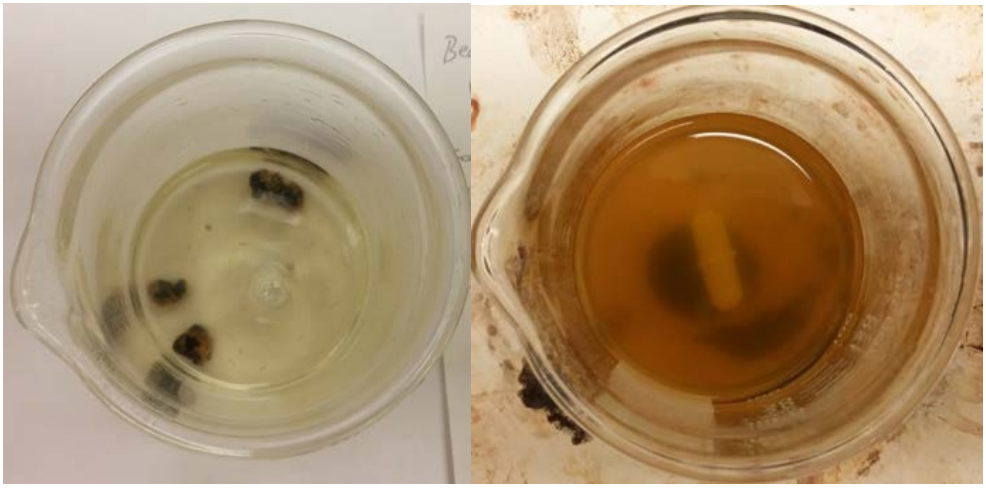

Figure 51. Brown Waxy Exudate (Stalagmite) Dissolving into R8 Fuel.

Figure 52 shows the filtration result after cooling indicating that 64% of the waxy exudate is soluble in fuel.

Figure 52.Filtration Result of Brown Waxy Exudate, Indicating that 64% of the Material is Soluble in Diesel Fuel.

Discussion

To aid discussion of the results, Figure 53 shows a modified pilot plant and test point diagram of Figure 1 where in this case the sample ports are labelled to identify sample locations in the results tables.

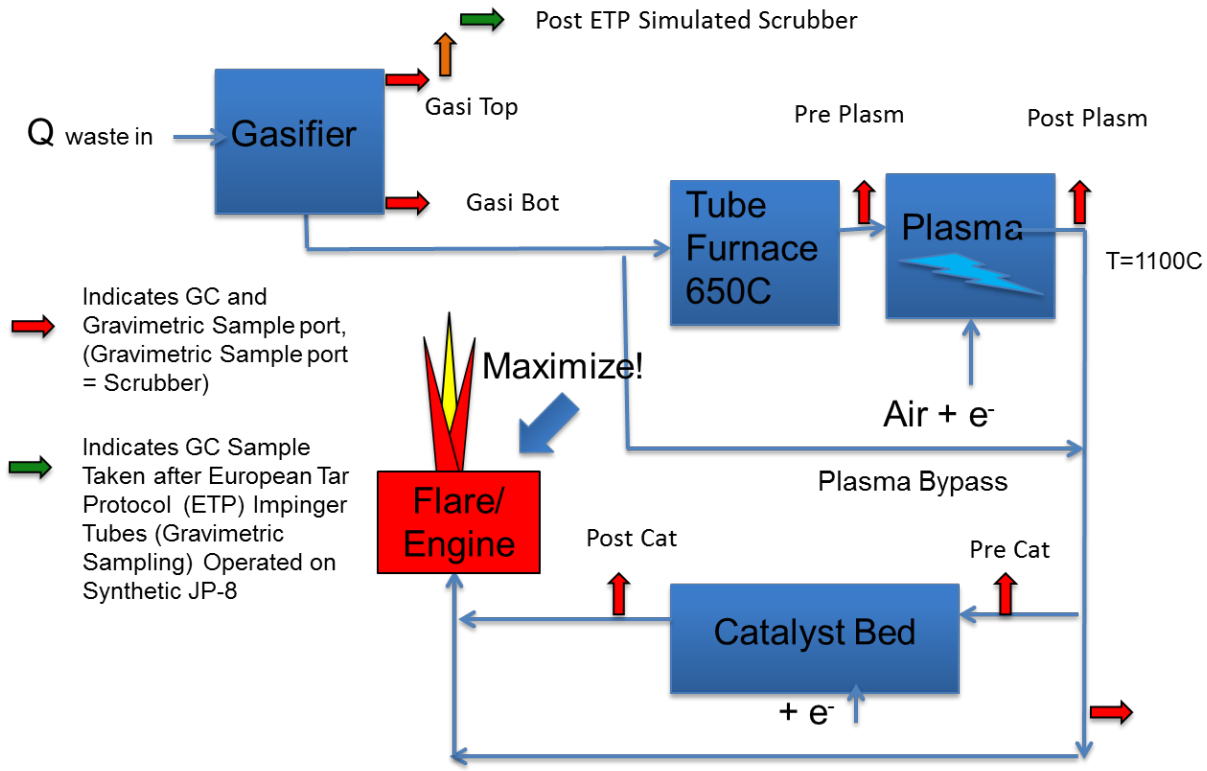

Figure 53. Pilot Plant Diagram with Test Ports Labelled.

It must first be stated that his project did not accomplish all experimentation goals originally planned. The system was not fully characterized ahead of time and the experimental runs had to be part of the initial burns to save schedule and labor hours. Further, the sampling was attempted as quickly as possible once stable temperatures were obtained out of concern for hard failures. The issues with the addition of the tube furnace at the recommendation of the plasma supplier, flow measurement issues, assembly and integration issues, feeder and PLC changes, and recovery from the plasma meltdown consumed resources and schedule. For the plasma related samples, the melted insulators made the experimenters concerned about repeating the damage.

8-14-14 Run Gas and Liquid Analysis Results Discussion

In Table 6 the Top-PS data was actually related to a premature stop run on 8-6-14 when the feeder plugged. The feed ram would not travel all the way forward and the temperature began to rise in the gasifier implying a bridge and material burnout in the mid-section. This run shows hydrogen increasing from Vial 1 to 4 (see Figure 16 for vial number description). If the sampling system were perfect the later vials would have more air and less hydrogen as a result of adding and mixing syngas into volumes initially full of air and in series. This must be the result of a leaky sampling system allowing air into vial 1 after sampling and pulling of the needle from the system and the septa. For the Top -1,2,4 sample vials it is difficult to explain why the H_2 concentration is so low, particularly when compared the Bottom -1,2,4 sample data right below it in the Table. The material flowed from the top of the gasifier to the bottom through the down-flow pipe. Obviously there were problems with the sampling system performance on the Top data as indicated by helium reading, which was added during this run at about 3.5% (see Top

Pre-light row). Bottom -1 & 2 samples had reasonable H_2 and He readings, but the Bottom-4 reading went to zero for H_2, He, CO and CH_4 implying a sampling, storage or processing issue. The fact that the O_2 went up while all these other gases (including N_2) went down is hard to hard to explain.

Samples Post Plasma 2-1,2,4 were taken when the plasma insulator was breaking down but was still operational. If the Bottom 1,2 vials are compared to the Post Plasma 1,2 vials the helium concentration went down as a result of the plasma air and reaction products being added to the stream. The reactions and or dilution that took place reduced the concentration of H_2, CO and CH_4.

While these gas phase changes were taking place from the bottom of the gasifier to post plasma, the liquid samples had methanol and ethanol as the primary liquids showing up in the data and being affected by the plasma. From the top of the gasifier to the bottom they show up in the 500 to 3000ppm range (benzene and xylene show up at less than 500 ppm). These species are insignificantly affected by the plasma and essentially eliminated by the catalyst. The xylene content increased, this may have been the result of some other species (one that didn't have calibration data) being modified to xylene or it may be errant data.

12-3-14 Run Gas and Liquid Analysis Results Discussion

For this run the Helium flow controller was not operated so the He data was not reported. The Top vials 2, 3 show reasonable amounts of H_2 and CO for an updraft gasifier. Top vial 1 had obvious problems as all the gases were low and did not add to 100%. The "Post ETP" Vials are another sampling from the top of the gasifier. In this case the large impinger tubes of the sampling bench per the European Tar Protocol were filled with R-8 (renewable JP-8) and the effluent from the sampling bench was forced into the GC vials as opposed to drawing the process gas into them. This tested how well the R-8 cleaned the gas of tars and developed GC samples with positive pressure. These samples have the highest hydrogen and lowest nitrogen readings of all.

In comparing the liquid results from the Top to the Post ETP samples it can be seen that all target chemicals are present at the top of the gasifier at almost 1000 to 4000 ppm concentrations (ethanol data is not understood, it was consistently negative in these results). Only methanol and IPA are apparent after the simulated R8 scrubbing. The IPA obviously came out of the tar sampling bench. The IPA was transferred to the pump, flow meter and totalizing meter during previous runs where the impinger tubes were filled with IPA. During the Post ETP run when the pump pulled the gas through the R-8 filled impinger tubes and then pushed the gas through the meter and into the GC sampling tubes residual IPA was transferred as well. It may well be that methanol was in such abundance and transferred through the vials and impinger tubes easily enough that it became apparent in the Post ETP samples through a similar transfer mechanism.

When the system was back up and operational for the 12-3-14 run, arc instability problems upon opening the plasma valves caused concern that repeat damage was likely. The flow rate was maximized to what the plasmatron could take while keeping the arc voltage and amperage in an acceptable range. It appears that what was actually was happening was that the plasma air injection (high pressure point in the system) was flowing backwards through the plasma toward the bypass process line to the flare (vacuum source) and this is what caused the pure air readings

at the pre- and post- plasma samples. This likely also delivered excess air to the catalyst bed, resulting in an exothermic condition such that the flow valves had to be throttled to keep the temperature under control and resulted in all the O_2 present at pre-catalyst being consumed by the syngas tar mix and coming out as CO_2. The liquid samples of the tar stream going into the catalyst approximate what was at the top of the gasifier (BTX, naphthalene, phenol and the alcohols), as discussed these are all consumed by the combustion that took place in the catalyst bed.

Some sampling problems were addressed but some require further modification. It is apparent that the sampling method introduced air into the samples, most likely because of residual vacuum resulting from sampling of a process operating at a vacuum. The air may enter while sampling, over time after sampling, or at the very least enters the GC sampling needle after it extracts the sample from the vial. The GC needle and syringe will have residual vacuum and upon withdrawal from the sample vial will fill with air to equalize this pressure. This air leak and residual vacuum theory is supported by the "Post ETP" results of Table 7 where, as discussed, the sampling bench drew gas from the top of the gasifier through the impinger tubes (loaded with R-8) and forced the gas into the GC sampling apparatus. These "Post ETP" vials have the lowest O_2 and N_2 values and highest H_2, CO values of all other samples collected.

The fact that O_2 is present at the top of the gasifier at all (particularly in the "Post ETP" results) implies that air is leaking in to the system, either through the double flap valves, the safety pressure release (which did vent a couple times) or all of the above.

For the liquid sample results, there is a lack of data pre- and post-plasma and catalyst because there was a lack of process gas. This was due to fact that the input air for the plasma was forcing the syngas away from the plasma. When the blending of bulk flow process gas with plasma effluent was supposed to be occurring, the system was simply adding excess air to the catalyst bed. The bed at 750°C ignited this air-fuel mix and a rapid rise in bed temperature occurred.

For the gravimetric results, the primary discussion point is that an increase in the amount of heavy tars occurs from the top of the gasifier to the down flow exit, probably a result of increased time and temperature causing crosslinking or transformation of primary tar to secondary or tertiary tar as described by Milne. Any implementation of the scrubbed updraft gasifier approach should extract material off the top of the gasifier and quench it as quickly as possible.

One of the goals of this work was to investigate capture of tars in a fluid that could be burned via the liquid fuel injection system of an engine. BTX should be fine based on engine manuals that allow 35% aromatic, and the JP-8 Spec that allows 25% aromatic hydrocarbon. The stalagmite poses another interesting source of liquid fuel from waste. The FTIR and DSC results imply that the stalagmite material is about a 30 carbon long, straight chain hydrocarbon. This is essentially bunker fuel (used for ships). It can probably safely be postulated that since the material is mostly soluble in R-8 it should be an acceptable additive to JP-8 or other fuels as a very energy rich stream.

Energy Content Analysis & Discussion

Table 12 contains the analysis of the liquid tars captured from the top of the gasifier in the GC sampling (12-4-14 run) based on calibration curves for the target molecules.

Table 12 Target Tar Concentration and Energy Analysis

		Target Tar concentration. Basis: 3 Liters of gas went through impingers, each had 8 ml of MCF in them.						
	Methanol (PPM)	Ethanol (PPM)	IPA (PPM)	Benzene (PPM)	Toluene (PPM)	Xylene (PPM)	Naphthalene (PPM)	Phenol (PPM)
Top Vial 1	2044	-1466	924	3405	1730	3903	1105	626
Top Vial 2	2011	-260	230	0	0	0	0	521
Top Vial 3	879	-238	123	0	0	0	0	168
Top Vial 4	795	325	116	0	0	0	0	84
Top Vial 5	0	-78	116	0	0	0	0	82
Total Tar ppm by type	5729	na	1509	3405	1730	3903	1105	1481
Density Methyl Chloroform		1.32g/cc	Mol Weight	134				
Moles Methyl Chloroform/cc		0.0099	moles x 8 ml =	0.0791	moles Methyl Chloroform			
Moles Tar	4.53E-04		1.19E-04	2.69E-04	1.37E-04	3.09E-04	8.74E-05	1.17E-04
Mol Weight (g/mole)	20	NA	60	80	92	106	128	94
Tar Weight (g)	9.06E-03		7.16E-03	2.15E-02	1.26E-02	3.27E-02	1.12E-02	1.10E-02
Target Tar Concentration in Syngas (g/m3)	**35**	**grams target tars/m3**						

What Table 12 shows is that the concentration of the target tars at the top of the gasifier is 35g/m^3 (ethanol was not considered in this analysis due to the errant data). The true concentration of tars should be considerably higher (perhaps 3-5X) as this summation is based on only 8 chemical species. From the GCMS run of Figure 42 at least 45 peaks can be seen. Each peak corresponds to a molecular species that this analysis could be repeated on and added to this potential chemical energy. The assumption here is that if the material diffused through the GC column the molecular weight is probably in the 200 g/mole or less range and has somewhat reasonable volatility. This analysis provides insight into the volatile tars that could be added to the liquid fuel stream, or could actually be taken into the intake manifold if a scrubber were operating at high enough temperature and the pipeline leading to the intake manifold were kept above tar condensation temperatures.

To further this analysis to the nonvolatile tars, from Table 10 can be seen to be as much as 113gr/m^3. Table 10 provides information on the nonvolatile tars that would either be non-usable polyaromatic (tertiary tars), non-usable solid particulates, or the usable high boil point alkanes and other species estimated at 64% by the filtration analysis following Figure 51.

In summary, the total liquid tar energy content is a minimum of 113*0.64+ 35 = 107 grams of potentially usable tars per cubic meter of syngas coming off the top of the gasifier. This number is a low estimate as there could easily be more than 64% of the tars usable. This is only the amount that ran out of the flare and hardened. Other material may have run out and evaporated or certainly been lost to the flare. The material may have been reduced in solubility by exposure to the flare which caused additional heating and possibly thermal degradation.

The original intent of this work was to repeat this type of analysis after the plasma and after the catalyst to determine a reasonable approximation of engine fuel energy potential after each process step.

The chromatography results are available upon request. They are not attached as file size for this document has become excessive and led to some software shutdown and document recovery occurrences.

Lessons Learned, Conclusions and Implications for Future Research/Implementation

1.) Implementation of a more accurate flow measurement system, perhaps a higher sensitivity pressure sensor with the existing (or smaller) orifice plates, would have resulted in flow values that are usable. The GEK PCU board used in these experiments has 4 pressure sensors that are ± 28 inH_2O and 2 that are ± 7 inH_2O. The digital readings only changed with relatively large changes in flow rate. Use of smaller orifice plates would give more accurate readings, but at the potential risk of plugging with tar prematurely. It is difficult to perform energy balance calculations after each process step without more accurate flow data.

2.) Perform gas phase sampling with a flow through all-steel chamber design with dual valves to allow material to be drawn into the sample chamber without concerns about puncturing septa (that are prone to leakage and solvent swelling). Consideration should also be made to shutting down the venturi drive system to eliminate vacuum in the system (and sample chamber) at the end of sample taking to reduce air intake into sample chamber or GC injection syringe. Along with this change, a modified sample injection system would have to be developed for the GCMS system. The value of the system at hand is that when coupled to the auto handler many samples can be processed unattended greatly saving labor hours associated with testing and analysis.

3.) The method used to characterize the tar quantity: establishing calibration curves of a few likely tar molecules (BTX, methanol, etc.) and trying to determine their concentration was probably not the best way to proceed. It would have been better to do gravimetric sampling into JP-8 or even better, a pure high boiling point alkane, and then perform rotary vacuum distillation at approximately 80^oC. This would indicate how many light tars are being captured and distilled regardless of the specific organic species. In this case, the amount that distilled out of the sample would indicate useful energy from light tars available under the reasonable assumption that anything in that boiling range would likely burn in the engine. The remaining sample should then be passed through a wetted filter to determine the amount of insoluble material left behind. The indications are that the material passing through the filter would likely be very useful as fuel like the bulk of the stalagmite of 30 carbon long alkane. To determine the total amount of the high boil point tars it would be necessary to perform the classical European Tar Protocol test with alcohol and rotary evaporation. In this case the material left behind would be the solids (high molecular weight aromatics) and the good alkane. Subtracting off the solids from a filtration step would provide an estimate of the usable material in the sample.

Summary

Waste materials and biomass are potentially a valuable energy resource if they can be gasified and the products combusted in electricity generation. Co-produced tars and gas cleanup have hindered utilization and reduced conversion efficiency. This study used an updraft gasifier to generate a tar rich gas stream and then attempted to evaluate plasma and catalytic reformation of the tars in a pilot plant configuration to make a higher percent of the tars usable as fuel. The feedstock used was a blend of wood chips, paper, plastic (halide free), and dry dog food. Gas was sampled at several process steps with techniques that allowed analytical and gravimetric analysis of the gas and tar stream. The sampling techniques simulated a scrubber using methyl chloroform, isopropyl alcohol and a renewable JP-8 (R8) engine fuel as the working fluid in

impinger tubes. The purpose of the simulated scrubber aspect of this work was to investigate capture of the tars in a fluid that could later be burned via the liquid fuel injection system of existing generator sets to enable maximum conversion of the waste to electricity. The captured gas and tar liquids were analyzed using gas chromatography (GC), flame ionization detection (FID), thermal conductivity detection (TCD), and mass spectroscopy (MS). The non-volatile constituents were evaluated for total mass. The numbers of experiments performed were limited due to the difficulty in getting the numerous systems and sampling systems to work together for the first time.

Hydrogen was generated at over 16% max (10% average) concentration immediately following the gasifier. Readings at later process steps were lower implying that the tar cracking experiment had excess air (leaks or plasma air injection) resulting in combustion or dilution of the products. The plasma had operational problems in terms of flow, arc stability and plugging which are debugged to the degree that meaningful data may be obtained moving forward. Tar reformation via the catalyst bed was accomplished in terms of gravimetric results and analytical results, but this could have been a result of combustion occurring in the bed due to excess air added to the plasma that was not effectively operating. The scrubber captured light and heavy tars in the very simple simulation and there is a conservative estimate of 107g of engine usable tars per cubic meter of syngas leaving the gasifier. It was inadvertently discovered that the pyrolyzed plastic from the waste is forming a 30 carbon alkane chain material that is solid at room temperature but soluble in R-8 with considerable energy potential. It may be possible to filter the fuel containing this material and use it in the engine while sending the only the filter cake back to the gasifier.

Conclusion

The conclusion is that this experimental system is complex. The very high temperatures, hydrogen activation of the catalyst, preheating for the plasma, electrical control and interference problems associated with the plasma, precise controls of flow rates and hazards associated with air fuel mixes led to issues that limited acquisition of all data planned. The system is capable of taking more data but funding has run out.

A plasma or catalytic reactor system is probably too complex for a FOB waste to energy system and the focus for future work should fall back to the simplest method of getting the waste energy into the engine. This is likely gas scrubbing with a fuel, filtration of the fuel, passing the fuel and the cleaned gas to the engine. The filter cake should return to the gasifier per Figure 54.

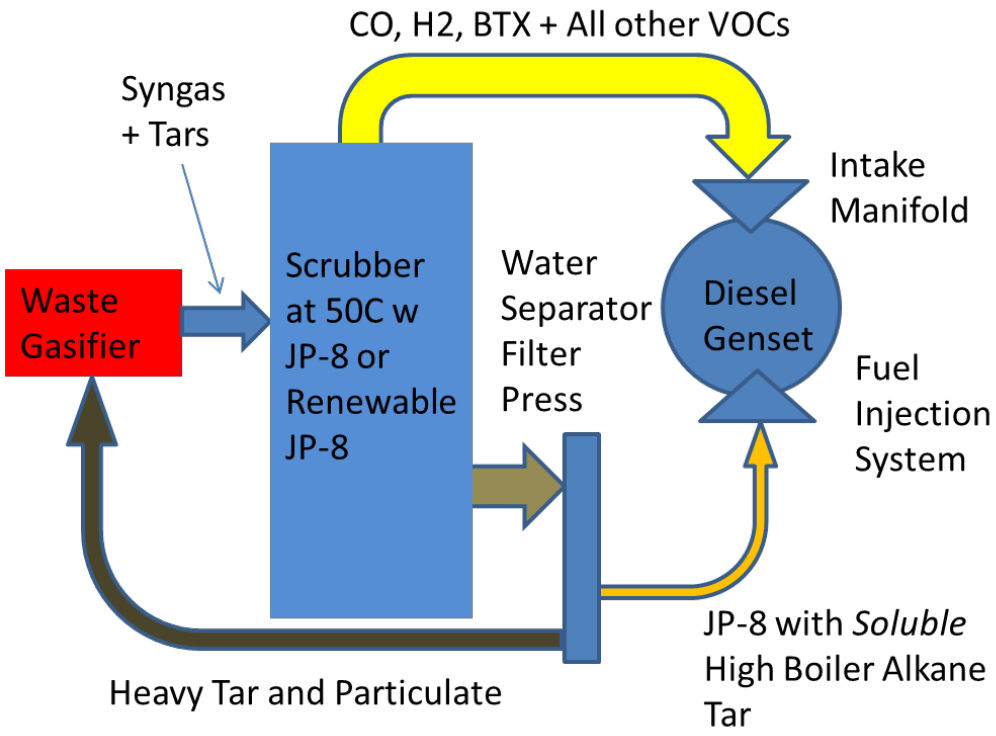

Figure 54. Optimized Waste to Energy System for Maximized Conversion of Waste Energy into Electricity

There are 3 sources of chemical energy coming from a gasifier: Syngas, light tars and heavy tars. The syngas obviously should be burned in the engine via the intake manifold. The light tars could be sent to the engine via the intake manifold if the scrubber and syngas stream is kept hot enough to keep the light tars from condensing. These consist of BTX, alcohols, aldehydes, acids, ketones, furans and some lighter mixed oxygenates. They may also be added to the liquid fuel stream and would burn acceptably provided they didn't damage seals or injectors. These may be reactive, but if diluted in fuel immediately upon generation and relatively quickly consumed in the generator engine there shouldn't be major detriment. It should be stated that feeding these light tars as vapors may be beneficial as they will less likely form soot if they enter the engine as vapors as opposed to injected droplets.

In terms of being usable in an engine, the heavy (high boil point) tars come in 3 general types: 1.) the high molecular weight polyaromatics (generally insoluble in JP-8 or even R-8 fuel and probably not usable except as gasifier feed); 2.) the mixed oxygenates, sugars, cellulose or lignin fractions from wood or paper that may be usable but requires further evaluation, 3.) as discussed in this work, the waxy alkanes discovered accidentally as the "stalagmite" under the flare which come from the plastics in the MSW which are very likely an excellent energy source.

Diesel engine fuels are ideally straight chained hydrocarbons which have low autoignition temperatures and burn very fast. Classically they "unzip" during combustion upon first contact of carbon from the center points of the chain with atomic oxygen or free radicals. Because of this diesel engines are injected during power stroke. The whole fuel load cannot be injected on intake

stroke or even near top dead center of power stroke because excessive pressure or “knocking” will occur. This feature of diesel engines and their fuel provides the path forward for future work.

Recommendation for Future Work

There are several recommendations.

1.) Continue work regarding further delivery of waste energy to engines by enhancing liquid phase capture of the tar while cleaning the syngas as shown in Figure 54.

    a. Create enough liquid fuel to run a small diesel engine generator and measure the engine output chemistry with GCMS.

    b. Document the difference in engine exhaust constituents relative to the engine running on virgin diesel fuel and characterize emissions cleanup requirements and potential solutions.

    c. Determine the amount of light tars which should go to the intake manifold and the heavy tars which should be split between the engine injector system (heavy alkanes soluble in fuel) and the gasifier (as sludge).

2.) Tune the engine injection system to allow more of the fuel to be injected towards the beginning of each stroke.

    a. Modern diesel engines inject many times during the power stroke on millisecond intervals. Tuning the injection cycle could allow longer residence time and more time for the tar molecules to burn, subject to engine knock limitations may be the path forward. Lockheed has an 18kW diesel genset that has been run on simulated syngas and JP-8 spiked with toluene as proof of concept. It is proposed to operate on fuel created in the scrubber (described next) and see what can be done to reduce non-desirables from the exhaust stream and reduce engine detrimental effects from the tars.

3.) Lastly, Figure 55 is an existing 3Ton/day scrubber built with LM capital and ready to be mated to an acceptable gasification system like the rotary gasifier of SERDP project WP-2211 or the Concord Blue waste to energy reformer slated for construction at the Lockheed Martin-Owego, NY facility in 2015. The work product would be to establish the light vs heavy tar split in the gasifier effluent, ASPEN model this scrubber for that mix, establish quench and recycle flow rates, mate and operate the scrubber system feeding syngas and the fuel mix to the engine. The engine was modified to enable a rapid switch to tar laden diesel and back again while enabling fuel use rate measurements. A load bank is available to determine derate factors occurring while the genset operates under load with this alternate fuel.

Figure 55. Existing Lockheed Capital Scrubber Ready for Integration to a Gasification Unit.

Appendices

Appendix A: Exceptions to the European Tar Protocol

In order to make use of available equipment and materials, there were a number of exceptions to the published *European Tar Protocol 2006* in this project. The exceptions listed here all pertain to tar sampling and analysis.

- No thimble filter was used in the sampling train. As a result it also follows that there was no thermocouple at this point to read the temperature of incoming gases and also there was no need for a Soxhlet extraction in order to collect all tars for analysis.

- The six impinger bottles used were of different dimensions than described. The bottle dimensions were O.D. 35mm x 300mm high. Since these are close to the larger prescribed bottles, 100mls of isopropyl alcohol was used in bottles 1 through 5.

- Glass beads were used in place of glass frits. The glass beads were 0.080" diameter (as opposed to 6mm). No amount of beads is prescribed in the protocol. A volume of 50mls of beads was introduced into each of impinger bottles 2, 3, 5 & 6 in this series of experiments.

- The temperature of the cold bath was maintained at 0C with ice and water instead of the prescribed -15C to -20C.

- The collected samples were stored in capped brown 1-liter bottles but at room temperature instead of at 5C or below.

- One sample was collected using JP-8 fuel instead of isopropyl alcohol.

Literature Cited

[i] Work sheet on Bagram air base operating cost. https://view.officeapps.live.com/op/view.aspx?src=http%3A%2F%2Fwww.aepi.army.mil%2Fdocs%2Fwhatsnew%2FFully%2520burdened%2520cost%2520of%2520waste%2520worksheet.xlsx

[ii] http://www.businessinsider.com/open-air-burn-pits-leave-troops-sickly-2013-11

[iii] Website to register for military personnel to register health complaints: http://www.publichealth.va.gov/exposures/burnpits/index.asp

[iv] NREL/TP-570-25357 Milne, T.A.; Evans R.J.; BiomassGasifier "Tars": Their Nature, Formation and Conversion

[v] Basu, Prabir, Gasification and Pyrolysis: Practical Design and Theory. June 2010; Academic Press.

[vi] SERI/SP-271-3022DE88001135; March 1988; Handbook of Biomass Downdraft Gasifier Engine Systems

[vii] On-Site Field Feeding Waste to Energy Converter; L. Knowlton* and D. Pickard -U.S. Army Natick Soldier Research, Development and Engineering Center,Natick, MA; J. Diebold, K. Lasnik, A. Lilley, and K. Browne Community Power Corporation, Littleton, CO; http://nsrdec.natick.army.mil/LIBRARY/00-09/R08-105.pdf

[viii] WASTE-TO-ENERGY White Paper; January 14, 2009; Dr. Igor Matveev, President, International Plasma Technology Center

[ix] Energy Fuels 2013;27(2):1174-81; Rodrigo Mpntiero, et.al.; Tar reforming under microwave plasma torch.

[x] Chemosphere 2007;68(10):1821-9; Van Durme, Jim, et. al; Abatement and degredation pathways of toluene of indoor air by positive corona discharge.

[xi] International Journal of Hydrogen Energy 32 (2007) 2848 – 2867; G. Petitpasa, J.-D. Rollier, A. Darmon, J. Gonzalez-Aguilar, R. Metkemeijer, L. Fulcheri; Acomparative study of non-thermal plasma assisted reforming technologies

[xii] Topics in Catalysis. DOI 10.1007/s11244-012-9789-z; Kimberly A. Magrini-Bair; Whitney S. Jablonski; Yves O. Parent; Matthew M. Yung: Bench- and Pilot-Scale Studies of Reaction and Regeneration of Ni–Mg–K/Al2O3 for Catalytic Conditioning of Biomass-Derived Syngas

[xiii] Bioresource Technology 102 (2011) 543–549 ; Thana Phuphuakrat; Tomoaki Namioka; Kunio Yoshikawa: Absorptive removal of biomass tar using water and oily materials

[xiv] US Patent 7,803,845; Boerrigter , et al.; Process for removing tar from synthesis gas

[xv] US Patent 8,783,215; Scott, P; Tongue, B.; Tar Scrubber for Energy Recovery from Gasifier Operations

[xvi] CEN BT/TF 143; July 2005; J. Good; L. Ventress; H Knoef; U. Zielke; et. al. Sampling and analysis of tar and particles in biomass producer gases.

[xviii] SERI/SP-271-3022DE88001135 March 1988 Handbook of Biomass Downdraft Gasifier Engine Systems

[xix] GEK Gasifier website.

[xx] Himmelblau, David M., Basic Principles and Calculations in Chemical Engineering 4th Edition. 1982; Prentice-Hall